The metabolic basis of MYC-induced apoptosis

Huizhong Su

苏慧中



THE UNIVERSITY
of EDINBURGH

Thesis submitted for the degree of Doctor of Philosophy
The University of Edinburgh
2018

Declaration

I declare that this thesis was written and composed solely by myself, and that it has not been submitted in any previous application for a degree. Except where stated otherwise by reference or acknowledgment, the work presented is entirely my own.

Huizhong Su

Acknowledgements

I would like to take this opportunity to thank my supervisor, Dr. Andrew Finch, who has been very supportive and patient, guiding and inspiring me throughout my PhD. He has taught me every little detail during my study, including experimental design, critical thinking and presentation and writing skills. And I would like to thank my secondary supervisor, Dr. Kamil Kranc, for the valuable feedback on my project and huge support on the mouse work. I would also like to thank my previous supervisor, Dr. Patrick Pollard who first invited me to the fascinating field of cancer metabolism. I am lucky to have had Joy Edwards-Hicks and Asimina Pantazi as lab members working together, sharing knowledge and ideas and also as friends sharing laughter and tears. Joy helped me a great deal with the project and her contribution is also acknowledged through the thesis. I wish them all the best for their new journeys ahead. I would like to express my thanks to all the other current and previous mentors and colleagues for all their help during my PhD: Dr. Heather Barker, who started and contributed a great deal to the project; Dr. Jimi Wills for his tremendous work on mass spectrometry, without whose support my project could not have progressed; Dr. Ming Yang, who is always passionate and critical about research and taught me much more than just essential wet lab techniques; and many names not listed here, including the thesis committee members, collaborators, everyone who joined our lab meetings, all colleagues on ECRC level 3, IGMM technical facilities, my thanks for all their support during these four years.

I probably would not have been able to pursue my PhD without all the help and support from my parents, both mentally and financially. Words cannot express my gratitude and love for them. Last but not least, thanks to my husband, Rui Chen, for the love and support throughout these years and many years to come.

Abstract

Programmed cell death, known as apoptosis, is widely accepted as a key tumour suppression mechanism. The oncogene *MYC* promotes cell growth and proliferation but also sensitises cells to apoptosis, which limits its oncogenic potential. MYC-induced apoptosis requires the pro-apoptotic BCL2 family proteins BAX/BAK and can be blocked by anti-apoptotic family members such as BCL2 and BCL-xL. Previous studies have identified glutamine withdrawal as a trigger for MYC-induced apoptosis. Through untargeted metabolomic analyses of cells with perturbed BCL2 family member composition and of cells undergoing glutamine-dependent MYC-induced apoptosis, we found that nucleosides and nucleotides were altered in correlation with apoptotic status. Glutamine is an important biosynthetic substrate and energy source and we show global transcription and translation of the cells decreased upon glutamine withdrawal. However, MYC-activated cells promote transcription and translation even in the absence of glutamine and thus still drive huge demand for energy. Deregulated MYC promotes nucleotide catabolism and depletes cellular energy charge upon glutamine withdrawal, indicating energy shortage driven by MYC. Nucleotide conversion and remodeling by adenylate kinase 2 (AK2) protects cellular energy charge and inhibits MYC-induced apoptosis. These results indicate a homeostatic model for MYC-induced apoptosis based upon mitochondrial energy supply and demand. We propose that the transcriptional activity of MYC drives huge demand for energy to support global transcription and translation and thereby sensitises cells to apoptosis under conditions of limiting energy supply.

Lay summary

Apoptosis is the process of programmed cell death (almost like cellular suicide) that often occurs when cells experience great stress. Resistance to cell death helps many cancer cells to survive and uncovering how such cells bypass apoptosis could allow for development of therapies to restore it. The *MYC* oncogene leads to tumour formation through promotion of cell growth and proliferation but it also sensitises cells to apoptosis. Blocking apoptosis therefore speeds up tumour formation by MYC. Because it promotes such rapid cell growth, MYC changes the ways cells use nutrients and energy, processes known as cell metabolism. Glutamine is an amino acid that is used in cells for multiple roles and MYC-activated cells undergo apoptosis when deprived of glutamine. This suggests that there is a link between cell metabolism and apoptosis, particularly driven by MYC. Using cells with activated MYC, we work on how cancer cell metabolism affects the onset of apoptosis. We found that imbalance of energy supply and demand is the key driver of apoptosis in MYC-expressing cells. This finding provides valuable information on targeting tumours with high levels of MYC and also sheds light on how cells in general undergo apoptosis.

Table of contents

Declaration **2**
Acknowledgements **3**
Abstract **4**
Lay summary **5**
Table of contents **6**
Chapter 1 - Introduction **8**
Apoptosis and cancer 8
BCL2 family and apoptosis 9
BCL2 family and metabolism 11
Discovery and structure of MYC 13
MYC in cancer 14
The undruggable MYC 15
Function of MYC 16
MYC and apoptosis 17
MYC and metabolism 19
Glycolysis 20
Glutaminolysis 22
Nucleotide biosynthesis 23
Lipid metabolism 24
Ribosome biogenesis 24
Mitochondrial biogenesis 25
Glutamine metabolism in cancer 27
Clinical applications of glutamine 29
Metabolic profiling 31
Chapter 2 - Materials and Methods **33**
Cell culture 33
Construction of retroviral expression vectors 34
Polymerase chain reaction (PCR) 34
Digestion 35
Ligation 35
Transformation 35
Construction of retroviral shRNA vectors 36
Lentiviral shRNA vector 36
Retroviral/lentiviral production and infection 36
Transfection for production of viral particles 36
Viral transduction 37
siRNA transfection 37
Western Blotting 38

qPCR 39
Apoptosis assay 41
IncuCyte 41
EU transcription assay 41
Metabolites extraction and metabolomic analysis 42
Metabolite extraction 42
LC-MS 42
Analysis 42
Seahorse mitochondrial function analysis 43
Statistical analysis 43
Chapter 3 - Metabolic changes during MYC-induced apoptosis 44
MYC drives continued demand for transcription and translation after withdrawal of glutamine 45
Glutamine withdrawal promotes nucleotide remodeling to a lower energy state 48
Accumulation of nucleosides and bases indicates nucleotide catabolism 50
Depletion of TCA cycle metabolites upon glutamine withdrawal 53
Mitochondrial adenylate kinase 2 is MYC-regulated and protects from apoptosis 54
Summary 59
Discussion 60
Chapter 4 - Oxidative stress and MYC-induced apoptosis 61
Glutathione depletion is not primarily the cause of MYC-induced apoptosis triggered by glutamine withdrawal 61
Mitochondrial control of oxidative stress 63
Proton leak and oxidative stress 67
Summary 70
Discussion 71
Chapter 5 - The BCL2 protein family and their role in metabolism 72
Metabolite changes in the pro-apoptotic state - overexpression of pro-apoptotic members 73
Metabolite changes in the anti-apoptotic state - knockdown of pro-apoptotic members or overexpression of anti-apoptotic members 77
Discussion 82
Chapter 6 - Discussion 84
Nucleotide catabolism 84
Undruggable MYC - synthetic lethal approaches 86
Membrane potential 87
Model 88
Chapter 7 - Bibliography 90

Apoptosis and cancer

Douglas Hanahan and Robert A. Weinberg proposed the hallmark capabilities that cancer cells can adopt to become tumourigenic and ultimately malignant. They initially proposed six hallmarks, namely sustaining proliferative signaling, evading growth suppressors, activating invasion and metastasis, enabling replicative immortality, inducing angiogenesis and resisting cell death (Hanahan and Weinberg, 2000). A growing body of research and progress now suggests that two additional hallmarks of cancer are involved: reprogramming of energy metabolism and evading immune destruction. Underlying these hallmarks are genome instability, which generates the genetic alterations that drive tumour progression, and inflammation, which sustains multiple hallmark functions (Fig 1.1) (Hanahan and Weinberg, 2011).

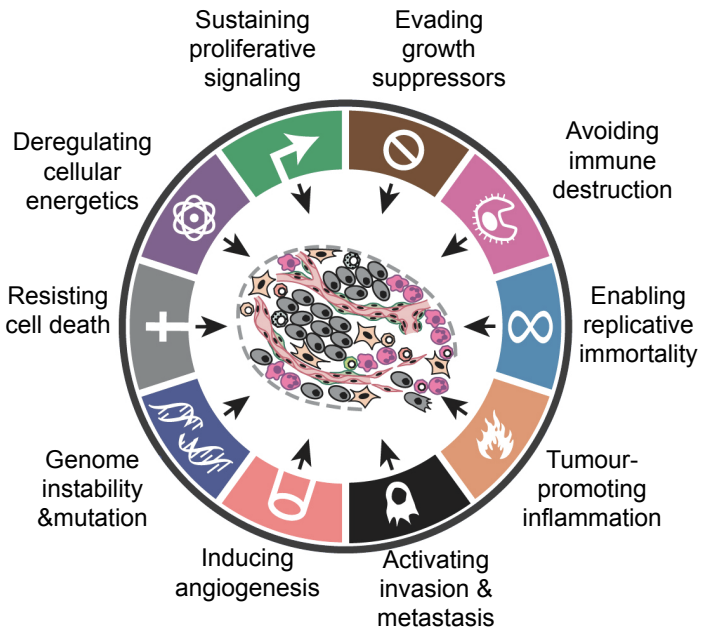


Figure 1.1. Hallmarks of cancer cells (reproduced from Hanahan and Weinberg, 2011)

Apoptosis is a cellular suicide program that organisms have evolved to eliminate unwanted cells during development and damaged or abnormal cells following cellular stress. Programmed cell death exerts strong selective pressure on cancer cells, and accordingly they acquire various strategies to override this process (Fernald and Kurokawa, 2013). It has been shown from several studies that cancer development is limited by apoptosis and tumours that are high-grade or resistant to therapy often exhibit attenuated apoptosis (Adams and Cory, 2007; Lowe et al., 2004; Evan and Littlewood, 1998).

BCL2 family and apoptosis

B-cell lymphoma 2 (BCL2) was discovered as an oncogene linked to an immunoglobulin heavy chain enhancer by t (14;18) chromosome translocation in follicular lymphoma (Fukuhara and Rowley, 1978). The Bcl2 protein promotes cell survival by inhibiting apoptosis rather than affecting proliferation (Vaux et al., 1988). More BCL2-like proteins were subsequently identified, some of which are anti-apoptotic and others pro-apoptotic, and together they form the BCL2 family (Fig 1.2).

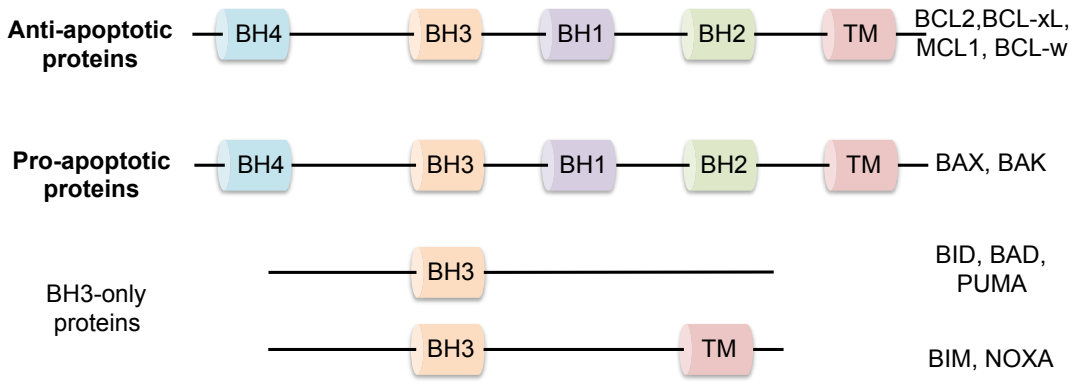


Figure 1.2. Key members of the BCL2 family (adapted from Delbridge et al., 2016)
BCL2 homology (BH) domains facilitate classification of BCL2 family members into three subgroups: anti-apoptotic, pro-apoptotic and BH3-only proteins. Some members also contain a transmembrane (TM) domain.

BCL2 family members all share combinations of α-helical regions, known as BCL2 homology (BH) domains. BH1-4 domains are highly conserved among family members and are crucial for their function. The BH3 domain mediates interaction between family members. Some members also contain a transmembrane (TM) domain to facilitate association with the outer mitochondrial membrane (Tsujimoto et al., 1987; Chen-Levy and Cleary, 1990; Krajewski et al., 1993).

BCL2 family proteins are divided into pro- and anti-apoptotic members (Fig 1.2). The pro-apoptotic BCL2 family proteins (e.g., BAX, BAK, BID, BIM, BAD, PUMA, and NOXA) all contain a single amphipathic BH3 domain. BAX and BAK possess multiple BH domains, while the rest of the pro-apoptotic members are known as "BH3-only proteins". BCL2 family proteins govern the mitochondrial control of apoptosis (Fig 1.3). BAX and BAK are the gateway controllers of mitochondrial outer membrane permeabilisation (MOMP), whilst activation of BAK/BAK and the consequent release of cytochrome c through MOMP are held in check by the anti-apoptotic BCL2 family proteins BCL2, BCL-xL, BCL-W and MCL1. The release of cytochrome c activates caspase-9 which can then activate caspase-3 and caspase-7 that are responsible for destroying the cell. BH3-only proteins often act as triggers to apoptosis in response to certain stimuli. For example, BIM can be induced by serum withdrawal (Weston et al., 2003), BID can be cleaved by caspase-8 to form the functionally active truncated BID (tBID) (Li et al., 1998), and PUMA and NOXA can be upregulated by p53-dependent DNA damage responses (Nakano and Vousden, 2001; Oda et al., 2000). The precise mechanisms by which individual BH3-only proteins promote apoptosis can differ. Some, like BID and BIM, are thought to interact with and promote the activation of BAX and BAK directly. In contrast, BAD, PUMA and NOXA can act as "derepressors", neutralising the activity of anti-apoptotic members to facilitate BAX/BAK activation (Andersen and Kornbluth, 2013).

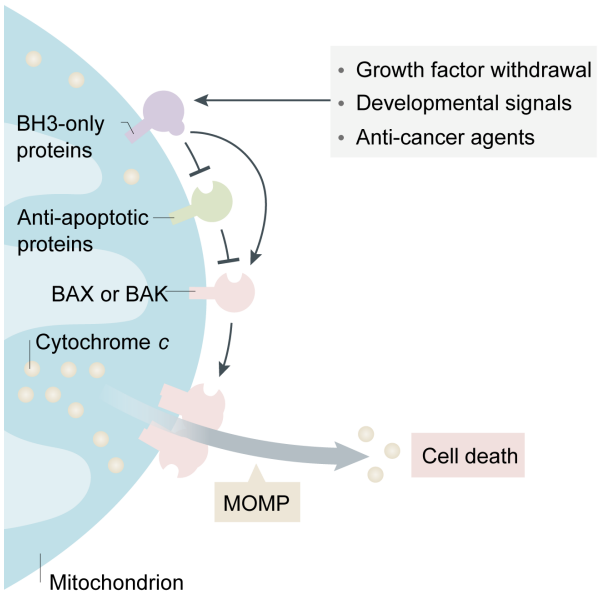


Figure 1.3. BCL2-regulated apoptosis signaling (reproduced from Delbridge et al., 2016)
BH3-only proteins, anti-apoptotic proteins and BAX/BAK work together to control release of cytochrome c through MOMP that consequently activates caspases and induces cell death.

BCL2 family and metabolism

In addition to their roles in regulating apoptosis, BCL2 family proteins have been found to control metabolic circuitries such as the efficiency of mitochondrial ATP synthesis (by binding to the F_1F_O ATP synthase), ATP/ADP exchange and cellular redox states. Moreover, several metabolic intermediates including ATP, acetyl–coenzyme A (acetyl-CoA), NAD^+, $NADP^+$, and reactive oxygen species (ROS) are intimately involved in signal transduction cascades that influence cell death (Green et al., 2014).

BAX and BCL2 interact with two mitochondrial channels, the voltage dependent anion channel (VDAC) and the adenine nucleotide transporter (ANT), which bridge the mitochondrial membranes and control mitochondrial import of ADP and export of ATP (Brenner et al., 2000; Marzo et al., 1998). The interaction of BAX and BCL2 alters the conductivity of these channels and is thought to affect apoptosis as a result. BCL-xL can promote an open conformation of the VDAC so that adenine nucleotide

exchange is maintained under conditions where apoptosis is associated with impaired ATP/ADP exchange (Vander Heiden et al., 1999). Moreover, BCL-xL interacts directly with the F_1F_O ATP synthase, thereby increasing its enzymatic activity and ATP production (Alavian et al., 2011).

Many studies have shown that reducing oxidative stress inhibits apoptosis. BCL2 prevents excessive mitochondrial ROS production by reducing the activity of the mitochondrial electron transport chain (ETC) (Chen et al., 2007), one of the major sources of ROS, and increasing cellular levels (Meredith et al., 1998) or shifting intracellular distribution of glutathione (Voehringer et al., 1998). BCL2 has also been shown to protect cells from H_2O_2-induced oxidative death and suppress lipid peroxidation when overexpressed (Hockenbery et al., 1993). Conversely, BAX expression in mammalian and heterologous models increases ROS generation and oxidative damage (Naderi et al., 2006) and H_2O_2-induced apoptosis is blocked in BAX null cells (Ahmad et al., 2004). Cells with higher intracellular levels of the antioxidant glutathione exhibit inactivation of the apoptotic function of cytochrome c by keeping it in its reduced state (Vaughn and Deshmukh, 2008). In this report, the authors suggest that cells with high pentose phosphate pathway activity, and consequent production of reduced NADPH and glutathione, are resistant to caspase activation downstream of MOMP. NOXA, when phosphorylated, may also modulate metabolism by enhancing the pentose phosphate pathway (Lowman et al., 2010).

In summary, the BCL2 family has been heavily implicated in the regulation of metabolism, especially nucleotide exchange/production and cellular redox state. However, despite these many reports, a clear unifying model for a metabolic basis for apoptosis is still lacking. This is in large part because most of the reports detail different apoptotic triggers and the involvement of specific BCL2 family members in a specific circumstance. Furthermore, many studies predate the advent of current mass spectrometric analyses, which are a mainstay of modern metabolic research. A major goal of this thesis was to address metabolic roles of the BCL2 family in a comprehensive and systematic way.

Discovery and structure of MYC

MYC, also known as *c-MYC*, is a human homologue of the retroviral oncogene *v-gag-myc*. The *v-myc* oncogene was first identified as the transforming element of the retrovirus MC29 which was isolated from a chicken with spontaneous myelocytomatosis (Ivanov et al., 1964). MC29 is an acute transforming, replication defective virus in which a large part of its gag, pol and env sequences are replaced by the host-derived myc sequence, the exons 2 and 3 of chicken *c-myc* (Reddy et al., 1983).

c-MYC was first discovered in Burkitt's lymphoma which is characterised by deregulation of *c-MYC* through chromosomal translocation to the immunoglobulin locus (Taub et al., 1982). The *MYC* gene family is comprised of three members, *MYC*, *N-MYC* and *L-MYC*. They are proto-oncogenic transcription factors sharing related functions while retaining distinct roles and association with different diseases (Nesbit et al., 1999).

Figure 1.4. illustrates the domain structure of *MYC*. The N-terminus of *MYC* contains a transactivation domain (TAD) and several highly conserved motifs known as MYC homologue boxes. The C-terminus contains a primary nuclear localization signal (NLS), a basic region (BR) and a basic helix-loop-helix-leucine-zipper (HLH-LZ) domain. The HLH-LZ domain allows the heterodimerisation of *MYC* with another HLH-LZ protein MYC-associated-factor-X (MAX). This dimer is responsible for sequence specific DNA binding that binds the enhancer box (E box) element CACGTG and activates the transcription of various genes (Blackwood and Eisenman, 1991). MYC-interacting Zn finger protein-1 (MIZ1) that specifically interacts with MYC also interacts through the HLH-LZ domain: this dimerisation forms a transcriptional repressor complex (Peukert et al., 1997).

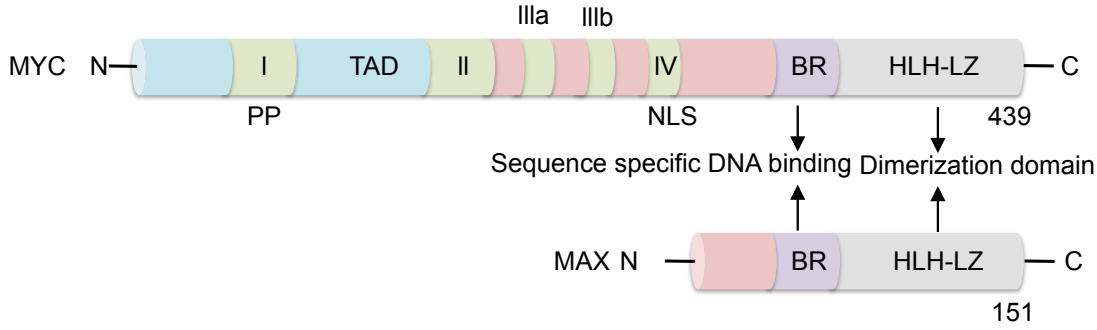


Figure 1.4. Domains of MYC and MAX (adapted from Meyer and Penn, 2008)
The figure illustrates the key domains of MYC and MAX. Black arrows indicate the BR domain for sequencing specific DNA binding and HLH-LZ for dimerization. TAD, transactivation domain; I, II, IIIa, IIIb, IV, MYC homology box I, II, IIIa, IIIb, IV; NLS, nuclear localisation signal; BR, basic region; HLH-LZ, helix-loop-helix-leucine-zipper.

MYC in cancer

Overexpression or activation of the transcription factor MYC occurs in more than half of human cancers arising from almost every tissue type and this deregulation of MYC expression can occur by many mechanisms (reviewed by Meyer and Penn, 2014). Deregulation commonly occurs as a consequence of genetic abnormalities that affect the *MYC* locus, including insertional mutagenesis, gene amplification and chromosomal translocation. Moreover, many additional mechanisms, including activation of upstream regulatory factors such as the oncogene RAS (Sears et al., 1999; Magudia et al., 2012) or transcription factor NOTCH (Palomero et al., 2006; Weng et al., 2006) and loss of APC in colorectal cancer (He et al., 1998) can also deregulate MYC expression.

Even though *MYC* is one of the most commonly activated oncogenes, MYC overexpression in normal cells can induce proliferative arrest, senescence or apoptosis, all restraining its oncogenic potential (Evan et al., 1992; Gibson et al., 1995; Felsher and Bishop, 1999; Grandori et al. 2003; Nilsson and Cleveland, 2003; Hoffman and Liebermann, 2008). MYC activation alone is insufficient for oncogenic transformation, but by cooperating with other oncogenic events MYC can initiate tumourigenesis. Genetic events abolishing tumour-suppressive mechanisms, such as loss of p53 or $p19^{ARF}$ to evade proliferative arrest or overexpression of BCL2 to

escape from apoptosis, can synergise with MYC to induce tumourigenesis. (Green, 1997; Zindy et al., 1998; Jacobs et al., 1999; Schmitt and Lowe, 2001; Finch et al., 2006).

MYC is usually required to maintain tumour growth and upon MYC inactivation, tumour cells appear to restore normal checkpoint mechanisms and undergo proliferative arrest, differentiation, cellular senescence, and/or apoptosis (Felsher and Bishop, 1999; Jain et al., 2002). A successful therapeutic strategy targeting MYC overexpression could have a great impact on cancer therapy, as demonstrated by Soucek et al (Soucek et al., 2008). However, MYC has yet to be successfully targeted for the treatment of cancer, as most transcription factors are generally considered "undruggable" (Verdine and Walensky, 2007; Filippakopoulos et al., 2010; Delmore et al., 2011; Yan and Higgins, 2013).

The undruggable MYC

Many known cancer drivers such as RAS, MYC and fusion transcription factors have been considered undruggable due to large protein–protein interaction (PPI) interfaces or lack of deep protein pockets (Whitfield et al., 2017; McCormick, 2015).

However, advances in drug development have made it possible for undruggable targets to become druggable. A good example is the BCL2 family, whose members were once considered undruggable: this was because they do not have hydrophobic pockets, they have an intracellular location and flat contact surfaces, all of which are undesirable from a pharmacological point of view. Due to the availability of a growing body of information about their biochemical and structural properties, BH3 mimetics have now been developed and have proven capable of inhibiting BCL2 (Delbridge and Strasser, 2015).

As targeting MYC has thus far proven to be challenging, much effort has been focused on indirect strategies. Work has been done to show that Aurora kinase A (AURKA) controls N-MYC stability (Otto et al., 2009) and therefore may represent an attractive target. A class of inhibitors has been reported that disrupts the native

conformation of AURKA and drives the degradation of the N-MYC protein in N-MYC-driven cancers (Gustafson et al., 2014).

Oncogenic MYC deregulates the cancer transcriptome, proteome, and metabolome, revealing many downstream pathways whose targeting may bring therapeutic benefit. An increasing number of studies has provided evidence that targeting metabolic pathways can cause vulnerability in MYC-driven cancers. Potential targets have been found that are involved in metabolic pathways that are synthetic lethal with MYC (reviewed by Hsieh and Dang, 2016). Although they are not specific for targeting MYC itself, understanding the metabolic rewiring driven by MYC will allow the development of therapies for targeting MYC-driven cancer. Whether these approaches will actually result in clinically useful therapies will require a good deal more research.

Function of MYC

MYC is a transcription factor that can bind to approximately 10-15% of the genome (Dang et al., 2006; Patel et al., 2004). During cellular and tissue homeostasis, MYC is a key regulator of organismal growth through promotion of several basic cellular programmes such as cell proliferation, cell growth, apoptosis, energy metabolism and various biosynthetic pathways (Eilers and Eisenman, 2008).

A summary of the most consistently identified MYC-induced genes in independent studies (Kress et al., 2015) is given in Figure 1.5. These target genes are involved in cell growth (ribosome biogenesis and protein synthesis), cell cycle control, energy production (glycolysis, glutaminolysis and mitochondrial biogenesis), anabolic metabolism (synthesis of amino acids, nucleotides and lipids) and DNA replication (Kress et al., 2015). Cell growth and proliferation require energy and building blocks and an important role of MYC is to transcriptionally regulate the production of key components of almost all cellular biosynthetic pathways in order to support this wide-ranging growth programme (Dang, 2013).

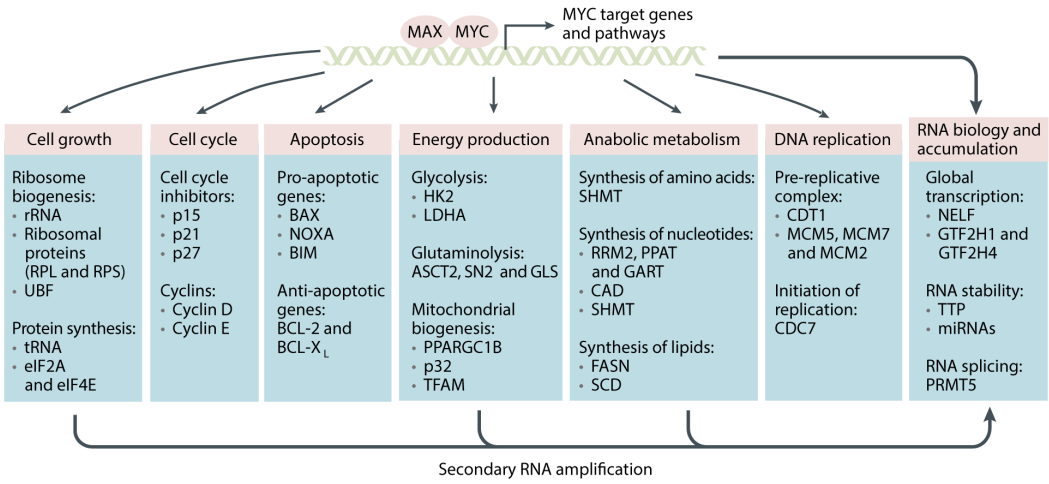


Figure 1.5. The main cellular processes regulated by MYC (reproduced from Kress et al., 2015)
The figure shows the main cellular processes and target genes involved in these processes that regulated by MYC. Several of the regulated gene products and pathways drive physiological changes in cells that have the potential to feed back on global RNA production, as indicated in the figure as secondary RNA amplification.

MYC and apoptosis

In addition to its promotion of growth and proliferation, MYC also sensitises cells to apoptosis, as mentioned above. MYC-induced apoptosis requires BAX/BAK (Dansen et al., 2006; Juin et al., 2002), release of cytochrome c (Juin et al., 1999), activation of effector caspases (Hotti A et al., 2000), and can be blocked by co-expression of anti-apoptotic family proteins such as BCL2 and BCL-xL (Bissonnette et al., 1992; Fanidi et al., 1992; Pelengaris et al., 2002). MYC protein expression may be crucial for the conformational change that activates BAX under certain conditions (Soucie et al., 2001). MYC also indirectly suppresses the anti-apoptotic proteins BCL2 and BCL-xL and thereby sensitises cells to gamma-irradiation-induced apoptosis (Eischen et al., 2001a; Maclean et al., 2003). In MYC-null cells treated with apoptotic stimuli that trigger MYC-independent cell death, Bax is not activated and cytochrome c is not released into the cytoplasm. Thus, Myc enhances cellular apoptotic potential by producing apoptotic signals at the mitochondria involving Bax activation and cytochrome c release (Soucie et al., 2001). It has also been shown that activated Myc-deficient primary B lymphocytes are resistant to

different apoptotic stimuli such as staurosporine and CD-95, suggesting that these stimuli induce apoptosis via mitochondrial signals. Non-activated Myc-deficient B cells have reduced spontaneous cell death compared to their wild-type counterparts (de Alborán et al., 2004). The precise molecular mechanisms of how MYC induces apoptosis remain unclear, however, it appears that multiple pathways are regulated by MYC to potentiate this biological activity.

In addition to involvement of mitochondrial signals involving the BCL2 family, MYC-induced apoptosis has been reported to be regulated by the ARF-p53 pathway. Overexpression of MYC induces accumulation of $p19^{ARF}$ ($p14^{ARF}$ in human cells), which inhibits MDM2-mediated degradation of p53 (Kamijo et al., 1998; Stott et al., 1998; Zindy et al., 1998; Eischen et al., 1999; Schmitt et al., 1999). Activated p53 in turn can induce apoptosis via transcriptional upregulation of BH3-only proteins PUMA and NOXA (Nakano and Vousden, 2001; Villunger et al., 2003). However, several groups have reported MYC-induced apoptosis in the absence of either $p19^{ARF}$ or p53, indicating that ARF and p53 are not essential for MYC-induced apoptosis (Hsu et al., 1995; Blyth et al., 2000; Eischen et al., 2001b; Finch et al., 2006). The recent identification of BIM as a transcriptional target of MYC suggests that this BH3-only protein may directly mediate the pro-apoptotic signal of MYC (Campone et al., 2011; Lee et al., 2013). MYC induces Bim accumulation in murine B cell lymphoma cells and MYC point mutants that fail to induce Bim (but still activate $p19^{ARF}$ and p53) fail to induce apoptosis (Hemann et al., 2005). Furthermore, it has been suggested that BIM is the primary mediator of MYC-induced apoptosis in multiple solid tissues (Muthalagu N. et al., 2014).

Abrogation of the apoptotic response is crucial for MYC-driven cellular transformation and tumourigenesis. Numerous oncogene cooperation studies involving *MYC* indicate that an important function of cooperating mutations is the abrogation of apoptosis induced by MYC. The anti-apoptotic gene *BCL2* cooperates with MYC to promote proliferation of B-cell precursors *in vitro* and promotes tumorigenesis *in vivo* (Vaux et al., 1988). Transgenic mice harbouring Bcl2 cDNA under the control of the IgH enhancer develop a large accumulation of B lymphocytes but no tumour within 12 months. When these mice were crossed with

the Eμ-Myc strain that carries a normal *Myc* gene coupled to the Ig heavy chain enhancer (Harris et al., 1988), they showed hyperproliferation of pre-B and B cells and developed greatly accelerated tumourigenesis compared to the Eμ-Myc mice (Strasser et al., 1990). Around 50% of the infrequent lymphomas arising in Bcl2 single transgenic mice had somatic translocations activating Myc, confirming a selective pressure during lymphomagenesis for cooperation between Bcl2 and Myc (McDonnell and Korsmeyer, 1991). Serum starvation can trigger Myc-expressing fibroblasts to undergo apoptosis and this can be abolished by overexpression of the anti-apoptotic proteins Bcl2 or Bcl-xL (Fanidi et al., 1992; Hueber et al., 1997). Bcl-xL overexpression synergises with Myc in oncogenesis by blocking Myc-induced apoptosis (Pelengaris et al., 2002).

The dependence of MYC-induced apoptosis upon BAX/BAK and its inhibition by BCL2 and BCL-xL suggest that MYC shares a unifying apoptotic mechanism with the BCL2 family. Understanding the molecular mechanisms underlying this apoptosis could provide new therapeutic avenues for treatment of MYC-driven cancers and those that have evaded apoptosis.

MYC and metabolism

As described above, MYC activates transcriptional programmes that promote cell growth and proliferation. Increasing cell growth requires increased metabolism and an essential component of the transcriptional programme of MYC, therefore, is the regulation of energetic and biosynthetic pathways to support cell growth. Fig 1.6 shows a summary of MYC target genes involved in metabolism.

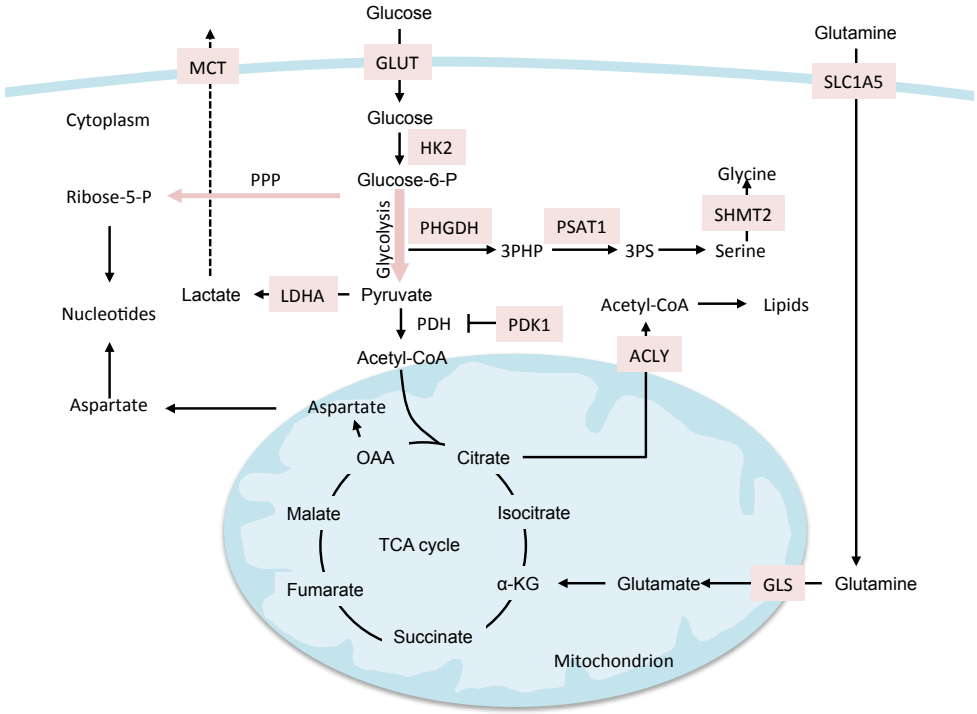


Figure 1.6. Key MYC target genes/pathways involved in metabolism (adapted from Stine et al., 2015)
Key metabolic pathways driven by MYC, including glycolysis, pentose phosphate pathway, serine synthesis, glutaminolysis, and nucleotide and lipid biosynthesis. Direct MYC target genes are shown in red shading.

Glycolysis

In growing cells, the expression of glucose and amino acid transporters are increased in order to support glycolysis and glutaminolysis for energy production and biosynthesis (Vander Heiden, 2011; Cantor and Sabatini, 2012; Dang, 2012). Glucose is imported into the cell and is subsequently phosphorylated by hexokinase to form glucose-6-phosphate (G6P) and G6P is then rearranged into fructose 6-phosphate (F6P) by glucose phosphate isomerase. F6P is phosphorylated by phosphofructokinase 1 (PFK-1) to form β-D-fructose 1, 6-bisphosphate (F1, 6BP) which is subsequently split into the 3-carbon molecules dihydroxyacetone phosphate (DHAP), and glyceraldehyde 3-phosphate (G3P) by fructose-bisphosphate aldolase (ALDO). G3P is further converted to pyruvate via 3- and 2-phosphoglycerate (3PG and 2PG) and phosphoenolpyruvate (PEP). Glycolysis results in a net gain of 2

moles of ATP and reduction of 2 moles of NAD^+ to NADH per mole of glucose. G6P is also metabolised into the pentose phosphate pathway (PPP) for the production of NADPH for reductive biosynthetic reactions and ribose-5-phosphate for nucleotide biosynthesis. The glycolytic intermediate 3PG is a substrate for the synthesis of lipids, as well as a precursor for serine and glycine biosynthesis. In growing cells, a significant amount of pyruvate is converted to lactate, a phenomenon known as aerobic glycolysis or the Warburg effect (Warburg, 1956). The shunting of pyruvate to lactate, catalyzed by lactate dehydrogenase (LDH), is necessary for the rapid regeneration of NAD^+ from NADH. This NAD^+ is required for continued activity of glyceraldehyde 3-phosphate dehydrogenase (GADPH), one of the intermediate steps of the glycolytic pathway, to maintain glycolytic flux for cytosolic ATP production (Le et al., 2010).

Pyruvate can be further oxidised in mitochondria through its conversion to acetyl-CoA, which combines with oxaloacetate to produce citrate for subsequent metabolism in the tricarboxylic acid (TCA) cycle. Citrate can also be exported to the cytosol and converted to acetyl-CoA by ATP citrate lyase (ACLY) for fatty acid synthesis. Pyruvate dehydrogenase (PDH), which converts pyruvate to acetyl-CoA, is a key regulatory step in the utilisation of pyruvate in the mitochondria. PDH is regulated by pyruvate dehydrogenase kinases (PDKs), which phosphorylate and inhibit PDH activity (Kim et al., 2006; Papandreou et al., 2006).

MYC upregulates most genes involved in glycolysis, starting from the glucose transporter GLUT1 (Osthus et al., 2000). MYC can also bind to the promoter and activate the expression of lactate dehydrogenase A (LDHA) that generates lactate from pyruvate to maintain glycolytic flux (Shim et al., 1997). Inhibition of lactate export by the MYC target monocarboxylate transporter (MCT1) has been shown to reduce cell growth and tumourigenesis (Doherty et al., 2014; Brahimi-Horn et al., 2011), indicating that LDHA supports MYC-induced transformation. In contrast, MYC reduces mitochondrial fates of glucose through induction of pyruvate dehydrogenase kinase-1 (PDK1) and the M2 isoform of pyruvate kinase (PKM2). PDK1 inhibits PDH by phosphorylation, stopping conversion of pyruvate to acetyl-CoA (Kim et al., 2007). MYC has also been shown to promote RNA splicing leading

to the expression of PKM2, which slows the catalytic conversion of phosphoenolpyruvate to pyruvate (David et al., 2010). Induction of PDK1 and PKM2 allow glucose-derived carbon to be used for biosynthetic pathways, rather than being metabolised in the mitochondrion for energy (Chaneton and Gottlieb, 2012).

In addition to induction of glycolytic genes and their regulators, MYC has also been shown to promote metabolic flux through carbon-utilising pathways. It has been shown that lymphocytes harbouring deregulated MYC exhibit increased flux through glycolysis and the pentose phosphate pathway (Wang et al., 2011) and MYC expression also increased labeling of ribose and purine nucleotides from ^{13}C-containing glucose (Morrish et al., 2009). Moreover, MYC can induce flux from 3PG towards the synthesis of serine and glycine, promoting donation of 1-carbon units to folate in a pathway which is essential for nucleotide biosynthesis, methionine metabolism and glutathione synthesis. In this pathway, phosphoglycerate dehydrogenase (PHGDH), which converts 3PG to 3-phosphohydroxypyruvate (3PHP), and phosphoserine aminotransferase 1 (PSAT1) that converts 3PHP into 3-phosphoserine (3PS), are both induced by MYC (Vazquez et al., 2011). Serine hydroxymethyltransferase 2 (SHMT2), which converts serine to glycine, is an established MYC target and has been shown to partially rescue the growth of Myc null rat fibroblasts (Nikiforov et al., 2002).

In summary, MYC promotes high metabolic flux through glycolysis and pathways that diverge from it, thereby providing growing cells with an important source of ATP as well as biosynthetic precursors for the synthesis of nucleotides and other key metabolites.

Glutaminolysis

In addition to glucose uptake and metabolism, MYC also stimulates glutamine consumption and catabolism. MYC was found to induce glutamine transporters SLC1A5 and SLC7A5 for glutamine import (Wise et al., 2008). Glutaminase (GLS) converts glutamine to glutamate, which feeds into the TCA cycle and glutathione synthesis and acts as the major intracellular amine donor for many transamination reactions: it has been shown that Myc induces *Gls* in mouse embryonic fibroblasts

(MEFs) (Wise et al. 2008). Another study in a P493-6 B-cell model of human Burkitt's lymphoma showed that mitochondrial GLS protein levels were increased by MYC. The mechanism for this was identified as occurring through the repression of microRNA miR23a/b leading to the elevation of GLS expression (Chang et al., 2008; Gao et al., 2009).

Glutamine can also provide carbon for the TCA cycle intermediates necessary for oxidative phosphorylation and mitochondrial ATP production in MYC. In growing B cells, both glucose and glutamine contribute carbons to TCA cycle intermediates (DeBerardinis and Cheng, 2010; Le et al., 2012), whilst metabolic stable heavy-isotope tracer studies confirmed that MYC increases glutaminolysis (Murphy et al., 2013). MYC sensitises cells to glutamine-deprivation-induced apoptosis, indicating that it promotes dependence upon glutamine (Yuneva et al., 2007). However, the mechanism of MYC-induced apoptosis triggered by glutamine withdrawal remains unclear.

Nucleotide biosynthesis

MYC drives nucleotide biosynthesis through multiple pathways. As described above, MYC drives the pentose phosphate pathway leading to ribose 5-phosphate production, thereby promoting synthesis of purine and pyrimidine nucleotides. Furthermore, MYC promotes glycine synthesis, which feeds one-carbon units into the purine synthesis pathway via folate. MYC also induces the expression of the multifunctional gene **c**arbamoyl phosphate synthetase 2, **a**spartate transcarbamylase and **d**ihydroorotase (CAD), which encodes the rate-limiting enzyme of pyrimidine synthesis (Miltenberger et al., 1995)，and dihydroorotate dehydrogenase (DHODH) that converts dihydroorotate to orotic acid, a precursor for pyrimidine synthesis (Liu et al., 2008). Glutamine donates its amide group in both pathways of nucleotide biosynthesis and is required for the production of aspartate via the TCA cycle (Zhang et al., 2014; Sullivan et al., 2015). Aspartate, in turn, is a substrate for CAD in the pyrimidine synthesis pathway and also donates the amine group that converts inosine monophosphate (IMP) to adenosine monophosphate (AMP) in the purine synthesis pathway.

Lipid metabolism

Membrane genesis is essential for growing cells and, accordingly, MYC plays a key role in stimulating fatty acid synthesis. Citrate generated from pyruvate is exported into the cytosol and converted by ATP citrate lyase (ACLY) to acetyl-CoA. Cytosolic acetyl-CoA is then converted to malonyl-CoA by acetyl-CoA carboxylase (ACACA). Both of these enzymes have been shown to be induced by MYC (Morrish et al., 2008). Fatty acid synthase (FASN), which catalyses fatty acid chain elongation, and stearoyl-CoA desaturase (SCD), which introduces double bonds to form unsaturated fatty acids, are also both induced by MYC (Zeller et al., 2003; Loven et al., 2012).

Ribosome biogenesis

Regulation of ribosome biogenesis is perhaps the core and most ancient function of MYC, since increased protein synthesis is absolutely required to support cell proliferation (van Riggelen et al., 2010). MYC regulates multiple stages of ribosome biogenesis (reviewed by van Riggelen et al., 2010). It directly regulates the RNA pol I-dependent transcription of ribosomal RNA (rRNAs) (Grandori et al., 2005; Arabi et al., 2005), the RNA pol III-dependent transcription of the 5S rRNA (Gomez-Roman et al., 2003) and the transcription of ribosomal proteins through RNA pol II-dependent transcription (Schlosser et al., 2003). MYC promotes the transcription of genes required for the processing of rRNA precursors and transport of mature ribosomal subunits, most importantly, nucleolin (NCL) and nucleophosmin (NPM1) (Watson et al., 2002). MYC also regulates mRNA translation through the transcription of translation initiation factors (Schmidt, 2004). By regulating both ribosome biogenesis and translation, MYC exerts control over cellular protein production.

Intriguing links have been identified between MYC-driven tumourigenesis and longevity. It has been shown that *Myc* haploinsufficient ($Myc^{+/-}$) mice exhibit increased lifespan compare to $Myc^{+/+}$ mice (Hofmann et al., 2015). Downregulation of ribosomal proteins and ribosome biogenesis genes and decreased translation rates were found in $Myc^{+/-}$ mice and these correlated with the longevity of mammalian

healthspan. In Eμ-Myc transgenic mice, loss of one allele of the core ribosomal proteins Rpl24 or Rpl38 decreased the occurrence of lymphoma by 20% and delayed tumour onset by over 100 days (Barna et al., 2008). This study suggests an opposing relationship between MYC and growth promotion on one hand and tumour suppression and longevity on the other.

Mitochondrial biogenesis

As described above, the many biosynthetic programmes driven by MYC require a great deal of energy and the mitochondrion is by far the most efficient cellular source of ATP. Accordingly, MYC has been shown to increase cellular mitochondrial content through direct activation of many genes involved in mitochondrial biogenesis (Morrish et al., 2003; Li et al., 2005; Zhang et al., 2007; Kim et al., 2008). Induction of MYC expression is accompanied by increased mitochondrial mass and expression of PGC-1β, a coactivator of mitochondrial biogenesis (Zhang et al., 2007). Knockdown of PGC-1β by siRNA diminished the increase of mitochondrial mass and O_2 consumption driven by MYC (Zhang et al., 2007). MYC has been shown to regulate both mitochondrial fission and fusion proteins in order to keep high levels of organelle turnover associated with its promotion of increased mitochondrial mass (Graves et al., 2012). The transferrin receptor TFRC, which imports iron, is a critical MYC target gene (O'Donnell et al., 2006) and iron is essential for mitochondrial biogenesis because of its key role in the function of iron-sulfur cluster and heme-containing proteins. MYC also induces the expression of C1QBP and p32, which are involved in mitochondrial protein synthesis (Fogal et al., 2010). Knockdown of p32 diminishes mitochondrial function and respiration and results in decreased cellular proliferation and remarkably diminished tumourigenesis.

As part of a coordinated programme for cell growth and proliferation, MYC drives a number of biosynthetic programmes, including nucleotide biosynthesis for globally elevated transcription and ribosome biogenesis for protein translation, placing tremendous energetic demand upon the cell. In order to maintain energetic homeostasis, MYC upregulates glucose transporters and glycolytic enzymes, promotes high metabolic flux through glycolysis and diverts glucose-derived carbon

into biosynthetic pathways, and at the same time induces expression of glutamine transporters and glutamine usage to maintain the TCA cycle for ATP production. Mitochondrial biogenesis ensures that the growing cells are adequately powered by both ATP production and increased biosynthetic flux through mitochondria (Li et al., 2005).

Glutamine metabolism in cancer

Glutamine, as a source of carbon and nitrogen to support biosynthesis, energy production and cellular homeostasis, is a critical metabolite for cell survival and growth, especially for cancer cells. Major glutamine metabolism pathways are summarized in Figure 1.7.

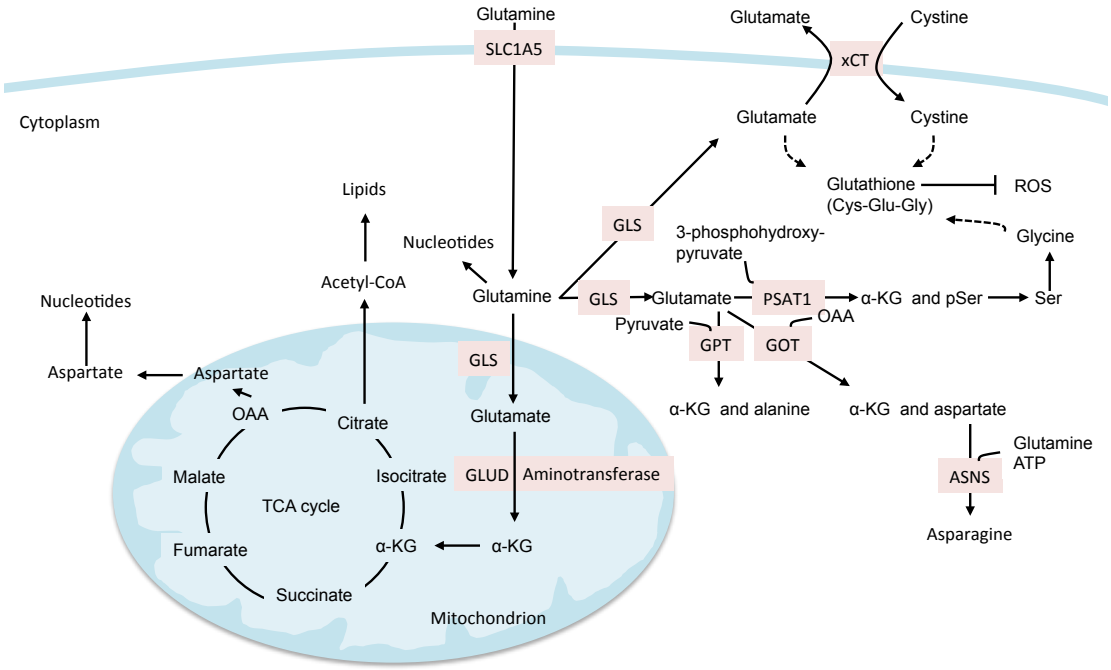


Figure 1.7. Major metabolic and biosynthetic fates of glutamine (adapted from Altman et al., 2016).
Glutamine is imported via SLC1A5 and other transporters and then enters a complex metabolic network by which its carbon and nitrogen are supplied to multiple pathways that promote cell survival and growth. Glutaminase (GLS) converts glutamine to glutamate, with release of the amide nitrogen as ammonia, whilst other glutamine-deaminating enzymes directly donate nitrogen to nucleotide biosynthesis (reviewed in Lane and Fan, 2015). Key enzymes discussed in the text are shown in red shading.

Glutamine is transported into cells through transporters such as SLC1A5, and can then be further metabolised or exported back out by antiporters in exchange for other amino acids (reviewed in Bhutia et al, 2015). Upon entry into cells, glutamine can be converted by glutaminase (GLS) to glutamate (Curthoys and Watford, 1995), which

is further catabolized to α-ketoglutarate (α-KG) through one of the two groups of enzymes, glutamate dehydrogenases (GDHs) or aminotransferases/transaminases (TAs) (Moreadith and Lehninger, 1984). α-KG then enters the TCA cycle to generate ATP through oxidative phosphorylation (Moreadith and Lehninger, 1984). Alternatively, α-KG can proceed backwards through the TCA cycle to produce citrate that supports acetyl-CoA and lipid synthesis (Metallo et al., 2012), although this alternative direction only occurs under conditions of mitochondrial metabolic perturbation. TAs are present in both the cytoplasm and the mitochondria and transfer nitrogen from glutamate to other organic acids to produce their corresponding amino acid. Thus glutamine-pyruvate transaminase (GPT), glutamate-oxaloacetate transaminase (GOT) and phosphoserine aminotransferase 1 (PSAT1) transfer nitrogen from glutamate to pyruvate, oxaloacetate and 3-PHP in the production of alanine, aspartate and phosphoserine, respectively. Aspartate is a key precursor for nucleotide biosynthesis and is required for generation of asparagine through asparagine synthetase (ASNS) in an ATP-consuming reaction that uses glutamine as the nitrogen donor. Phosphoserine supports the synthesis of serine and glycine, both important for one carbon metabolism and cellular antioxidative capacity. Glutamine-derived glutamate also contributes to the synthesis of glutathione (Welbourne, 1979) which neutralises ROS. Glutamate can be exchanged for cystine through the xCT antiporter, which has been shown to be important in various cancers and has been considered as a drug target (Ishimoto et al., 2011; Timmerman et al., 2013) and cysteine, which is rapidly produced from cystine, is joined by glutamate and glycine through sequential steps to form glutathione. Thus glutamine is an extraordinarily pleiotropic nutrient, providing carbon and nitrogen for multiple biosynthetic, energetic and reductive pathways.

Clinical applications of glutamine

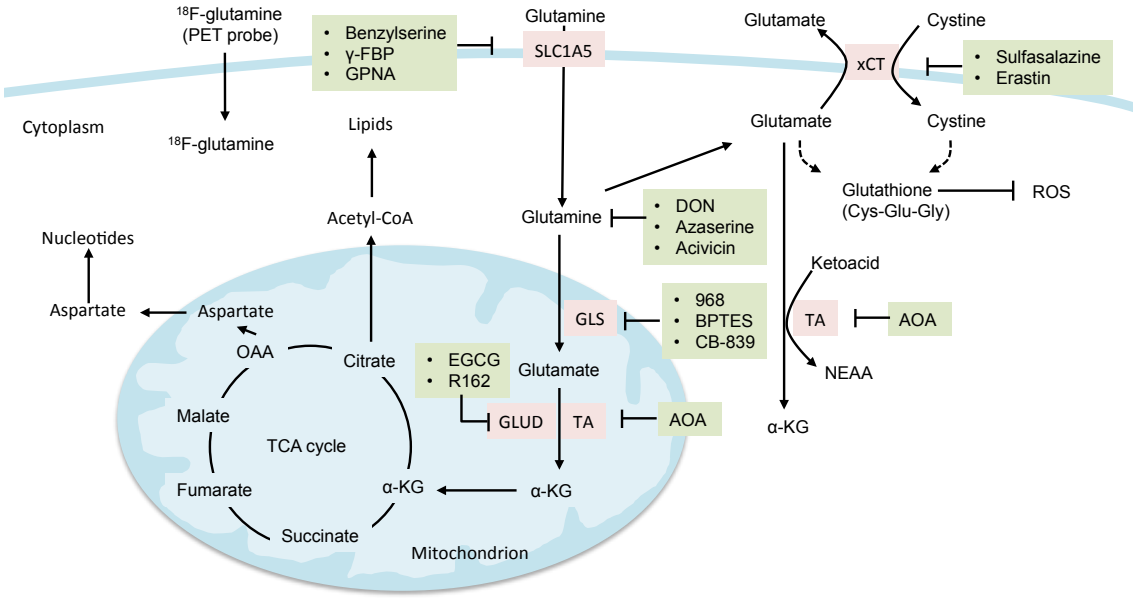


Figure 1.8. Glutamine metabolism as a target for cancer therapy and a tool for diagnostic imaging. (adapted from Hensley et al., 2013 and Altman et al., 2016)
^{18}F-labeled analogs of glutamine are under development as PET probes for localisation and prediction of glutamine dependence of tumour tissue. Key enzymes involved in glutamine metabolism are shown in red shading. Inhibitors that target various aspects of glutamine metabolism are shown in green shading. DON, 6-diazo-5-oxo-L-norleucine; NEAA, nonessential amino acids; OAA, oxaloacetate; TA, transaminase; 968, compound 968; α-KG, α-ketoglutarate; γ-FBP , γ-folate binding protein; GLS, kidney-type glutaminase; GLUD, glutamate dehydrogenase; GPNA, L-γ-glutamyl-p-nitroanilide.

The central role of glutamine in key metabolic pathways in cancer cells renders it an appealing target for clinical strategies to detect, monitor and treat cancer. Reprogrammed cancer metabolism can be used to image tumours and [^{18}F] (2S, 4R) 4-fluoroglutamine (^{18}F-FGln), which can be taken up by tumours, was developed as a potential tumour imaging tracer due to the relatively long half-life of ^{18}F. It has been validated both *in vitro* and *in vivo* (Ploessl et al., 2012; Lieberman et al., 2011) and ^{18}F-FGln positron emission tomography (PET) has since been assessed clinically and shown as a valuable tool in the clinical management of glioma (Venneti et al., 2015). Methods to image or quantify glutamine metabolism *in vivo* would be useful to

predict glutamine dependence of different tumours and their therapeutic response to inhibitors of glutamine metabolism (Rajagopalan and DeBerardinis, 2011).

As summarized by Brian J. Altman et al (Altman et al., 2016), there are many classes of compound that target glutamine metabolism, from targeting the plasma membrane transporters to the conversion to glutamate and further down to α-KG. Although most of the compounds are still in the preclinical stage or have been limited by toxicity, CB-839, an inhibitor of GLS, has shown promise in preclinical studies (Jacque et al., 2015; Gross et al., 2014) and is currently under study in several clinical trials.

Cells can acquire several mechanisms for glutaminase independence that lead to resistance to GLS inhibition. However, the multiple roles of glutamine in supporting cancer cell metabolism such as energy production, macromolecular synthesis and ROS homeostasis make GLS inhibition a potential candidate for combination therapy that sensitises cells to other treatments (reviewed by Altman et al., 2016). An increasing body of work has been done on identifying treatments that are synthetically lethal with inhibition of glutamine metabolism. Specific inhibition of the anti-apoptotic protein BCL2 synergizes with GLS inhibition leading to induction of apoptosis in acute myeloid leukemia (Jacque et al., 2015). It has been suggested that glutamine depletion in MYC-transformed cells induces apoptosis through ATF4-dependent PUMA and NOXA induction (Qing et al., 2012). ATF4 activation by agonists cooperates with inhibitors of glutamine metabolism in inducing apoptosis *in vitro* and inhibiting tumor growth *in vivo* (Qing et al., 2012). Glutamine deprivation can result in energy depletion while MYC constitutively drives transcription and translation (described in detail in Chapter 3). The resulting lack of energy supply for protein translation may result in protein mis-folding and ER accumulation, leading to ER stress pathway activation and induction of ATF4.

Understanding the mechanisms underlying the glutamine dependence of cancer cells should enable the identification of new anticancer treatments and new candidates for combination therapies based upon inhibition of glutamine metabolism.

Class	Drug	Status
Glutamine mimic	• DON • Azaserine • Acivicin	•Off-target effect on nucleotide biosynthesis • Limited by toxicity
Glutamine depletion	L-Asparaginase	•Off-target toxic conversion of glutamine to glutamate • Limited by toxicity • FDA-approved to treat ALL
GLS inhibitors	968	Preclinical tool
	BPTES	Preclinical tool
	CB-839	Phase I clinical trial
SLC1A5 inhibitors	• Benzylserine • γ-FBP • GPNA	Preclinical tools
GLUD inhibitors	EGCG	Tool compound
	R162	Preclinical tool compound
Aminotransferase inhibitors	AOA	• Clinically used to treat tinnitus • Toxic at higher doses
SLC7A11 or xCT system inhibitors	Sulfasalazine	FDA approved for arthritis
	Erastin	Tool compound, induces iron-dependent ferroptosis

Table 1.1. Strategies to target glutamine metabolism in cancer pharmacologically (reproduced from Altman et al., 2016).

ALL, acute lymphoblastic leukaemia; AOA, aminooxyacetate; DON, 6-diazo-5-oxo-l-norleucine; FDA, US Food and Drug Administration; γ-FBP , γ-folate binding protein; GLS, kidney-type glutaminase; GLUD, glutamate dehydrogenase; GPNA, L-γ-glutamyl-p-nitroanilide.

Metabolic profiling

Gene-expression studies (transcriptomic) or protein profiles (proteomic) have led to identification of new tumour subtypes, as well as transcriptional and protein biomarkers for diagnostic/prognostic purposes in cancer. Metabolic activity can also be quantified, as various analytical tools have been developed to measure concentrations of low-molecular-weight metabolites. Mass spectrometry can be used to characterise the metabolic profile of cells, tissues or organisms. With the rapid development of LC-MS, global metabolites can be analysed increasingly accurately and quickly. Perhaps more important from a clinical perspective is the cost required to perform comprehensive metabolite profiling: this too is dropping on a yearly basis, raising the possibility of biopsy-based (or even intraoperative) decision making on therapeutic approaches in patients. Through detecting changes in the

metabolic network, metabolomic approaches offers a particularly sensitive method to monitor changes in biological systems that can provide important information about tumourigenesis and reveal new therapeutic targets (Griffin and Shockcor, 2004).

Understanding one of the hallmarks of cancer, how cells resist apoptosis, has been an important topic for decades and would certainly be beneficial for cancer therapy. Another newly added hallmark, the reprogramming of energy metabolism in cancer cells, is an area of increasing focus. Previous studies indicate the roles of the BCL2 protein family and MYC in metabolism. However, whether or not their role in metabolism is connected to their apoptotic function remains unclear. The lack of systematic studies of the metabolic roles of the BCL2 family using current mass spectrometric technology and the unsolved mechanism for MYC-induced apoptosis together lead to the main goal of my thesis - to discover the metabolic basis of BCL2 family-mediated MYC-induced apoptosis.

Our hypothesis is that MYC-induced apoptosis is caused by imbalance of energy supply and demand. Chapter 3 shows MYC-overexpressed cells drive the energetic demand and suffer from energy crisis upon glutamine withdrawal. We found that adenlyte kinase 2 regulates cellular energy charges and therefore protects MYC-induced apoptosis. Chapter 4 explores the role of oxidative stress in MYC-induced apoptosis. The results indicate the protective role of glutamine is not primarily through production of glutathione but there is still a component of ROS involved in MYC-induced apoptosis. Chapter 5 studies the metabolic functions of the BCL2 family. Our data support a model in which energy supply and demand are key determinants of apoptosis regulated by BCL2 family.

Chapter 2 - Materials and Methods

Cell culture

All cell lines were maintained in humidified incubators at 37°C and 5% CO_2. HEK293ET human embryonic kidney cells were a kind gift of Dr. Felix Randow at the MRC Laboratory of Molecular Biology, Cambridge. Cells were cultured in Dulbecco's modified Eagle's medium (DMEM) supplemented with 10% fetal bovine serum (FBS).

MRC5 early passage primary human lung fibroblasts were obtained from the European Collection of Authenticated Cell Cultures (ECACC) via Public Health England. Cells were cultured in DMEM supplemented with 10% FBS. MRC5 cells were immortalized by transduction of retroviral hTERT, followed by retroviral infection with vectors pM6P-blast/pM6P-puro (kind gift of Dr. Felix Randow, MRC Laboratory of Molecular Biology, Cambridge UK) containing target genes of interest.

Murine lymphoma cells were extracted from the lymph nodes of Eμ-Myc mice. After CO_2 euthanasia, lymph nodes were dissected, minced in PBS, and filtered through a 35μm nylon mesh. Single cell suspensions of freshly extracted lymphoma cells were plated on irradiated (30 Gy) or mitomycin C treated feeder layer (106 NIH-3T3 cells/2.4-cm plate) in 45% Iscove's Modified Dulbecco's Medium (IMDM), 45% DMEM, 10% FBS, 1% penicillin and streptomycin, 4mM L-glutamine, and 25μM 2-mercaptoethanol.

Table 2.1. Culture Media

Reagent	Supplier	Catalog No.
DMEM	Thermo Fisher	41965
FBS	Thermo Fisher	10270-106
Penicillin and streptomycin	HGU	
L-glutamine(200mM)	Thermo Fisher	25030
IMDM	Thermo Fisher	12440
DMEM, no glucose, no glutamine, no phenol red	Thermo Fisher	A14430
Krebs-Ringer Solution, bicarbonate-buffered	Alfa Aesar	J67591
Vitamin mix	Sigma	M6895
2-mercaptoethanol	Sigma	M6250
Mitomycin C	Sigma	M0503

Construction of retroviral expression vectors

Either cDNA from HEK293ET cells or plasmids of the genes of interest were used as template for cDNA synthesis by polymerase chain reaction. cDNA of genes of interest were cloned into the retroviral vector pM6P-puro/pM6P-blast.

Polymerase chain reaction (PCR)

PCR was carried out on an Applied Biosystems VeritiTM Thermal Cycler. DNA was amplified using the following general reaction mixture (Table 2.2 and Table 2.3)

Table 2.2. PCR reaction setup

Component	Volume
DMSO	5% when use cDNA as tempelete
Pfu turbo	1 µl
10xPfu Buffer	5 µl
10 mM dNTP	1 µl
Primer Mix	1 µl (final conc.= 0.3 uM each)
DNA template	70 µg plasmid/850 µg cDNA
ddH_2O	to 50 µl

Table 2.3. Routine PCR cycling progamme

Segment	Cycle	T/°C	Time
1	1	94	2 min
2	30	94	30 sec
		55	45 sec
		72	1 min/kb
3	1	72	10 min

Samples were then held at 4°C before removal from the cycler and storage at -20°C. PCR products were checked for correct sizing by DNA agarose gel electrophoresis and were subsequently purified using a QIAGEN PCR purification kit.

Digestion

Purified PCR products were digested by specific restriction enzymes (New England Biolabs) and then loaded for DNA agarose gel electrophoresis. DNA fragments were extracted from the gel using the QIAquick Gel Extraction kit.

Ligation

T4 DNA ligase (New England Biolabs) was used for the ligation of target genes into retroviral vectors according to the manufacturer's instructions.

Transformation

The ligation products were used directly for transformation into XL10-Gold Ultracompetent Cells or DH10β Max efficiency competent cells. Colonies were selected on agar plates with 100 μg/ml of Ampicillin and were picked for DNA miniprep and sequencing. Sequencing was performed by the MRC Human Genetics Unit sequencing service.

Table 2.4. Constructs cloned (√ means successfully generated by myself)

	BAX	BAK1	BIM	BCL2	MCL1
pM6P-puro	√	√	√	√	√
pM6P-blast	√	√	√	√	√
	BCL-xL	SOD2	GPX1	PRDX3	AK2
pM6P-puro	√	√	√	√	√
pM6P-blast	√	√		√	

Construction of retroviral shRNA vectors

shRNA constructs were designed and cloned into the pSUPER-retro-puro vector (OligoEngine, VEC-PRT-0002) following the pSUPER-retro-puro protocol from OligoEngine.

Table 2.5. shRNA sequence for target genes

Target gene	Sequence
Ak2-a	CCGGGAAATGGTTGTGGAGCTAATTCTCGAGAATTAGCTCCACAA CCATTTCTTTTTG
Ak2-b	CCGGGATAAGGAGACATGGTATTATCTCGAGATAATACCATGTCTC CTTATCTTTTTG
Ak2-c	CCGGGAAACTGGTGAGTGACGAAATCTCGAGATTTCGTCACTCA CCAGTTTCTTTTTG
Ak2-d	CCGGCCGGTCCTACCATGAGGAATTCTCGAGAATTCCTCATGGTA GGACCGGTTTTT
Ak2-e	CCGGGAAACTGGTGAGTGACGAAATCTCGAGATTTCGTCACTCA CCAGTTTCTTTTT

Lentiviral shRNA vector

Lentiviral shRNA plamids (MISSION® TRC shRNAs) were obtained from Sigma and used for lentiviral shRNA knockdown of target genes.

Table 2.6. List of lentiviral shRNA plamids

Target gene	Supplier	Catalog No.
AK2-1	Sigma	TRCN0000315319
AK2-2	Sigma	TRCN0000315321
AK2-3	Sigma	TRCN0000315322
AK2-4	Sigma	TRCN0000006024
AK2-5	Sigma	TRCN0000006026

Retroviral/lentiviral production and infection

Transfection for production of viral particles

The production of viral particles was carried out by transfection of HEK293ET cells. For lentiviral production the cells were transfected with the packaging vector

psPAX2, the envelope vector pMD2.G encoding the protein VSV-G (Addgene) and the viral transfer vector. For retroviral production, pGag-Pol was used instead of psPAX2. Typically, 10 μg of each plasmid was mixed with 80 μl of 1μg/μl polyethyleneimine (PEI), incubated at room temperature for 20 minutes before adding DMEM to a final volume of 500 μl. This mix was added to a 75 cm^2 flask of HEK293ET cells at 70% confluence containing 10 ml of DMEM/10% FBS and incubated overnight. The following day, the medium was replaced with fresh culture medium. 24 hours after that, the viral supernatant was harvested and used for infection.

Viral transduction

The viral supernatant was mixed with polybrene (hexadimethrene bromide) at a final concentration of 5 μg/ml. The viral mix was diluted with DMEM/10% FBS to the desired concentration, filtered through a 0.45 μm filter unit and used to infect the recipient cells at 40% confluence. 24 hours post-infection the medium was replaced with fresh viral mix and after another 24 hours the cells were split into selection in the appropriate antibiotic. Puromycin was used at 1-2 μg/ml and blasticidin at 5 μg/ml for a period of 4-6 days, until all uninfected control cells had died.

siRNA transfection

DharmaFect 1 transfection reagent (Dharmacon) was used to deliver Dharmacon SMARTpool siRNA mix by reverse transfection at 30 nM final concentration. 3000 cells and 0.1 μl of transfection reagent were used per well for 96-well plates and 1x10^5 cells and 2 μl of transfection reagent per well were used for 6-well plates.

Table 2.7. List of siRNA SMARTpools

No.	siRNA
1	ON-TARGETplus Non-targeting Pool siRNA
2	ON-TARGETplus Human BAX(581) siRNA
3	ON-TARGETplus Human BAK(578) siRNA
4	ON-TARGETplus Human BIM(10018) siRNA
5	ON-TARGETplus Human AK1 (203) siRNA
6	ON-TARGETplus Human AK2 (204) siRNA
7	ON-TARGETplus Human AK3 (50808) siRNA
8	ON-TARGETplus Human AK4 (205) siRNA
9	ON-TARGETplus Human AK5 (26289) siRNA
10	ON-TARGETplus Human AK7 (122481) siRNA
11	ON-TARGETplus Human AK8 (158067) siRNA
12	ON-TARGETplus Human AK9 (221264) siRNA
13	ON-TARGETplus Human GPX1 (2876) siRNA
14	ON-TARGETplus Human PRDX3 (10935) siRNA

Western Blotting

Cells were washed once with PBS before lysis in cell lysis buffer on ice for 5 minutes. Cell lysates were then centrifuged for 5 minutes at 13000 rpm and 4°C to remove insoluble material. Protein was quantified using a Pierce™ BCA protein assay kit (ThermoFisher) according to the manufacturer's guidelines. Protein samples mixed with 6x protein sample buffer were boiled for 10 minutes at 95°C and analyzed by SDS-PAGE. 20-40 μg protein was loaded per well onto 8-16% nUView Tris-Glycine Precast Gels (NuSep) and separated on the gel in running buffer at 100-170V. Proteins were transferred to transfer membrane (Immobilon-P, pore size 0.45 μm) in transfer buffer at 0.32 mA for 20 minutes per gel. The membranes were incubated in blocking buffer (5% skimmed milk in TBST) for one hour at room temperature. Membranes were then incubated overnight on an orbital shaker with primary antibody diluted in blocking buffer at 4°C. Primary antibody was washed off from the membranes by TBST three times before incubating with the appropriate HRP-linked secondary antibody diluted in blocking buffer for an hour. The membranes were washed another three times in TBST before proteins were detected using the SuperSignal West Pico chemoluminescent reagent (ThermoFisher) and imaging (Bio-RAD, Chemi-Doc MP Imaging system).

Table 2.8. Buffers for West blotting

Substance	Composition
TBS-Tween	10 mM Tris (pH 7.5), 154 mM NaCl, 0.5% Tween
Cell lysis buffer	20 mM Tris (pH 7.5), 100 mM NaCl, 5 mM MgCl2, 0.5% IGEPAL
Running buffer	2.5 mM Tris, 19.2 mM glycine, 0.01% SDS
Transfer buffer	2.5 mM Tris, 19.2 mM glycine, 10%Methanol

Table 2.9. List of antibodies used

Reagent	Supplier	Cat No.	Dilution
Anti-Bcl2 antibody	Abcam	ab18210	1:1000
Anti-Bcl-xL/S [EPR16642] antibody	Abcam	ab178844	1:1000
Mcl-1 Antibody (S-19)	Santa cruz	sc-819	1:500
Bax (N-20) rabbit polyclonal antibody	Santa Cruz	sc-493	1:1000
Bak NT rabbit polyclonal	Millipore,	2370748	1:625
Bim Rabbit mAb #2933	Cell signaling	C34C5	1:500
GPX1 rabbit monoclone antibody	Abcam	ab108427	1:1000
Anti-Peroxiredoxin 3 antibody [EPR8115]	Abcam	ab128953	1:10000
Anti-SOD2 antibody	Abcam	ab13533	1:3000
Anti-AK2 Antibody	Atlas	HPA018479	1:400
Anti-AK4 Antibody	Atlas	HPA049461	1:500
β-actin Mouse Monoclonal	Proteintech	60008-1-Ig	1:5000
Anti-Mouse-HRP	Cell signaling	7076S	1:1000
Anti-Rabbit Immunoglobulins/HRP	DAKO	P0399	1:1000

qPCR

qPCR primers were designed using the Primer3web (version 4.0.0) online tool (Untergasser et al. 2012; Koressaar and Remm, 2007). Primers were designed to span exon/exon boundaries to ensure only mRNA was amplified.

Table 2.10. Sequences of qPCR primers

Gene ID	Forward	Reverse
AK1	CACTGCTGCTGTATGTGGAC	GGTCTCCTCATTGTCGTCCA
AK2	TGGTAGTGGAGCTCATTGAGA	CATTTCTGCCTGCCTCACA
AK3	AAACAACGCCTTACTGCTCG	AGTCAGGTCATCAATGCCCA
AK4	CTTGCGGGAGAACATCAAGG	CGGACATCATTAGGCGTGTG
AK5	ACACATCTCTCAACTGGCGA	CCAGGTCTCCACGTTCCATA
AK6	ACAAGGAAGAAATCGTGCATCA	CTTTGATCCACTGCTCAATCCA
AK7	GAGGCTCAGTCAATTCCCCT	AATCAACAGGGTCTTCGGGT
AK8	CAGTGGGAAAAGTCTGCAGG	AAACGTGGTCCTATCTGCCA
AK9	TCGTGTTGAAGCTTTGCCAA	GGAATGCTTTGACCGCTGAT

Cells were scraped in PBS, centrifuged at 6000 rpm and used fresh or frozen at -80 °C for later processing. RNA was extracted using RNeasy Mini kit (Qiagen) and reverse-transcribed using qScript cDNA Supermix (Quanta Biosciences) according to the manufacturer's protocol (Table 2.11, 2.12). qPCR was performed on a StepOne RT-PCR system (ThermoFisher) using Sybr Select Master Mix (Life Technologies) and the primers for genes of interest (Table 2.13, 2.14). A threshold was established in the linear phase of the amplification plot, and the log Ct (the number of cycles to reach the threshold) for each sample was used for quantification. During setup of qPCR methods, melt curves for the reactions were used to assess primer quality.

Table 2.11. Mix for reverse transcription of cDNA

Components	Volume
RNA	0.5 µg
5x qScript cDNA Supermix	4 µl
RNAse-free H_2O	to 20 µl

Table 2.12. PCR progamme for reverse transcription of cDNA

Segment	Cycle	T/°C	Time
1	1	25	5 min
2	1	42	30 min
3	1	85	5 min
4		4	Inf.

Table 2.13. qPCR mix

Components	Volume
cDNA	1 µl
Primers	0.8 ul from each 5 µM primer stock
2xSYBR selection master mix	10 µl
H_2O	to 20 µl

Table 2.14. qPCR program

Segment	Cycle	T/°C	Time
1	1	95	10 min
2	40	95	15 sec
		60	30 sec
		75	15 sec
3	1	95	15 sec
4	1	60	1 min
5	1	95	15 sec

Apoptosis assay

Cells were seeded in 6-well plates for different treatments (where stated). For determination of apoptosis, floating cells in medium were collected by centrifuging at 6000 rpm and attached cells were trypsinised and collected into the same tube. Pellets were resuspended in 100 µl binding buffer (BD Bioscience) with 5 µl annexin V-FITC and 5 µl propidium iodide stock (BD Bioscience FITC Annexin V Apoptosis Detection Kit). Data were acquired using a BD Accuri flow cytometer and analysed using FlowJo software, reporting single- and double-positive populations as apoptotic.

IncuCyte

Cells were seeded in 96-well plates for different treatments (where stated). 5 µM Caspase-3/7 Reagent (Essen bioscience, Cat No. 4440) was added at the end of treatment. Plates were placed into the IncuCyte® live-cell analysis system, 4 images were taken per well every 2 or 3 hrs for up to 48 hrs and analysed by IncuCyte ZOOM software. Percentage of apoptosis area was calculated by apoptotic cell confluence divided by phase cell confluence.

EU transcription assay

Click-iT RNA Alexa Fluor 488 HCS Assay (Thermo Fisher) was performed for determination of global transcription. Cells were seeded in 96-well plates, triplicate wells for each condition, treated as described, incubated with 5-ethynyl uridine (EU) for an hour before fixation using 3.7% formaldehyde in PBS followed by a 0.5% Triton® X-100 permeabilization step. Alexa Fluor azide was added for EU detection. Cells were then washed with Click-iT reaction rinse buffer and counterstained with DAPI. Images were taken using the ImageXpress Micro XLS Widefield High-Content Analysis System (Molecular Devices LLC, CA). Analysis was performed using the software MetaXpress 5.1.0.46 (Molecular Devices). EU incorporation was calculated by the average FITC intensity of each nucleus in a 5x5 image grid from each well.

Metabolites extraction and metabolomic analysis

Metabolite extraction

Metabolites were extracted from 6-well plates by washing individual wells with ice-cold PBS and addition of cold extraction buffer (50% methanol, 30% acetonitrile, 20% water solution at -20°C or lower) to each well for 10 seconds. Extracts were clarified and stored at -80°C until required. Remaining cells were fixed and stained with DAPI for normalization purposes. Cell numbers were counted using the ImageXpress (as for EU incorporation above) and calculated by the sum of the DAPI count of each well.

LC-MS

LC-MS was carried out using a 100 mm x 4.6 mm ZIC-pHILIC column (Merck-Millipore) using a Thermo Ultimate 3000 HPLC inline with a Q Exactive mass spectrometer. A 32 min gradient was developed over the column from 10% buffer A (20 mM ammonium carbonate), 90% buffer B (acetonitrile) to 95% buffer A, 5% buffer B. 10 µl of metabolite extract was applied to the column equilibrated in 5% buffer A, 95% buffer B. Q Exactive data were usually acquired in negative mode (although positive/negative switching were also used) and standard ESI source and spectrometer settings were applied (typical scan range 75-1050). Metabolites were identified based upon m/z values and retention time matching to standards.

Analysis

Xcalibur is a data processing software suite provided with the Thermo scientific LC-MS system. It provides tools for method setup, data acquisition, data processing and reporting. Processing methods were setup for metabolites of interest so that the LC/MS samples could be analysed in a targeted manner. Following data processing, excel files were exported containing peak areas for each specified metabolite in all of the samples. For the purpose of analysis, isotopologs were considered as separate metabolites. For untargeted analysis of metabolomic datasets, SIEVE v2.1(Thermo scientific) and XCMS (Smith et al. 2006) were used. They compare samples between

two biological conditions. The output highlights ions that have different intensity between the two biological conditions. These ions were then further analysed for peak integrity by inspection of chromatograms and assigned metabolite IDs by accurate mass and standard retention time. Targeted analyses using Xcalibur were carried out on the ions and related pathways highlighted by untargeted analysis. Metabolites identified in the study were validated by accurate mass and retention time in order to meet the reporting requirement for non-novel metabolite identification for chemical analysis (Sumner et al., 2007; Sumner et al., 2014).

Seahorse mitochondrial function analysis

Cells were seeded at 12000/well in Seahorse V7 plates and 4-OHT was added to all wells on the following day. After a further 24 hours incubation, glutamine was withdrawn (where stated) for 12 hrs before the plate was placed in a Seahorse XF-24 analyzer (Seahorse Bioscience) for mitochondrial stress tests. Four inhibitors were added in the following order: 1μM Oligomycin (ATP synthase inhibitor), 2 μM FCCP (MMP uncoupler), 2 μM Antimycin (complex III inhibitor), 2 μM Rotenone (complex I inhibitor) to determine the functional status of mitochondria.

Statistical analysis

Student's T-tests was used to compare sample conditions consisting of at least three biological replicates. For all experiments, p-values ≤ 0.05 were considered to be significant, as indicated by a single asterisk (*).

Chapter 3 - Metabolic changes during MYC-induced apoptosis

MYC drives a number of biosynthetic programs, including nucleotide biosynthesis for globally elevated transcription and ribosome biogenesis for protein translation, placing huge energetic demand upon the cell (Sabò et al., 2014; Kress et al., 2015). MYC deregulation sensitises cells to apoptosis induced by different triggers, such as death receptor ligands TNF (Klefstrom et al., 1994) or TRAIL (Lutz et al., 1998) and withdrawal of serum (Evan et al., 1992) or glutamine (Yuneva et al., 2007).

Normal human lung fibroblasts MRC5 were transduced with pM6P-blast empty vector (VEC) or pM6P-blast-MYC-ER^{T2} (MYC). In the presence of 4-OHT, MYC-ER^{T2} is activated and translocates to the nucleus to function. MYC-activated cells were highly sensitive to glutamine withdrawal (Fig 3.1).

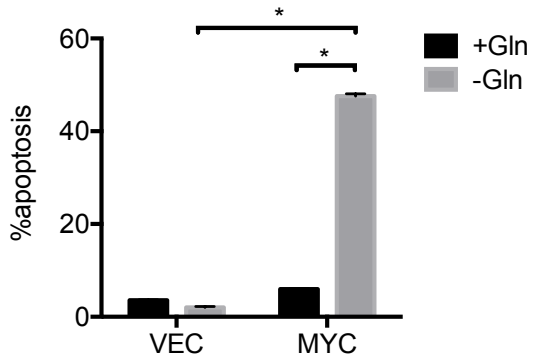


Figure 3.1. Glutamine withdrawal sensitises MYC-activated cells to apoptosis. MRC5 cells expressing MYC-ER^{T2} or VEC were stimulated for 24 hrs with 200 nM 4-OHT and glutamine was then withdrawn for 16 hrs. Apoptosis was assessed by Annexin V/PI staining and flow cytometry (n=3). Data are mean ± SEM of triplicate wells for each condition in one representative experiment.

Glutamine is a pivotal biosynthetic substrate, and is involved in a variety of metabolic pathways. One might predict similar effects on MYC-activated cells of deprivation of other amino acids, many of which are utilized in biosynthetic pathways in addition to protein translation. To test whether other amino acids could induce apoptosis in MYC cells, 15 amino acids were omitted individually from the tissue culture medium. Krebs-Ringer Solution was used as base medium and glucose,

FBS, vitamin mix and amino acids were added back. Only glutamine withdrawal induced apoptosis that was specific for MYC-activated cells (Fig 3.2). Both MYC and VEC could not survive without cystine, but this was at a later time point compared to glutamine. The role of cystine in GSH synthesis is discussed in Chapter 4. Thus, of all of the amino acids provided in DMEM, the apoptotic response of MYC-activated cells is specific to glutamine withdrawal.

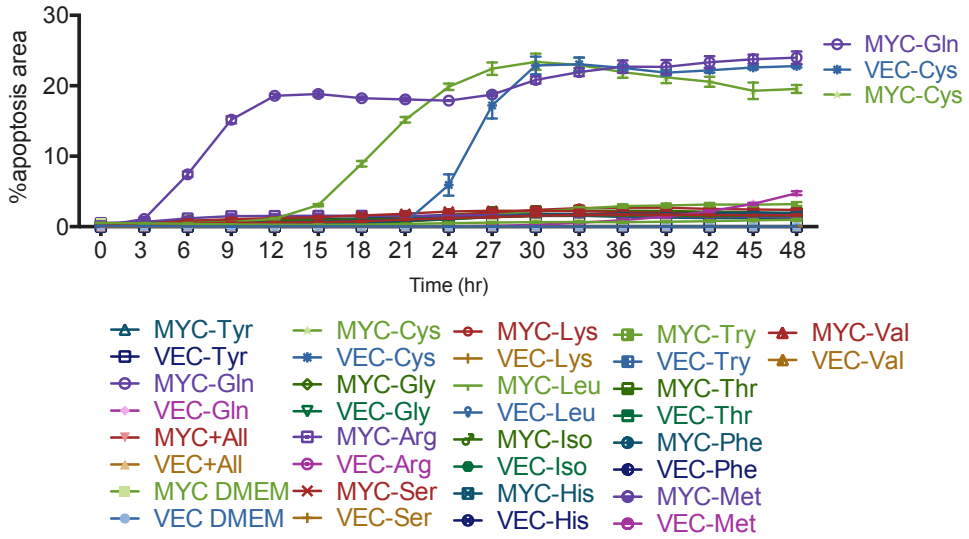


Figure 3.2. Glutamine starvation induces apoptosis specifically in MYC.
MRC5 cells (MYC-ER^{T2}) were treated with 4-OHT for 24 hrs. DMEM was then changed to medium that was deficient in the indicated amino acids. Cell viability was measured every three hours using the IncuCyte live-cell analysis system for 2 days with 5μM Caspase3/7 apoptotic reagent (n=2). Percent apoptosis area of each condition was calculated as outlined in materials and methods. Data are mean ± SEM of triplicate wells for each condition in one representative experiment.

MYC drives continued demand for transcription and translation after withdrawal of glutamine

Glutamine is required for nucleotide and amino acid biosynthesis and its withdrawal is expected to impact upon transcription and translation.

Ethenyluridine (EU) incorporation was used to measure global transcription in the cell. Both VEC and MYC cells reduced their transcription upon glutamine withdrawal, whilst MYC activation led to an increase in transcription under

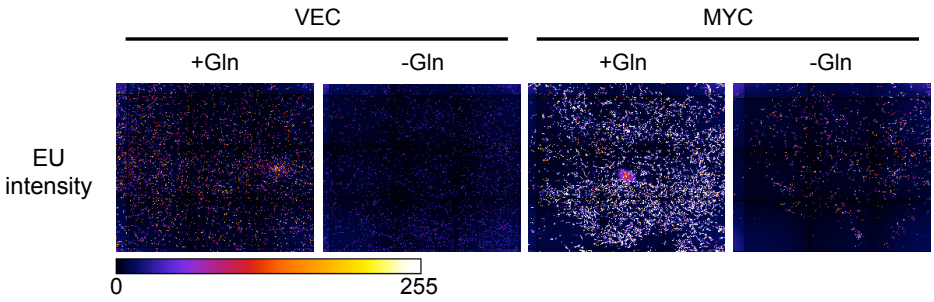
conditions either with or without glutamine (Fig 3.3 a,b). MYC activation even maintained the global transcription under glutamine withdrawal to a similar level as VEC under normal growth condition (Fig 3.3 a,b). Thus, despite the absence of glutamine as an essential precursor for nucleotide biosynthesis, MYC drives continued demand for nucleotides to support transcription.

VEC or MYC cells treated with 4-OHT for 24 hrs were pulsed with $^{13}C_6$, $^{15}N_2$-lysine for 6 hours. Cells were then collected for shotgun proteomic analysis to assess global translation. The values of heavy to light protein indicate for the extent of protein translation during the labelling period. Among the labeled samples, the translational rate was decreased in both MYC and VEC upon glutamine withdrawal (Fig 3.3 c), as expected considering the role of glutamine in protein synthesis. As with transcription, MYC had a higher translational rate than VEC irrespective of whether glutamine was present or not (Fig 3.3 c). This indicates that even though translation is impaired upon glutamine withdrawal, MYC continues to drive translation, in addition to transcription.

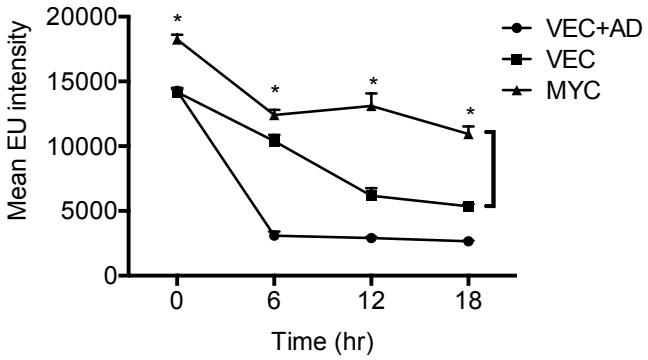
Transcription and translation are energy-consuming processes and therefore MYC sets up huge demand for nucleotides, amino acids and energy. In order to understand the metabolic impact of glutamine withdrawal on normal fibroblasts with MYC activation in an unbiased way, discovery-based (unbiased) relative quantitation of metabolites was applied. This technique allows for determination of relative metabolite changes in one sample group relative to other sample groups without prior knowledge of the metabolites involved. Signals corresponding to individual metabolite ions were integrated over the LC time scale and compared between runs. The Orbitrap-based Q Exactive mass spectrometer provided the high-resolution, accurate-mass measurements required for LC-MS relative quantitation experiments. The software SIEVE v2.1 (Thermo Scientific) for chapter 5 and XCMS (Smith et al. 2006) for chapter 3 were used to perform untargeted metabolomic analyses. This untargeted method is a powerful technique for identifying and quantifying relative changes in complex samples. Metabolites that have different abundances from control group were putatively identified by matching their accurate mass with that provided by METLIN (Smith et al., 2005). Xcalibur targeted quantitation software

(Thermo Scientific) was then applied to confirm the identification and provide relative quantitation of the metabolites. Metabolite identification was validated by accurate mass and retention time in order to meet the reporting requirement for non-novel metabolite identification (Sumner et al., 2007; Sumner et al., 2014). These applied to all the metabolites identified in the thesis.

a.



b.



c.

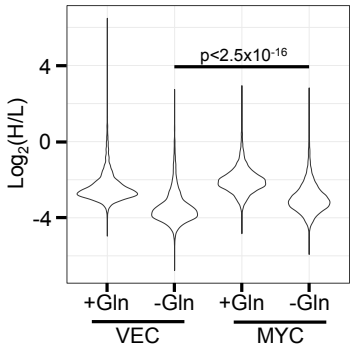


Figure 3.3. MYC maintains metabolic and energetic demand to support continued transcription and translation upon glutamine withdrawal.

a. MRC5 cells (VEC or MYC-ER^{T2}) were treated with 4-OHT for 24 hrs and glutamine was then withdrawn for 16 hrs. Cells were pulsed for 1 hr with 1mM ethenyluridine (EU) which is incorporated into nascent transcripts. EU incorporation was revealed by click chemistry with a fluorescent azide (n=3). Each one of the 4 photos in the figure is a composite of 9 separate images taken from one representative well from the 12 hr time point.

b. High content imaging was used to quantify EU incorporation at the stated times in MRC5 cells treated as above or with 500 μM actinomycin D (AD). Data are mean ± SEM of three wells in one representative experiment.

c. MRC5 cells were treated with 4-OHT for 24 hrs. Glutamine was then withdrawn and cells were pulsed with $^{13}C_6$, $^{15}N_2$-lysine for 6 hours (n=2). The figure shows the ratio of the heavy labeled protein to the light protein which indicates the translational rate of the cells. Cell pellets were collected and sent for shotgun proteomic analysis. *This was analysed by Dr. Jimi Wills.*

Glutamine withdrawal promotes nucleotide remodeling to a lower energy state

Changes in nucleotides upon glutamine withdrawal were picked up by untargeted metabolomic analyses. ATP levels were decreased in both VEC and MYC cells upon

glutamine deprivation (Fig 3.4 a). However, AMP and ADP levels were significantly increased only in MYC-activated cells (Fig 3.4 a). The changes were also seen in the other lower-energy nucleotides. Cellular energy status can be shown by cellular energy charge; NTP/NMP ratios shown by all four of nucleotides were depleted specifically in MYC without glutamine (Fig 3.3 b).

a.

b.

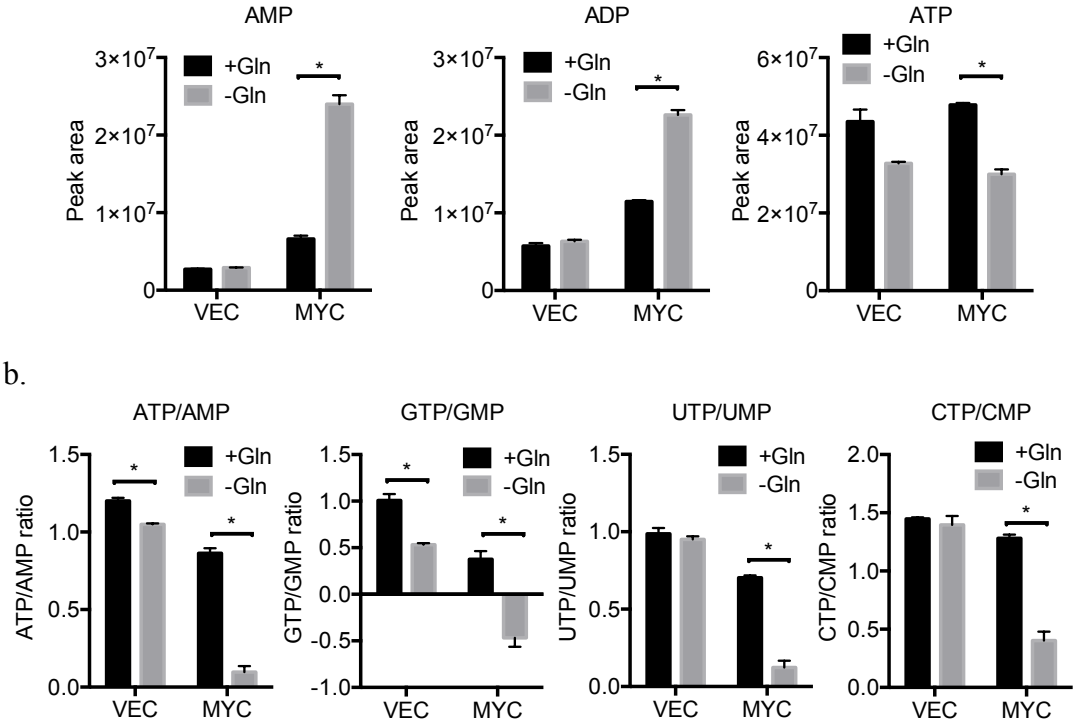


Figure 3.4. Glutamine withdrawal promotes nucleotide remodeling to a lower energy state.

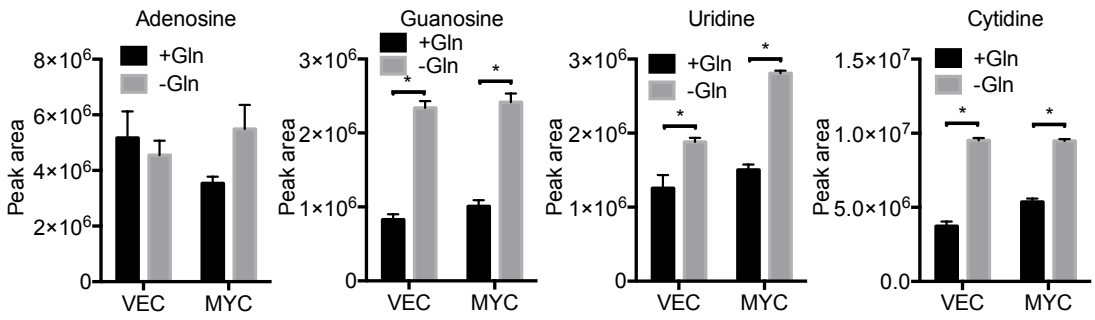
LC-MS was used to quantify levels of metabolites in MRC5 cells treated for 24 hrs with 4-OHT and glutamine was then withdrawn for 6 hrs (n=3). Data are mean ± SEM of triplicate wells in one representative experiment.

a. Histograms show levels of AMP (retention time, 13.92 min), ADP (retention time, 14.70 min) and ATP (retention time,15.37 min).
b. Histograms show levels of cellular energy charge (ratio of NTP/NMP). NTP/NMP ratio is calculated by $\log_2$(ratio).

Accumulation of nucleosides and bases indicates nucleotide catabolism

As there were clear changes in nucleotides, the levels of nucleosides and bases were also investigated. Nucleosides were accumulated upon glutamine withdrawal (Fig 3.5 a). Hypoxanthine and xanthine were increased after glutamine deprivation (Fig 3.5 b), other bases not shown were difficult to detect by LC-MS. Xanthine accumulation was correlated with the time of glutamine withdrawal specific in MYC-activated cells (Fig 3.5 b).

a.



b.

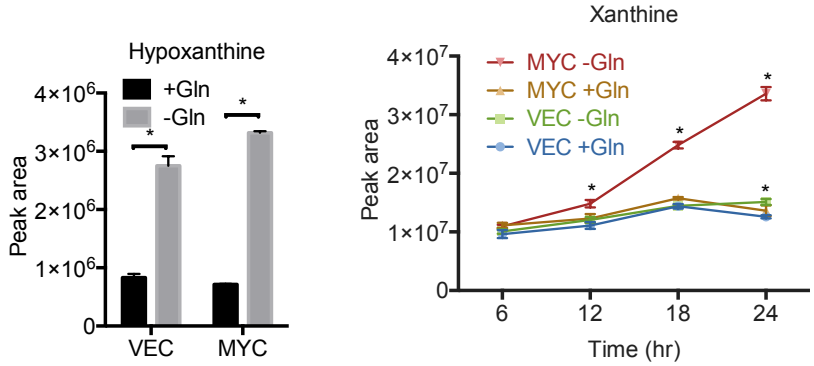


Figure 3.5. Accumulation of nucleosides and bases upon glutamine deprivation. LC-MS was used to quantify levels of metabolites in MRC5 cells treated for 24 hrs with 4-OHT and glutamine was then withdrawn for 6 hrs or as indicated in the figure (n=3). Data are mean ± SEM of triplicate wells in one representative experiment.

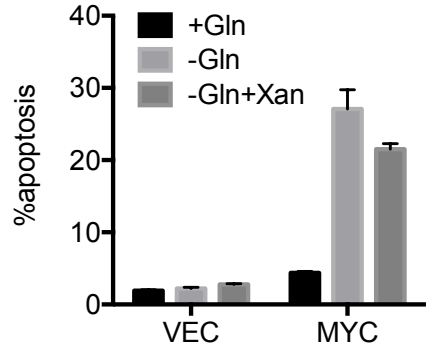
a. Histograms show levels of nucleosides.
b. Plots show levels of hypoxanthine and xanthine.

The accumulation of xanthine upon glutamine withdrawal correlates with MYC-induced apoptosis. In order to know whether xanthine is causative for apoptosis, exogenous xanthine was added to the cells at the point of glutamine withdrawal but no clear effect found on apoptosis was observed (Fig 3.6 a). Thus, xanthine accumulation is not causative for apoptosis.

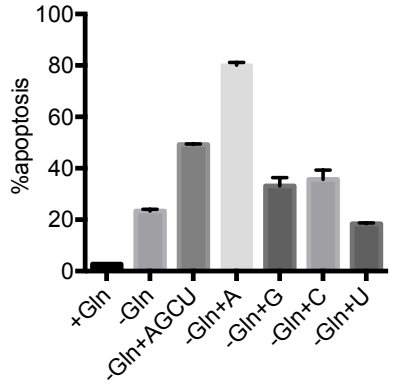
Glutamine supports nucleotide biosynthesis through energy generation and donation of carbon (via aspartate) and nitrogen. If loss of nucleotide biosynthesis was the cause of the apoptosis triggered by glutamine withdrawal, exogenous nucleosides should be able to rescue this. Nucleoside rescue experiments were performed to address this question. Addition of all four nucleosides enhanced MYC-induced apoptosis (Fig 3.6 b). Nucleosides were then added separately to the cells and adenosine enhanced apoptosis significantly, while the other three nucleosides had little effect on apoptosis (Fig 3.6 b). Importantly, none of them rescued apoptosis.

We further investigated the role of adenine nucleotides as exogenous adenosine had unique function among all the nucleosides. Exogenous AMP, ADP and ATP were added to MYC cells deprived of glutamine. AMP enhanced apoptosis to a similar level as adenosine (Fig 3.6 c). AMP could be converted to adenosine rapidly and could therefore enhance apoptosis through adenosine. However, cells have multiple adenosine receptors carrying out different functions which makes it difficult to predict a mechanism. Indeed, adenosine alone induced apoptosis in the presence of glutamine in MYC. Large amounts of adenosine and AMP may interfere with nucleotide catabolism and cellular energy charge which may contribute to apoptosis.

a.



b.



c.

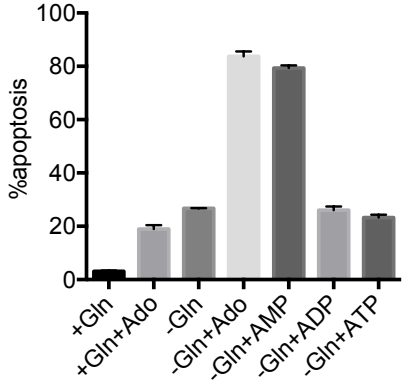


Figure 3.6. Effect of exogenous nucleosides and bases on MYC-induced apoptosis.
MRC5 cells (VEC or MYC-ER^{T2}) were treated with 4-OHT for 24 hrs and glutamine was then withdrawn for 16 hrs. Addition of (a) 1 mM xanthine, (b) nucleosides (1 mM singly or 250 μM each combined), (c) 1mM nucleotides as indicated in the figures. Apoptosis was assessed by Annexin V/PI apoptosis assay and flow cytometry (n=2). Data are mean ± SEM of triplicate wells in one representative experiment.

Addition of nucleosides was not able to rescue the apoptosis and their elevation under apoptotic conditions indicates nucleotide catabolism. Previously reports stated where nucleotide catabolism occurs include exercising skeletal muscle and hypoxia *in vivo* (Tullson and Terjung, 1991; Jennings and Steenbergen, 1985; Chouchani et al., 2014), both situations where energetic demand exceeds supply. When the rate of ATP hydrolysis exceeds the capacity of muscle fiber to phosphorylate ADP, the ADP and AMP levels increase, leading to the deamination of adenylates and their degradation to nucleosides and bases. The nucleotide catabolism and energy charge

depletion observed upon glutamine withdrawal clearly indicates energy shortage in MYC-activated cells. Accumulation of nucleosides and bases are markers for nucleotide catabolism, indicating insufficient energy supply during MYC-induced apoptosis.

Depletion of TCA cycle metabolites upon glutamine withdrawal

The energy shortage observed in MYC without glutamine led us to investigate the TCA cycle metabolites. Mitochondrial ATP is generated through oxidative phosphorylation driven by the TCA cycle. α-Ketoglutarate, fumarate and malate, major metabolites required for generation of mitochondrial NADH and ATP, were depleted upon glutamine withdrawal (Fig 3.7). This indicates that mitochondrial ATP generation is impaired and that the TCA cycle relies on glutamine in MRC5 cells. Aspartate, generated from glutamine and oxaloacetate by transamination, was also strongly decreased (Fig 3.7).

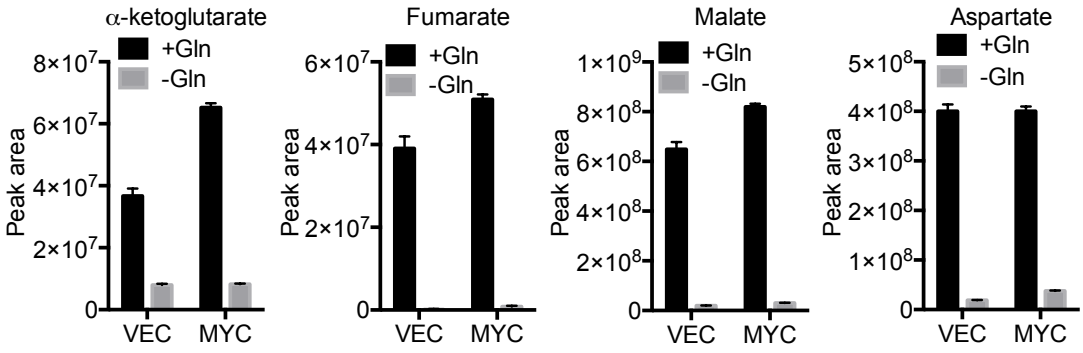


Figure 3.7. Depletion of TCA cycle metabolites upon glutamine withdrawal. MRC5 cells were treated for 24 hrs with 4-OHT and then glutamine was withdrawn for 6 hrs. Metabolites were extracted for LC-MS analysis (n=3). Histograms show levels of TCA cycle intermediates and aspartate. Data are mean ± SEM of triplicate wells in one representative experiment.

The MRC5 cells depend on glutamine for mitochondrial ATP production and glutamine withdrawal depletes cellular energy charge and triggers nucleotide catabolism, indicating insufficient energy supply. We hypothesise that glutamine withdrawal triggers MYC-induced apoptosis through a loss of energetic support.

Mitochondrial adenylate kinase 2 is MYC-regulated and protects from apoptosis

The catabolism of nucleotides is an indication of lack of energetic supply. However, the interconversion of nucleotides and nucleosides may be beneficial for cells to balance the accumulation of certain nucleotides. The enzyme adenylate kinase (AK) is important for ensuring maintenance of adequate levels of NTPs in cells such as liver and muscle. By constantly monitoring nucleotide levels inside the cell, AKs play an important role in cellular energy homeostasis (Dzeja and Terzic, 2009). The predominant reaction catalyzed by AKs is 2ADP ↔ AMP + ATP. AKs are present in both the cytosol and the mitochondria and assist the cell in remodeling and usage of nucleotides. Among the nine isoforms of AKs, AKs 2-4 are localized in the mitochondria. Since we found a correlation between mitochondrial ATP production and apoptosis, we examined whether the AKs are regulated by MYC. qPCR analysis shows that the expression of AKs 2-4 were strongly elevated upon MYC activation (Fig 3.8 a). Upregulation at the protein level was confirmed for AK2 and AK4 by western blotting (Fig 3.8 b). These results indicate that MYC activates the molecular machinery required for nucleotide interconversion or remodeling at the mitochondrion. Apoptosis was measured in cells in which AKs 1,2,3,4,5,7,8 and 9 were knocked down individually by siRNA during MYC activation and glutamine withdrawal. siRNAs targeting AK2 and AK5 enhanced apoptosis while knockdown of AK4 and AK8 rescued the apoptosis (Fig 3.9 a, b). As AKs catalyse reversible reactions and have different cellular localisations, it is not unexpected that different AKs may exert different effects on apoptosis. AK2 was the only mitochondrial AK whose knockdown protected from apoptosis and we hypothesised that AK2 plays a key role in nucleotide interconversion and remodeling to protect the mitochondrion from energy depletion.

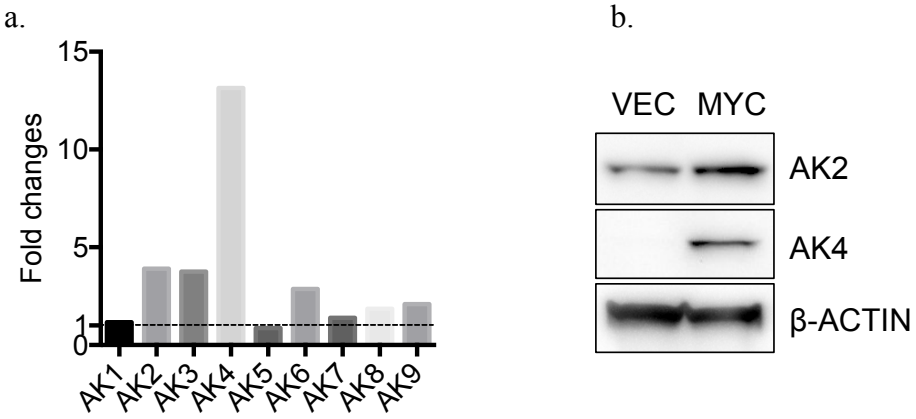


Figure 3.8. MYC induces expression of mitochondrial AKs.

a. Relative mRNA levels of the mitochondrial AKs measured by qPCR in MRC5 cells following 24hrs of MYC activation (n=2). Results are presented as fold-change of MYC to VEC normalised to β-ACTIN mRNA.

b. Protein levels of AK2 and AK4 were assessed by western blotting in MRC5 cells following 24 hrs of MYC activation.

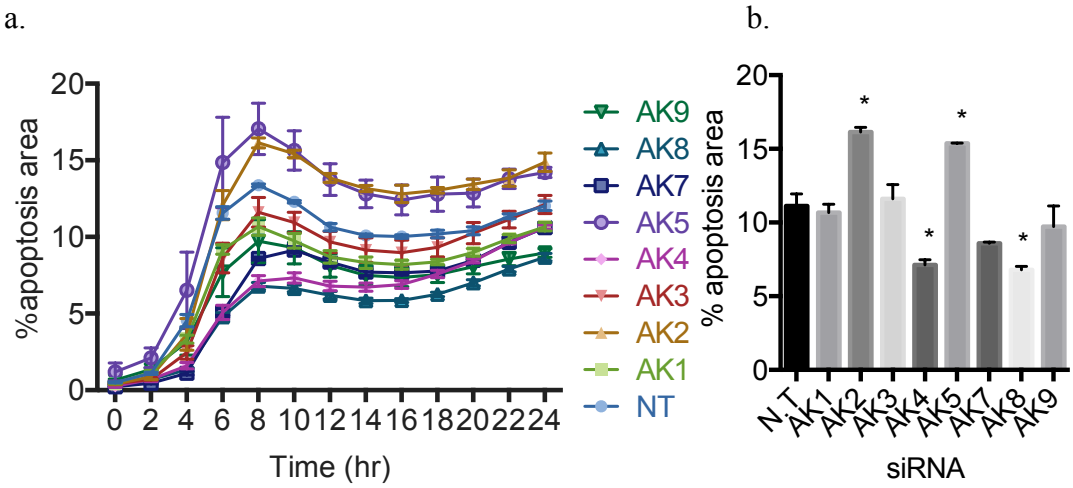


Figure 3.9. Effect of knockdown of AKs on MYC-induced apoptosis.

siRNAs were reverse transfected into MRC5 MYC-ER^{T2} cells following 24 hrs of MYC activation by 4-OHT. Glutamine was then withdrawn for 24 hrs. Cell viability was measured every two hours using the IncuCyte live-cell analysis system with 5μM Caspase3/7 apoptotic reagent. Percent apoptosis area of each siRNA was calculated as outlined in materials and methods (n=3). Data are mean ± SEM of triplicate wells for each condition in one representative experiment.

a. Plot shows the percent apoptosis area over 24 hours of glutamine withdrawal.

b. Histogram shows the percent apoptosis area at the 8 hr time point.

The enhancement of MYC-induced apoptosis by AK2 knockdown was further confirmed by the Annexin V/PI apoptosis assay (Fig 3.10 a). Parallel metabolomic analysis showed that ATP/AMP ratio was decreased upon AK2 knockdown (Fig 3.10 b). Furthermore, retroviral overexpression of AK2 rescued the apoptosis and energy charge depletion observed in MYC cells upon glutamine withdrawal (Fig 3.10 c, d). These results correlate with our hypothesis that AK2 plays an important role in nucleotide remodeling to protect the mitochondrion from energy depletion. AK2 is the only adenylate kinase localised in the mitochondrial intermembrane space and its main role is to convert ATP and AMP into 2 x ADP: the ADP can then be taken into the mitochondrial matrix where it is converted to ATP by the F_1F_O ATP synthase. Thus, although AK2 usually hydrolyses a single molecule of ATP, it leads to the net production of two molecules of ATP and it therefore acts to facilitate mitochondrial ATP production.

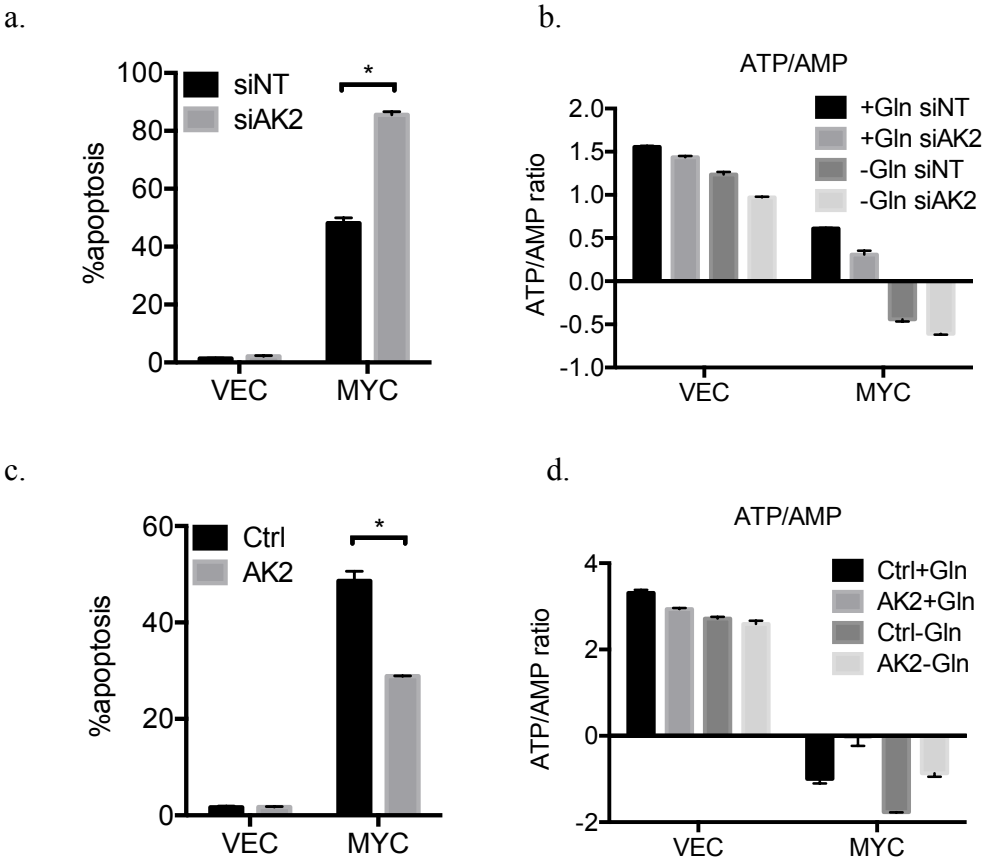


Figure 3.10. Effect of knockdown or overexpression of AK2 on MYC-induced apoptosis.

30 nM siRNA targeting AK2 was reverse transfected into MRC5 cells following 24 hrs of MYC activation by 4-OHT and glutamine was then withdrawn

a. for 16 hrs before apoptosis was assessed by Annexin V/PI apoptosis assay and flow cytometry (n=3).
b. for 6 hrs before metabolite extraction. ATP/AMP ratio is calculated by $\log_2$(ratio). *This experiment was performed by Joy Edwards-Hicks.*

MRC5 cells (VEC or MYC-ER^{T2}) overexpressing control vector or AK2 were treated with 4-OHT for 24 hrs and glutamine was then withdrawn

c. for 12hrs before apoptosis was assessed by Annexin V/PI apoptosis assay and flow cytometry (n=2).
d. for 6 hrs before metabolite extraction. ATP/AMP ratio is calculated by $\log_2$(ratio).

Data are mean ± SEM of triplicate wells for each condition in one representative experiment.

AK2 plays an essential role in helping the MYC-activated fibroblasts cope with energy shortage caused by glutamine withdrawal. If this system could be applied to a mouse model system, it would be more relevant to future clinical application. The Eμ-Myc transgenic mouse model carries a normal *Myc* gene coupled to the Ig heavy chain enhancer: the transgene is expressed exclusively in B-lymphoid cells (Harris et al., 1988). We wished to test whether manipulation of Ak2 would have an effect on the lymphoma development in Eμ-Myc mice. B lymphocytes were taken from Eμ-Myc mouse lymphoma, cultured and transduced with retroviral plasmids expressing shRNAs targeting Ak2. The transduced B lymphocytes were then triggered with glutamine deprivation and assayed for apoptosis. We expected to see enhancement of apoptosis with Ak2 knockdown and, if this was verified, we planned to inject the modified lymphoma cells back into mice to assess rate of lymphomagenesis. Unfortunately, the knockdown of Ak2 by shRNA was minimal (Fig 3.11) which led to very limited difference of apoptosis triggered by BPTES or glutamine withdrawal compared to control (Fig 3.12). The background apoptosis level was higher with Ak2 knockdown which may indicate that the cells were struggling with Ak2 loss and they may therefore have selected against the knockdown. Due to the poor knockdown of Ak2 in B lymphocytes and the inconclusive results, this experiment was not taken any further. We performed the same experiment in MRC5 cells but all of the cells transduced with shRNA targeting human AK2 could not survive.

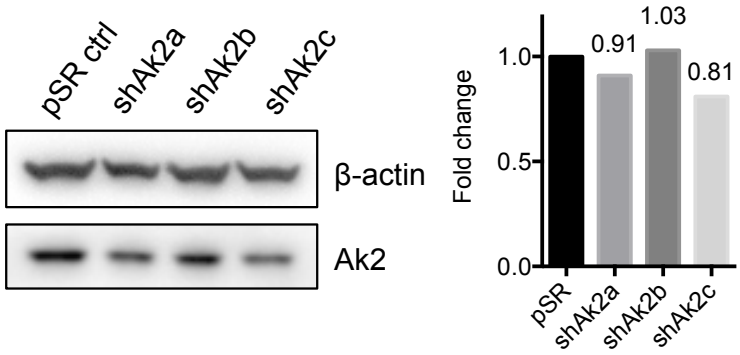


Figure 3.11. shRNA knockdown of Ak2 in B lymphoma cells.
Protein level of Eμ-Myc B lymphoma cells transduced with shRNA targeting Ak2 or control was determined by western blotting. Knockdown ratio of Ak2 to β-actin was analyzed by Image J.

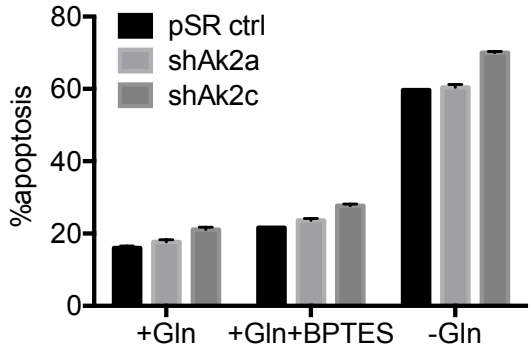


Figure 3.12. Effect of Ak2 knockdown on B lymphoma cells upon glutamine deprivation.
L-alanine, L-asparagine, L-aspartic acid, L-proline and pyruvate were added to DMEM lacking glutamine to replace the IMDM/DMEM media used for culture of Eμ-Myc B lymphoma cells. Media with 4 mM Gln or 5 μM BPTES was changed for 16 hrs. Apoptosis was measured by Annexin V/PI assay and flow cytometry (n=2). Data are mean ± SEM of triplicate wells for each condition in one representative experiment.

Summary

Glutamine withdrawal sensitises MYC-activated cells to apoptosis. As glutamine is an important amino acid involved in multiple biosynthetic and metabolic pathways, we employed metabolomic analyses in order to determine the effect of glutamine withdrawal in MYC-activated cells. Nucleotide catabolism, decrease of cellular energy charge and TCA cycle depletion were detected upon glutamine withdrawal, indicating insufficient energy supply. Elevated transcription and translation driven by MYC even in the absence of glutamine clearly shows MYC-driven demand for energy and other biosynthetic substrates. Nucleotide production from exogenous nucleosides could not rescue the apoptosis triggered by glutamine withdrawal, indicating that a lack of nucleotide biosynthesis was not responsible for the apoptosis. Therefore, imbalance of energetic supply and demand became our hypothesis of the molecular mechanism underlying MYC-induced apoptosis. Interconversion and remodeling of nucleotides by AK2 provided the cells with mitochondrial ATP, rescued the cellular energy charge and protected from apoptosis, further supporting our hypothesis.

Discussion

Yuneva et al. first discovered that IMR90 human fibroblasts overexpressing MYC are sensitive to glutamine withdrawal but the mechanism remains unclear (Yuneva et al., 2007). Cancer cell lines with MYC overexpression may already have other changes or lesions that could bring complexity to our study. Therefore, we chose a similar model as Yuneva et al.. We used normal human fibroblast MRC5 and activated MYC by 4-OHT to look at how MYC activation could have effect on cells undergoing glutamine withdrawal triggered apoptosis. We both found decrease in cellular ATP levels upon glutamine withdrawal, but our work discovered a huge increase in AMP, ADP levels in MYC. The decrease of cellular energy charge and elevated nucleotide catabolism clearly indicates energy crisis in MYC activated cells. Thus, we propose that energy imbalance leads to MYC-induced apoptosis. Qing et al. and Zhang et al. both suggested that ATF4 mediates MYC-induced apoptosis through ER stress (Qing et al., 2012; Zhang et al., 2014). This fits in well with our hypothesis. Energy shortage leads to unfolded protein responses, the disruption of TCA cycle leads to ROS accumulation, both contribute to ER stress and regulate ATF4. But the energy imbalance is still the key determinant of MYC-induced apoptosis.

Chapter 4 - Oxidative stress and MYC-induced apoptosis

As described in the introduction, oxidative stress is pro-apoptotic and BCL2 has been shown to protect cells from H_2O_2-induced oxidative death and suppress lipid peroxidation when overexpressed (Hockenbery et al., 1993). BAX expression in mammalian and heterologous models increases ROS generation and oxidative damage (Naderi et al., 2006). Thus, although we have shown that mitochondrial energetics play a key role in MYC-induced apoptosis, it is likely that there is a component of mitochondrial ROS in this process. We therefore examined mitochondrial ROS in more detail.

Glutathione depletion is not primarily the cause of MYC-induced apoptosis triggered by glutamine withdrawal

As mentioned in Chapter 3, glutamine is the only amino acid whose withdrawal from the culture medium triggered apoptosis specifically in MYC-activated cells. Withdrawal of cystine, the oxidised dimer of the amino acid cysteine, induced apoptosis in both VEC and MYC cells (Fig 4.1). Both glutamine and cysteine are precursors for the antioxidant glutathione (GSH) and therefore play an important role in reducing oxidative stress. Levels of GSH were measured upon glutamine or cystine starvation to assess how withdrawal of these amino acids might impact oxidative stress. After 6 hrs withdrawal of either amino acid, GSH levels dropped significantly (Fig 4.2 a). GSH was completely depleted after 18 hrs of cystine starvation but reasonable levels were maintained upon glutamine withdrawal at this time point (Fig 4.2 b). Without GSH, cells are likely to suffer from oxidative stress, which could lead to apoptosis. MYC was more sensitive than VEC as shown by the earlier onset of apoptosis elicited by cystine withdrawal (Fig 4.1). This may indicate that MYC sensitises cells to apoptosis under conditions of oxidative stress. The onset of apoptosis induced by glutamine withdrawal is much earlier than cystine regardless of the higher GSH level, indicating that GSH depletion is not primarily the cause of apoptosis triggered by glutamine withdrawal.

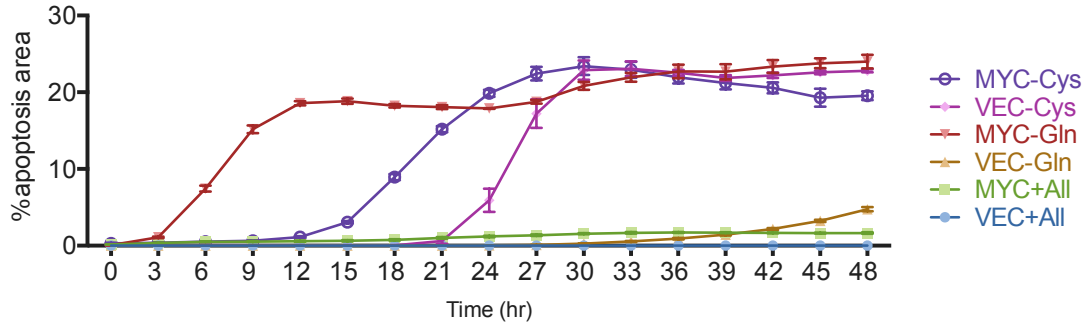
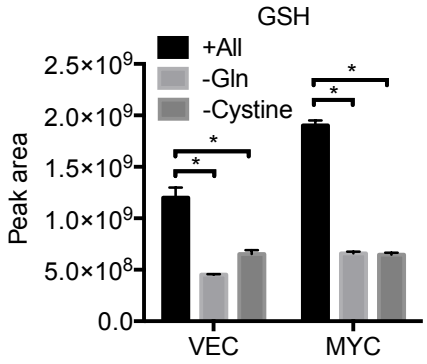


Figure 4.1. Effect of glutamine or cystine withdrawal on MYC-induced apoptosis.
MRC5 cells (VEC or MYC-ER^{T2}) were treated with 4-OHT for 24 hrs. DMEM was then changed to medium lacking glutamine or cystine. Cell viability was measured every three hours using the IncuCyte live-cell analysis system with 5 µM Caspase-3/7 apoptotic reagent for 2 days (n=2). Percent apoptosis area of each condition was calculated as outlined in materials and methods. Data are mean ± SEM of triplicate wells for each condition in one representative experiment. This figure is a reduced form of Fig 3.2.

a.



b.

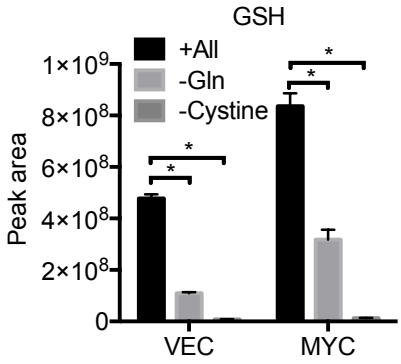


Figure 4.2. GSH levels upon glutamine or cystine withdrawal.
MRC5 cells (VEC or MYC-ER^{T2}) were treated with 4-OHT for 24 hrs and then transferred into medium lacking glutamine or cystine for (a) 6 hrs or (b) 18 hrs before metabolite extraction. Data are mean ± SEM of triplicate wells for each condition normalised to cell number.

Buthionine sulfoximine (BSO) is a sulfoximine that reduces levels of GSH by inhibiting glutamate-cysteine ligase (GCL), the enzyme that catalyses the first step of glutathione synthesis (Drew and Miners, 1984). BSO led to more efficient depletion of GSH than glutamine withdrawal, yet did not trigger apoptosis (Fig 4.3 a,

b). This confirms that GSH depletion is not primarily the cause of apoptosis in our system.

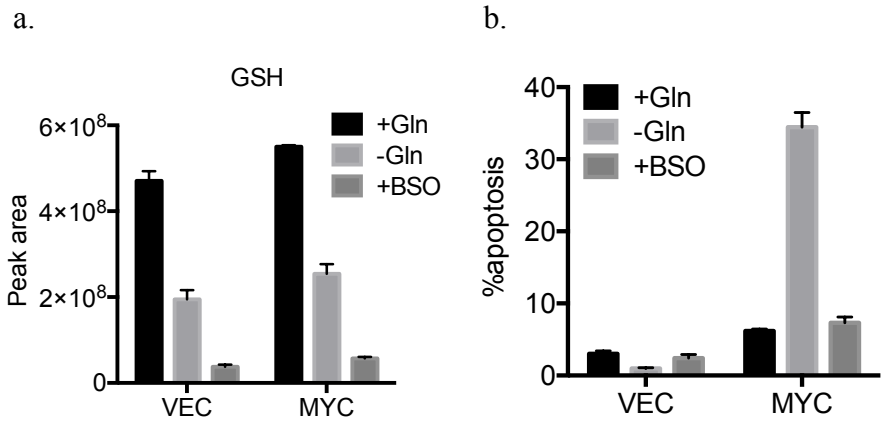


Figure 4.3. Effect of BSO treatment on apoptosis and GSH level.
MRC5 cells (VEC or MYC-ER^{T2}) were treated with 4-OHT for 24 hrs prior to transfer into medium containing 20 μM BSO or lacking glutamine. After a further 18 hrs, (a) metabolites were extracted for LC-MS or (b) apoptosis assays were carried out. Data are mean ± SEM of triplicate wells for each condition. *This experiment was performed by Dr. Heather Barker.*

Cystine starvation and BSO treatment both depleted GSH, but whilst 18 hrs cystine withdrawal induced cell death (Fig 4.1), BSO treatment for 18 hrs did not (Fig 4.3 a). It appears that BSO treatment is not as efficient as cystine starvation in depleting GSH and it is therefore possible that the oxidative stress triggered by BSO is insufficient to induce apoptosis. Even though depletion of GSH is not primarily the cause of glutamine withdrawal-triggered apoptosis, MYC did accelerate cystine-withdrawal triggered apoptosis, suggesting that oxidative stress can partially contribute to MYC-induced apoptosis.

Mitochondrial control of oxidative stress

Oxidative stress is caused by the imbalance of ROS generation and the ability to detoxify ROS or repair the damage. One major source of the ROS production is the electron transport chain in the inner mitochondrial membrane. Mitochondrial antioxidant enzymes therefore play an essential role in keeping cellular oxidative

stress in check. Figure 4.4 illustrates the mitochondrial control of oxidative stress. In order to investigate further the role of oxidative stress during MYC-induced apoptosis, antioxidant enzymes were perturbed by pharmacological or genetic tools.

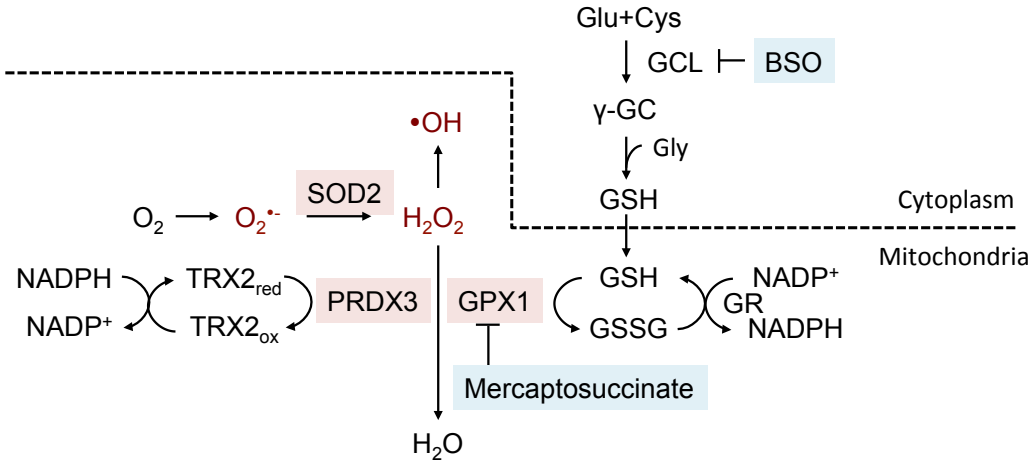


Figure 4.4. Mitochondrial control of oxidative stress.
The schematic diagram illustrates the pathways through which oxygen can be converted to either water or ROS by antioxidant enzymes and the pathway of GSH synthesis from glutamate, cysteine and glycine. Antioxidant enzymes are shown in red shading. Inhibitors are shown in blue shading. Reactive oxygen species that may cause damage are in dark red. SOD2, superoxide dismutase 2; GPX1, glutathione peroxidase 1; GR, glutathione reductase; PRDX3, mitochondrial peroxiredoxin; TRX2, mitochondrial thioredoxin shown in reduced and oxidized forms; GCL, glutamate-cysteine ligase.

Superoxide dismutases, thioredoxins, peroxiredoxins and glutathione peroxidases are enzymes involved in the clearance of superoxide anion and hydrogen peroxide. Glutathione peroxidase 1 (GPX1) is the most abundant among the GPX family and localises to both cytoplasm and mitochondria (Lubos et al., 2011). It encodes the major mitochondrial GPX in mouse liver (Esworthy et al., 1997) and is an important antioxidant enzyme clearing hydrogen peroxide in mitochondria. Mercaptosuccinate is one of the most effective and widely used inhibitors to GPX1 and it exerts its inhibitory effects through competition with GSH for binding to the active site of the enzyme (Chaudiere et al., 1984). BSO alone as described above did not trigger MYC-induced apoptosis. Mercaptosuccinate alone mildly promoted apoptosis in MYC-expressing cells, but the combination of BSO and mercaptosuccinate led to

robust apoptosis that matched that triggered by glutamine withdrawal (Fig 4.5). These data suggest that ROS can trigger MYC-induced apoptosis under certain conditions.

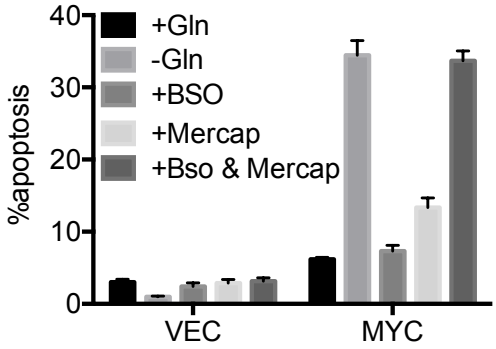


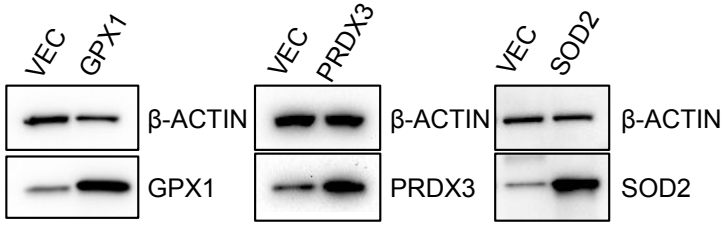
Figure 4.5. Effect of BSO and/or mercaptosuccinate treatment on MYC-induced apoptosis.
MRC5 cells (VEC or MYC-ER^{T2}) were treated with 4-OHT for 24 hrs and then transferred into medium containing 20 μM BSO, 100 μM mercaptosuccinate or lacking glutamine. After a further 18 hrs, cells were harvested for apoptosis assay. Data are mean ± SEM of triplicate wells for each condition. *This experiment was performed by Dr. Heather Barker.*

In addition to pharmacological regulation of ROS, the major mitochondrial antioxidant enzymes were overexpressed or knocked down to assess whether this could impact upon MYC-induced apoptosis triggered by glutamine withdrawal.

Constructs of retroviral vector pM6P-blast with GPX1, mitochondrial superoxide dismutase SOD2 or mitochondrial peroxiredoxin PRDX3 were cloned and transduced into pM6P-puro-MYC-ER^{T2} cells. Overexpression was confirmed by western blotting (Fig 4.6 a). Overexpression of GPX1 partially rescued MYC-induced apoptosis triggered by glutamine withdrawal (Fig 4.6 b). PRDX3 or SOD2 overexpression had little effect on apoptosis (Fig 4.6 b). Protein knockdown upon siRNA treatment was confirmed by western blotting (Fig 4.7 a). Knockdown of GPX1 but not PRDX3 enhanced the death in MYC cells (Fig 4.7 b). SOD2 is a highly efficient and abundant enzyme and it is likely that its expression is not limiting for clearance of superoxide. Thus the lack of an effect on apoptosis does not

necessarily rule out a role for mitochondrial ROS originating from this radical. The product of the SOD2 reaction is H_2O_2, which also needs to be cleared enzymatically and this step is more likely to be the limiting one in mitochondrial ROS resolution. PRDX3 uses thioredoxin (TRX) to recharge after reducing H_2O_2, whereas GPX1 uses GSH as a reductant. These different molecular mechanisms may give rise to the different results seen with these two enzymes. These results, together with the mercaptosuccinate/BSO results, confirm that GPX1 protects cells from MYC-induced apoptosis under conditions of lowered GSH levels.

a.



b.

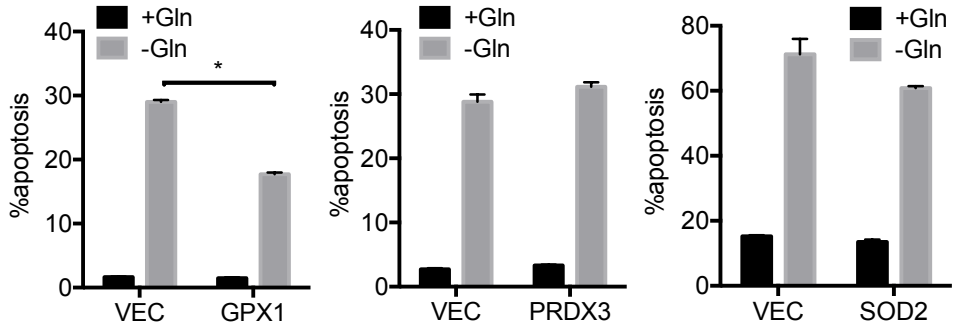
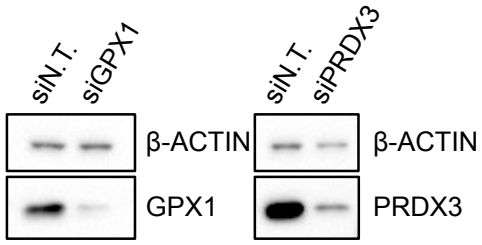


Figure 4.6. Effect of overexpression of antioxidant enzymes on MYC-induced apoptosis.

MRC5 MYC-ER^{T2} cells transduced with empty vector or GPX1, PRDX3 or SOD2 were treated with 4-OHT for 24 hrs and then glutamine was withdrawn for 16 hrs.

a. Western blots show the protein levels of GPX1, PRDX3 and SOD2.
b. Annexin V/PI apoptosis assay was performed (n=2). Data are mean ± SEM of triplicate wells for each condition in a representative experiment.

a.



b.

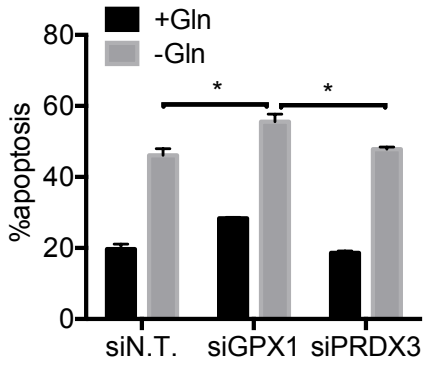


Figure 4.7. Effect of knockdown of PRDX3 and GPX1 on MYC-induced apoptosis.

30 nM siRNAs targeting GPX1 or PRDX3 were reverse transfected into MRC5 MYC-ER^{T2} cells. Cells were treated with 4-OHT for 24 hrs and glutamine was then withdrawn for 16 hrs.

a. Western blots show the protein levels of GPX1 and PRDX3 by siRNA knockdown.
b. Annexin V/PI apoptosis assay was performed (n=2). Data are mean ± SEM of triplicate wells for each condition in a representative experiment.

Proton leak and oxidative stress

As oxidative phosphorylation encompasses mitochondrial functions including ATP production and production of oxidative stress, it was decided that a method to assess multiple mitochondrial parameters might provide helpful information on the potential sources and levels of oxidative stress of the cells. Seahorse XF cell mitochondrial stress tests were performed to compare MYC cells to VEC cells under conditions with or without glutamine. Measuring the oxygen consumption rate (OCR) directly provides a standard and comprehensive method to assess the key parameters of mitochondrial function in live cells including basal respiration, ATP-linked respiration, proton leak, maximal respiration, spare respiratory capacity and non-mitochondrial respiration (Fig 4.8). With the help of several compounds that specifically target components of the electron transport chain (ETC), namely oligomycin, FCCP, and a mix of rotenone and antimycin A, the assay can determine key parameters of ETC function. As illustrated in figure 4.8, after measuring basal

respiration, the compounds are serially injected into the wells to enable measurement of ATP-linked respiration, maximal respiration, and non-mitochondrial respiration, respectively. Proton leak and spare respiratory capacity are then calculated from these parameters.

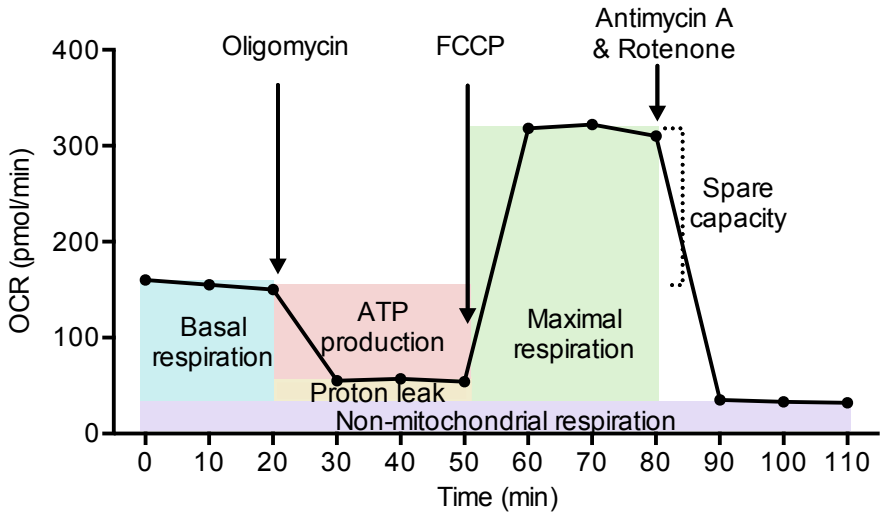


Figure 4.8. Scheme of mitochondrial respiration measured by Seahorse mitochondrial stress test (reproduced from the Seahorse website).
Oxygen consumption rate is measured by Seahorse every 10 minutes to determine the key parameters of mitochondrial respiration. 1μM oligomycin, 2μM FCCP, 2μM antimycin A and 2μM rotenone are added sequentially for assessment of different parameters.

Oxidative phosphorylation, the process whereby the mitochondrion produces ATP, involves the transport of protons across the inner mitochondrial membrane driven by the ETC. Electrons are passed through complexes I-IV via oxidation-reduction reactions (Fig 4.9). Under normal condition, complex IV reduces molecular oxygen, which acts as the terminal electron acceptor, forming H_2O. However, at other points of the chain, molecular oxygen may instead be prematurely and incompletely reduced by escaping electrons to give the superoxide radical ($O_2^{\bullet -}$) or other reactive oxygen species.

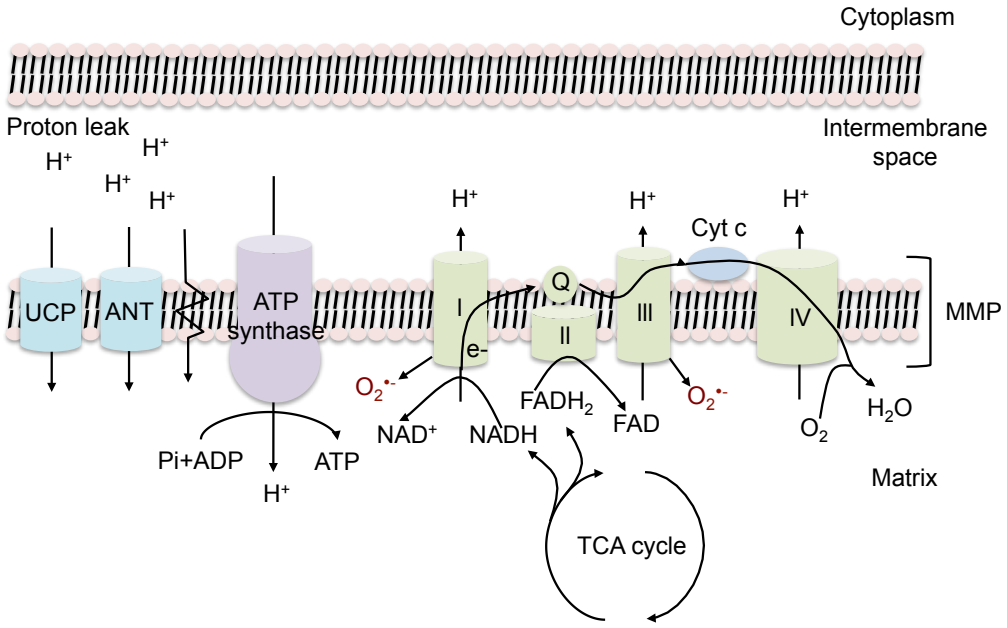


Figure 4.9. Scheme of electron transport chain and proton leak (adapted from Jastroch et al., 2010).
The scheme illustrates how electrons are passed through the complexes of the ETC, driving the efflux of protons to the intermembrane space. This gradient gives rise to the Mitochondrial Membrane Potential (MMP). Proton transport back to the matrix through the ATP synthase drives ATP generation. Protons can also leak back into the matrix spontaneously or through the adenine nucleotide translocase (ANT) and uncoupling proteins (UCPs) - shown in blue. Complexes I-IV are shown in green. Superoxide radical ($O_2^{\bullet -}$) generation along the ETC is shown in dark red.

The ETC pumps protons from the mitochondrial matrix into the intermembrane space, creating an electrochemical gradient that can drive protons back into the matrix through the ATP synthase to produce ATP. Protons can also return to the matrix independently of ATP synthase in a process known as “proton leak”. The total proton leak of a mitochondrion is the sum of two processes: basal leak, which is unregulated, and inducible leak, which is mediated by specific mitochondrial inner membrane proteins. The basal proton leak is cell-type specific and correlates with metabolic rate. The inducible leak through the adenine nucleotide translocase (ANT) and uncoupling proteins (UCPs) can be activated by fatty acids, superoxide, or peroxidation products (Jastroch et al., 2010). Therefore, proton leak can be an indicator of the level of mitochondrial oxidative stress.

With kind help from Dr. Roderick Carter (Centre for Cardiovascular Science, University of Edinburgh), Seahorse mitochondrial stress tests were performed. Basal respiration was slightly higher in MYC-activated cells, indicating higher oxidative phosphorylation activity (Fig 4.10). Basal respiration and mitochondrial ATP production were decreased upon glutamine withdrawal (Fig 4.10), comfirming that glutamine fuels the TCA cycle to drive ATP production and that the cells suffer from energy shortage in the absence of glutamine as described in Chapter 3. MYC has much higher proton leak compared to VEC (Fig 4.10), an indication of higher level of the mitochondrial oxidative stress.

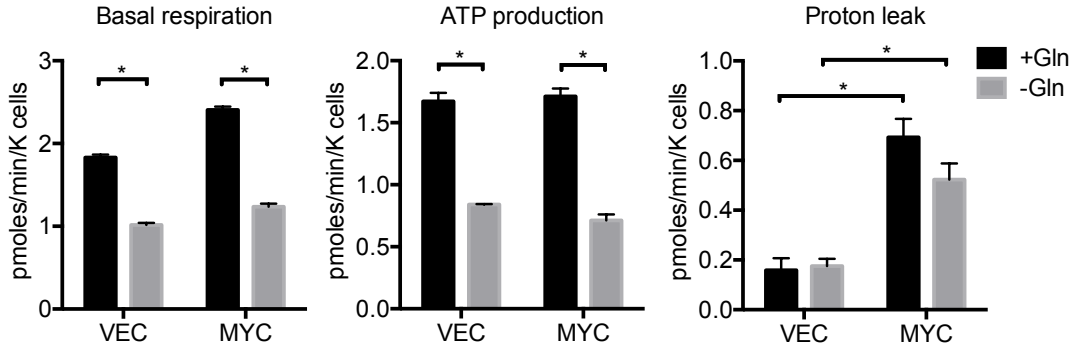


Figure 4.10. Seahorse mitochondrial stress tests on MRC5 cells upon glutamine withdrawal.
MRC5 cells (VEC or MYC-ER^{T2}) were plated in a Seahorse V7 plate, treated with 4-OHT for 24 hrs and glutamine was then withdrawn for 12 hrs before OCR was measured, using a Seahorse XF24 analyzer (n=3). Data are mean ± SEM of triplicate wells for each condition in a representative experiment.

Summary

The data presented in this chapter indicate that the protective function of glutamine is not primarily through production of glutathione to protect cells from ROS. However, there are indications that MYC-expressing cells are more likely to suffer from oxidative stress as indicated by higher basal respiration and proton leak measured by Seahorse mitochondrial stress tests. Furthermore, MYC can sensitise cells to apoptosis triggered by the combination of mercaptosuccinate and BSO, suggesting that ROS can be a determinant of MYC-induced apoptosis. Finally, the antioxidant

enzyme GPX1 protected MYC-expressing cells from glutamine withdrawal-triggered apoptosis, suggesting a component of ROS is present under these conditions.

Discussion

BCL2 has been shown to protect cells from H_2O_2-induced oxidative death and suppress lipid peroxidation but have no effect on peroxide generation (Hockenbery et al., 1993). GPX1 is a known inhibitor of lipid peroxidation, it can block IL-3 deprivation induced death (Hockenbery et al., 1993). Similarly, GPX1 also protects MYC-induced apoptosis triggered by glutamine withdrawal in our study. Our data of higher H^+ leak upon MYC activation also indicates lipid peroxidation of mitochondrial membrane. All suggesting that lipid peroxidation could play an important role in BCL2 family regulated MYC-induced apoptosis. The healthy and intact of mitochondrial membrane is essential for many processes, such as, energy production, maintaining membrane potential and apoptosis regulation. Taken together with the data from Chapter 3, a plausible unifying model may be one whereby MYC drives excessive demand for ATP from the mitochondrion and when the TCA cycle is compromised, there is production of mitochondrial ROS leading to lipid peroxidation and then apoptosis.

Chapter 5 - The BCL2 protein family and their role in metabolism

BCL2 is the founding member of the BCL2 family of proteins that play important roles in regulating apoptosis. Core members bind each other and work in antagonistic fashion, with BAX and BAK promoting apoptosis and BCL2, BCL-xL, MCL1 and BCL-W inhibiting apoptosis. Additional family members, known as the BH3-only proteins, act as inducible triggers of apoptosis (Willis et al., 2007). BCL2 family proteins have been found to control metabolic circuitries. They have been implicated in the regulation of mitochondrial nutrient and energy metabolism, such as mitochondrial ETC activity and mitochondrial import of substrates and metabolites (Brenner et al., 2000; Matsuyama et al., 1998; Marzo et al., 1998; Vander Heiden et al., 1999; Gottlieb et al., 2000; Chen et al., 2007; Alavian et al., 2011). Previous work on BCL2 family proteins suggests that the signaling pathways governing metabolism and apoptosis are linked, although a precise mechanism for such a link remains unclear. We aimed to investigate whether there is a unified metabolic mechanism that underpins the apoptotic function of this family and what role the BCL2 family plays in the link between metabolism and apoptosis. This work was based upon an enabling technology, high-resolution mass spectrometry, that allows for accurate, reliable and efficient analysis of metabolites. As already described, we not only studied the apoptosis directly regulated by BCL2 family but also MYC-induced apoptosis that gives additional insight into the links between metabolism and apoptosis (Chapter 3).

Previous work on the metabolic roles of the BCL2 family was based on different biological systems and focused on specific family members. In order to understand their role in metabolism in a more comprehensive, systematic and unbiased way, key family members including pro-apoptotic members BAX, BAK and BIM and anti-apoptotic members BCL2, BCL-xL and MCL1 were manipulated (by overexpression and/or RNAi-mediated knockdown) in MRC5 cells for untargeted metabolomic analysis. Pro-apoptotic state or anti-apoptotic state driven by different BCL2 family members were set up and studied separately. Metabolite changes in either pro or anti-apoptotic state were identified and verified by accurate mass and standard retention

time. We were particularly interested in metabolites that go in opposite directions in the two states as this would indicate metabolites regulated by BCL2 family that correlate with their apoptotic function.

Metabolite changes in the pro-apoptotic state - overexpression of pro-apoptotic members

The pro-apoptotic BCL2 family members BAX, BAK and BIM were transduced individually into MRC5 cells by retroviral infection. The infected cells underwent apoptosis which confirmed the expected proapoptotic function of these BCL2 family members. The cells were harvested before the onset of death in order to capture the metabolic changes prior to onset of apoptosis. The overexpression of BAX, BAK or BIM was confirmed by western blotting (Fig 5.1) and, in parallel, metabolites were extracted for untargeted metabolomic analysis (Fig 5.2 and Tables 5.1 & 5.2).

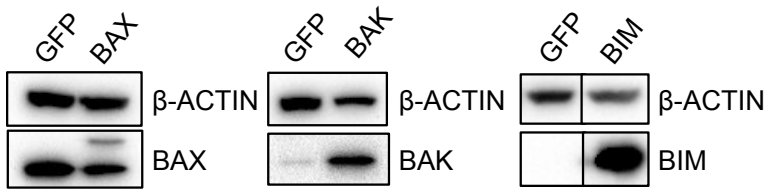


Figure 5.1. Overexpression of BAX, BAK and BIM.
Pro-apoptotic BCL2 family members, BAX, BAK and BIM were transduced into MRC5 cells by retroviral infection. Metabolites and proteins for BIM were extracted after 18 hrs of infection. For BAX and BAK, metabolites and proteins were extracted after 48 hrs of infection.

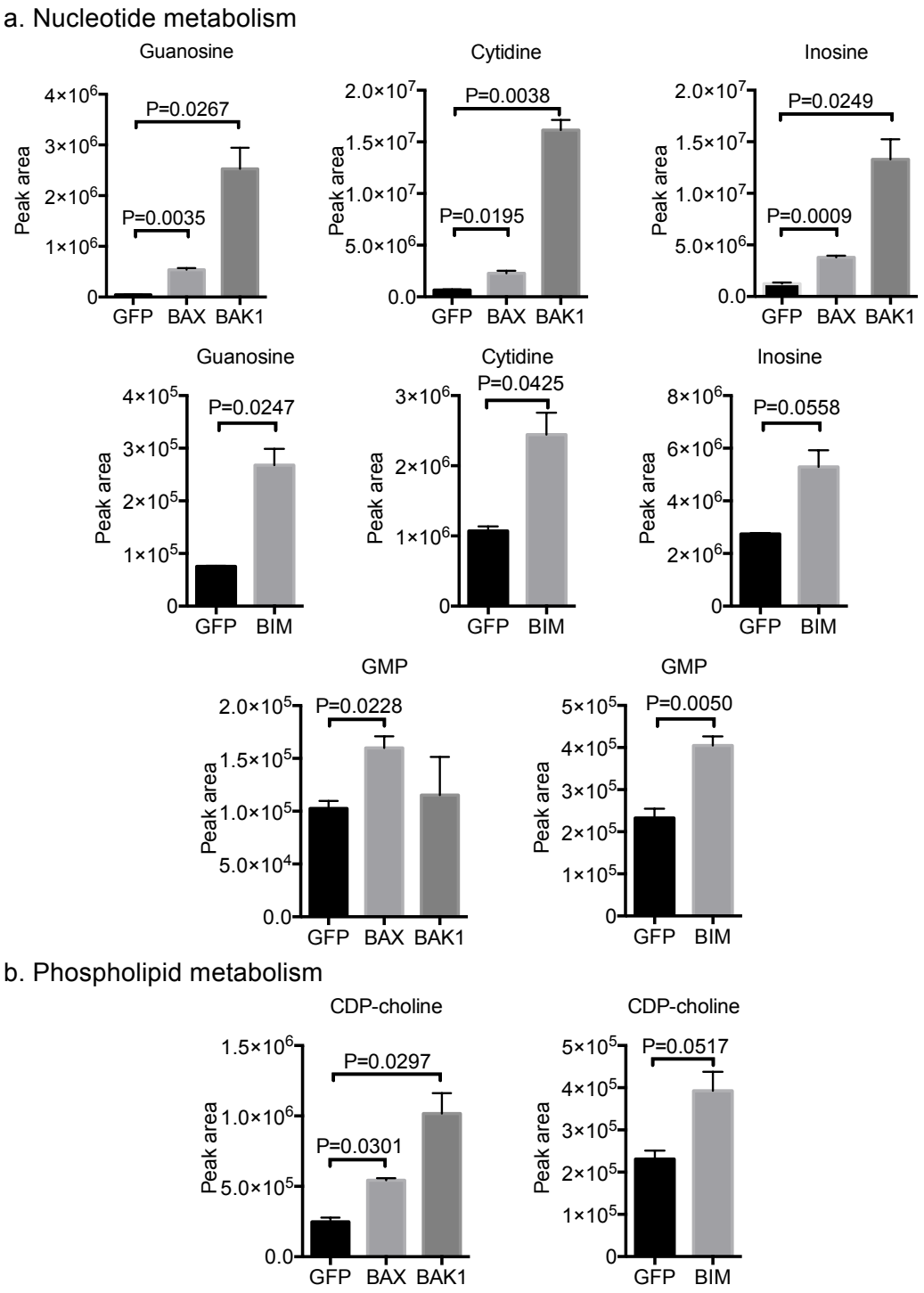


Figure 5.2. Metabolite changes upon BAX, BAK or BIM overexpression.
Histograms of metabolites changed in the pro-apoptotic state. Means, standard errors and p values of triplicates are shown. One of the three samples of the GFP from BAX and BAK1 group had problem with detection. Metabolites were consistently detected in all the other samples.

Table 5.1. Up-regulated metabolites upon pro-apoptotic state (metabolites in red shading are nucleobases, nucleosides and nucleotides)

BAX			BAK			BIM		
Metabolites	Ratio	P-value	Metabolites	Ratio	P-value	Metabolites	Ratio	P-value
Guanosine	12.03	0.004	Guanosine	56.59	0.027	Guanosine	3.55	0.025
SAH	8.4	0.002	SAH	38.77	0.024	SAH	3.48	0.030
Cytidine	3.54	0.020	Cytidine	25.23	0.004	Cytidine	2.28	0.042
Inosine	3.06	0.001	Cystine	12.78	0.03	Cystine	2.19	0.041
Thymidine	2.51	0.015	Inosine	10.7	0.025	Cysteine	1.94	0.033
Xanthine	2.28	0.016	Cysteine-S-sulfate	10.56	0.023	Inosine	1.93	0.056
Choline	2.22	0.059	Choline	9.55	0.03	GMP	1.74	0.005
CDP-choline	2.2	0.030	Xanthine	7.3	0.015	CDP-choline	1.7	0.052
CDP-ethanolamine	2.12	0.056	Thymidine	6.74	0.043	Cysteine-S-sulfate	1.29	0.030
Glycerophosphocholine	1.62	0.037	CDP-ethanolamine	5.15	0.012			
GMP	1.56	0.023	Adenosine	4.41	0.045			
			methionine	4.24	0.034			
			CDP-choline	4.11	0.030			
			Glycerophosphocholine	4.05	0.033			
			homocysteine	3.88	0.039			
			Glycine	3.78	0.047			
			Serine	3.29	0.037			
			Phosphatidylglycerol	3.27	0.038			
			Glycerylphosphorylethanolamine	3.02	0.017			
			Creatine	2.8	0.022			
			Taurine	2.31	0.018			
			GSSG	1.83	0.012			

Table 5.2. Down-regulated metabolites upon pro-apoptotic state (metabolites in blue shading are nucleotides)

BAX			BAK			BIM		
Metabolites	Ratio	P-value	Metabolites	Ratio	P-value	Metabolites	Ratio	P-value
Phospho-L-Serine	0.24	0.017	IMP	0.12	0.003	GTP	0.54	0.040
			Phospho-L-Serine	0.18	0.037	UDP	0.64	0.000
						Phospho-L-Serine	0.66	0.005
						ATP	0.78	0.016
						ADP	0.83	0.048

Metabolites identified in the tables were validated by accurate mass and retention time in order to meet the reporting requirement for non-novel metabolite identification (Sumner et al., 2007; Sumner et al., 2014).

Metabolite changes in the anti-apoptotic state - knockdown of pro-apoptotic members or overexpression of anti-apoptotic members

Pro-apoptotic members BAX, BAK and BIM were knocked down by siRNA and anti-apoptotic members BCL2, BCL-xL and MCL1 were retrovirally overexpressed in order to detect metabolic changes correlating with an anti-apoptotic state. Metabolite changes were analysed by untargeted methods. Since serum withdrawal is known to induce Bim expression (Weston et al., 2003), siRNA knockdown of BIM was performed and compared to non-target control under conditions both with and without FBS. Protein levels were demonstrated by western blotting (Fig 5.3).

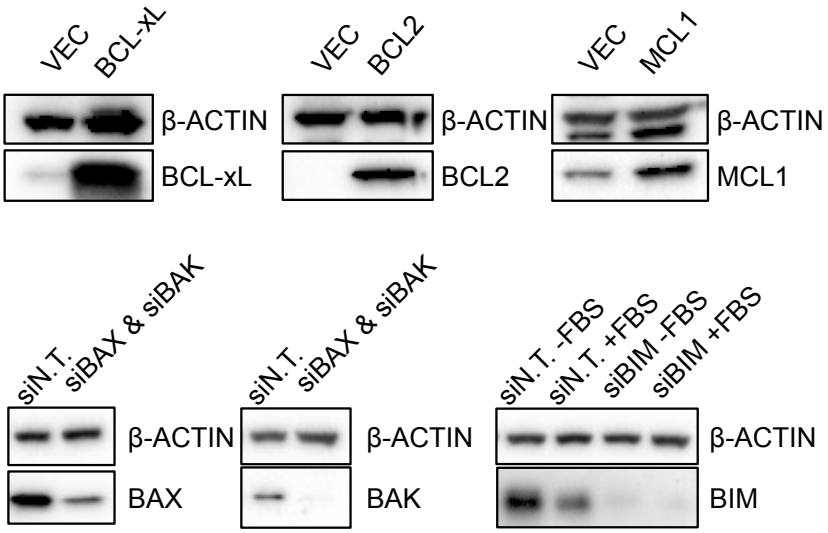


Figure 5.3. Knockdown of BAX, BAK or BIM and overexpression of BCL2, BCL-xL or MCL1.
siRNAs targeting BAX and BAK were simultaneously introduced into MRC5 cells by reverse transfection. 48 hrs post-transfection, protein and metabolites were extracted. siRNA targeting BIM was introduced into MRC5 for 24 hours and FBS was then withdrawn for another 24 hours, when protein and metabolites were extracted. Anti-apoptotic family members BCL2, BCL-xL and MCL1 were transduced into MRC5 cells by retroviral infection. Protein and metabolites were extracted 48 hrs post-infection. Western blots show the protein levels of BAX, BAK, BIM, BCL2, BCL-xL and MCL1.

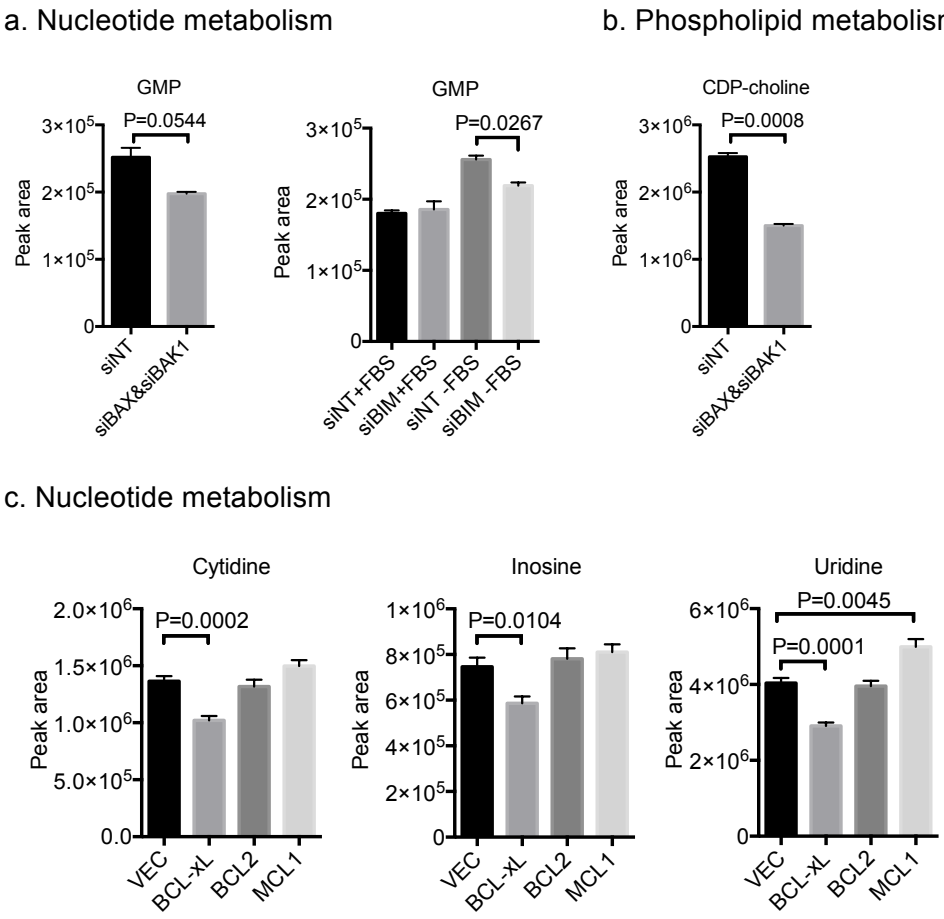


Figure 5.4. Metabolite changes upon anti-apoptotic status.
Histograms of metabolites changed in the anti-apoptotic state. Means, standard errors and p values are shown.

Table 5.3. Metabolite changes during the knockdown of pro-apoptotic members (metabolites in red or blue shading are nucleosides and nucleotides up or down-regulated)

siBAX & siBAK			siBIM +FBS			siBIM -FBS		
Metabolites	Ratio	P-value	Metabolites	Ratio	P-value	Metabolites	Ratio	P-value
Cysteine-S-sulfate	2.217	0.000	CDP-choline	1.332	0.029	Taurine	1.215	0.012
Hypotaurine	1.583	0.044	Hypotaurine	1.265	0.040	Hypotaurine	1.207	0.020
Taurine	1.489	0.059	Acetyl-L-Cysteine	1.232	0.017			
CDP-ethanolamine	1.48	0.026	NADH	1.186	0.018			
Inosine	1.262	0.047	Taurine	1.175	0.031			
Phosphocreatinine	1.229	0.053						
Phosphocreatine	1.227	0.042						

siBAX & siBAK			siBIM +FBS			siBIM -FBS		
Metabolites	Ratio	P-value	Metabolites	Ratio	P-value	Metabolites	Ratio	P-value
IMP	0.317	0.003	Phospho-L-Serine	0.704	0.027	Cysteine-S-sulfate	0.708	0.021
CDP	0.521	0.026	Cysteine-S-sulfate	0.77	0.039	Phospho-L-Serine	0.762	0.029
Acetyl-L-Cysteine	0.553	0.012	Cytidine	0.913	0.051	GMP	0.856	0.007
UDP	0.566	0.023						
CDP-choline	0.595	0.001						
ADP	0.669	0.052						
Phospho-L-Serine	0.725	0.026						
AMP	0.768	0.034						
GMP	0.784	0.054						

Table 5.4. Metabolite changes during the overexpression of anti-apoptotic members (metabolites in red or blue shading are nucleosides and nucleotides up or down-regulated)

BCL-xL			BCL2			MCL1		
Metabolites	Ratio	P-value	Metabolites	Ratio	P-value	Metabolites	Ratio	P-value
CDP-choline	1.833	0.001	Glycerophosphocholine	2.189	0.001	Cystine	1.754	0.002
Glycerophosphocholine	1.78	0.000	IMP	2.062	0.020	Phospho-L-Serine	1.726	0.000
GMP	1.378	0.007	CDP-choline	1.746	0.002	IMP	1.655	0.010
Glycerylphosphorylethanolamine	1.345	0.000	GSSG	1.663	0.004	Cystathionine	1.364	0.000
			Glycerylphosphorylethanolamine	1.542	0.000	CDP-ethanolamine	1.262	0.003
			Cysteine	1.35	0.009	Uridine	1.235	0.004
			Taurine	1.269	0.014	Phosphatidylglycerol	1.213	0.005
			Glycine	1.262	0.032	Choline	1.192	0.015
			Cysteate	1.247	0.021			
			Phosphatidylglycerol	1.203	0.025			
			Choline	1.148	0.050			
			Cystathionine	1.141	0.048			

BCL-xL			BCL2			MCL1		
Metabolites	Ratio	P-value	Metabolites	Ratio	P-value	Metabolites	Ratio	P-value
Phosphocreatinine	0.627	0.000	CDP-ethanolamine	0.46	0.000	CDP	0.512	0.006
CDP-ethanolamine	0.639	0.000	GDP	0.591	0.020	Glycerylphosphorylethanolamine	0.621	0.000
Phosphocreatine	0.688	0.000	GTP	0.603	0.000	Glycerophosphocholine	0.647	0.001
Uridine	0.72	0.000	Phospho-L-Serine	0.623	0.000	Cysteinesulfinate	0.726	0.000
NAD^+	0.722	0.000	Phosphocreatinine	0.636	0.000	GTP	0.744	0.025
Hypotaurine	0.729	0.000	Phosphocreatine	0.731	0.000	Taurine	0.764	0.004
Cytidine	0.747	0.000	CTP	0.739	0.005	CTP	0.824	0.048

Phospho-L-Serine	0.752	0.004	NAD^+	0.751	0.000	NAD^+	0.881	0.020
N_acetylaspartate	0.756	0.000	ATP	0.764	0.001	UDP_GlcNAc	0.882	0.003
Inosine	0.785	0.010	NADPH	0.781	0.000			
Cysteinesulfinate	0.791	0.000	UTP	0.785	0.004			
Serine	0.8	0.002	Hypotaurine	0.801	0.003			
Methionine	0.805	0.002	N_acetylaspartate	0.801	0.005			
Xanthine	0.833	0.009	UDP_GlcNAc	0.817	0.003			
NADPH	0.85	0.005						
Choline	0.856	0.004						
UDP_GlcNAc	0.86	0.000						
Creatine	0.9	0.027						

Metabolites identified in the tables were validated by accurate mass and retention time in order to meet the reporting requirement for non-novel metabolite identification (Sumner et al., 2007; Sumner et al., 2014).

Discussion

The metabolites identified in these analyses are mainly involved in nucleotide, cysteine and phospholipid metabolism. These pathways were consistently regulated when BCL2 family members were knocked down or overexpressed. Metabolite changes in the pro-apoptotic state were more robust with higher fold-changes especially in BAK-overexpressing cells. The anti-apoptotic state seems comparable to control cells as they appear healthy and have smaller fold-changes. However, metabolites that change in opposite directions are identified when comparing the changes of pro-apoptotic state against anti-apoptotic state. For example, GMP is reduced in both BAX and BAK double knockdown and BIM knockdown, but increased in BAX or BIM overexpression samples (Fig 5.2 a, fig 5.4 a). Similarly, CDP-choline is reduced in BAX and BAK double knockdown but increased in BAX or BAK overexpression samples (Fig 5.2 b, fig 5.4 b). The fact that the levels of these metabolites correlate with apoptotic status does suggest regulation of metabolism by the BCL2 family. Some of the phospholipid pathway metabolites contain nucleotides (e.g. CDP-choline) and it is possible that the changes observed in phospholipid metabolites are secondary to the changes in the nucleotides. Several nucleosides were significantly elevated in pro-apoptotic state and reduced in the anti-apoptotic state (Fig 5.2 a, fig 5.4 c). Indeed, guanosine, cytidine and inosine are the most changed metabolites in the pro-apoptotic state (Fig 5.2 a). As described in Chapter 3, nucleosides are not synthesized *de novo*, but rather arise through catabolism of the nucleotides. Thus there appears to be a strong induction of nucleotide catabolism upon transduction of pro-apoptotic BCL2 family members. Previous reports stated where nucleotide catabolism occurs including exercising skeletal muscle and hypoxia *in vivo* (Tullson and Terjung, 1991; Jennings and Steenbergen, 1985; Chouchani et al., 2014), situations where energetic demand exceeds supply. We observed the same pattern of nucleotide catabolism during MYC-induced apoptosis triggered by glutamine withdrawal (Chapter 3), which is also a condition where energetic demand exceeds supply.

In general, the nucleotide levels are also regulated by the BCL2 family, although not

with as clear a correlation with apoptotic status as the nucleosides (highlighted in red or blue shading in Table 5.1-4). Previous studies suggest that the BCL2 family can interact with mitochondrial proteins involved in the trafficking of intermediate metabolites, in particular in the exchange of ATP and ADP between the matrix and the cytosol (Vander Heiden et al., 1999; Marzo et al., 1998; Narita et al., 1998). Bcl2 and Bax have been found to regulate the channel activity of the mitochondrial ANT that exports ATP from the mitochondrial matrix and imports ADP into the matrix (Brenner et al., 2000). The ATP synthase, a proton pump that can operate in both directions creating ATP or consuming ATP, is required for Bax-induced apoptosis in both yeast and mammalian cells (Matsuyama et al., 1998). Moreover, Bcl-xL interacts directly with the ATP synthase, increasing its enzyme activity and ATP production in neurons (Alavian et al., 2011). Regulation of the exchange and generation of ATP and ADP between the mitochondrion and the cytosol by the BCL2 family is consistent with a model in which energetic supply and demand are determinants of apoptosis.

Taken together, our data support a model in which energy supply and demand are key determinants of the apoptosis regulated by the BCL2 family. This is consistent with many previous reports, as described above, and with a recent report linking Bim-induced apoptosis with the integrity of the mitochondrial electron transport chain (Jiang et al., 2016).

Initially, the untargeted analyses were only done for the intracellular metabolites. We then looked at certain metabolites in extracellular samples that highlighted from the untargeted analysis but could not get extra useful information than the intracellular samples alone. Therefore, we decided not to perform untargeted analysis for the extracellular metabolites. If there was plenty of time working on this part of the project, untargeted analysis for extracellular metabolites would potentially provide more information on the role of signal transduction of certain metabolites. Lipidomic analysis on BCL2 family could also contribute to an important angle of their role in metabolism.

Chapter 6 - Discussion

MYC-induced apoptosis requires the transactivation domain of Myc (Evan et al., 1992) and this has led to a widespread assumption that MYC-induced apoptosis is mediated by specific transcriptional targets of MYC. Sabò et al. investigated the role of MYC in gene expression during B cell lymphomagenesis and found that MYC directly regulates the expression of distinct subsets of genes that lead to the indirect amplification of global transcription through the activity of the induced MYC target genes (Sabò A et al., 2014). We confirmed that MYC drives potent amplification of global transcription and consequent activation of another energetically demanding process, translation. Here we propose a homeostatic model of MYC-induced apoptosis based upon energetic supply and demand. We present data showing the activation of global transcription and translation by MYC indicating elevated energetic demand, and a profound reduction in cellular energy charge in cells undergoing MYC-induced apoptosis triggered by glutamine withdrawal. Our data indicate that the homeostasis of energetic supply and demand is a key determinant of MYC-induced apoptosis.

Nucleotide catabolism

Nucleotide catabolism, in particular the accumulation of hypoxanthine and xanthine, has been observed in contracting skeletal muscle (Tullson and Terjung, 1991) and in ischaemic tissue (Harmsen et al., 1981; Jennings and Steenbergen, 1985; Chouchani et al., 2014). Combined with our findings that nucleotide catabolism is induced by MYC and enhanced in cells undergoing MYC-induced apoptosis, the common feature of these conditions is the imbalance of metabolic supply and demand. The exact mechanism of nucleotide catabolism under these conditions currently remains unclear. However, the accumulation of AMP during energetic imbalance may promote catalysis to adenosine purely based upon substrate concentration. This, in turn may fuel the cascade of reactions that result in catalysis to hypoxanthine and/or xanthine.

There are three major mechanisms that could lead to AMP accumulation. Firstly, cells with activated MYC demonstrate increased flux through the pentose phosphate and nucleotide biosynthesis pathways, leading to increased production of AMP. Secondly, AMP can be generated by phosphorylation of adenosine or addition of ribose 5-phosphate to adenine in the salvage pathway. Thirdly, hydrolysis of ATP in energy-consuming reactions leads to production of ADP (in the case of kinases) or AMP. ADP can also be remodeled to ATP and AMP through the action of the adenylate kinases. In times of high energy consumption, the ATP is consumed and the AMP accumulates. We observed indications that all three mechanisms contribute to AMP accumulation in MYC-activated cells, but the energetic hydrolysis of ATP was the only model that correlated with MYC-induced apoptosis.

The purine nucleotide cycle is a metabolic cycle in which AMP is deaminated to IMP, which is then converted back to AMP via adenylosuccinate. The conversion of IMP to AMP also consumes aspartate and produces fumarate, which can feed back into the TCA cycle to fuel mitochondrial ATP production. This cycle plays an important role in energy metabolism in skeletal muscle (Tullson and Terjung, 1991). The purine nucleotide cycle may be important in MYC-activated cells, as they are dependent upon glutamine-fueled TCA cycle activity and, when glutamine is limiting, the purine nucleotide cycle may act as a source for TCA metabolites. IMP and adenylosuccinate, two intermediates of the cycle, are significantly up-regulated in MYC-activated cells, although whether this is due to increased nucleotide biosynthesis or purine nucleotide cycle activity is currently unknown.

Nucleotide catabolism may rescue levels of AMP, thereby allowing continued conversion of ADP to ATP and AMP by AKs, supporting cellular ATP levels. Irrespective of potential benefit to cellular homeostasis, the products of nucleotide catabolism are diagnostic of shortfall between energetic supply and demand and may be used as a hallmark of MYC-activated cells or even MYC-driven tumours.

Undruggable MYC - synthetic lethal approaches

As targeting MYC itself has thus far proven to be challenging (Whitfield et al., 2017), much effort has been focused on indirect strategies. Resistance to apoptosis helps cells overexpressing MYC to survive and thus understanding how MYC induces apoptosis should enable development of therapies to restore or even enhance apoptosis to eliminate MYC-activated cells. MYC drives metabolic rewiring in cells through direct mechanisms (e.g. promotion of nucleotide biosynthesis) and indirect mechanisms (e.g. low energy charge) and this can cause metabolic vulnerability in MYC-driven cancers. Our data suggest that there are potential targets involved in metabolic pathways that are synthetic lethal with MYC. Understanding the metabolic basis for MYC-induced apoptosis will allow development of anti-metabolic interventions for cancer therapy.

Tumour cells depend upon mitochondrial metabolism to provide ATP and building blocks for macromolecule synthesis to support cell proliferation. Accumulating evidence suggests that mitochondrial bioenergetics, biosynthesis and signaling are required for tumourigenesis. Therefore, targeting mitochondrial ATP production, mitochondrial biosynthetic function and mitochondrial redox capacity are potential cancer therapies (reviewed by Weinberg and Chandel, 2014). Recent work shows that MYC and MCL1 cooperatively promote mitochondrial OXPHOS, which in turn induces HIF-1α and chemotherapy resistance of cancer stem cells in triple negative breast cancer (TNBC) (Lee et al., 2017). Targeting mitochondrial respiration and HIF-1α may reverse chemotherapy resistance in TNBC. Another study has shown that targeting mitochondrial biosynthetic function by inhibiting glutaminase is a promising strategy for targeting MYC-driven tumours (Le et al., 2012). Indeed, the GLS inhibitor CB-839 is currently in clinical trials. Yet another study demonstrated that SHMT2 is necessary for redox balance in Myc-transformed cells under conditions of hypoxia and, diminishing SHMT2 levels decreased tumour growth (Ye et al., 2014). However, because of the complexity of metabolic circuits, and the ability of cancer cells to utilize alternative metabolic routings (Mullen et al., 2011; Sullivan et al., 2015), treatments targeting multiple mitochondrial pathways may be more effective for targeting cancer cells with MYC overexpression. Our data indicate

that there is energetic shortfall during MYC-induced apoptosis and that interconversion of adenine nucleotides by AK2 supports mitochondrial ATP production required by MYC. AK2, therefore, may be a good target for combination therapy with inhibition of glutaminase: this combination should preferentially target the energy supply in cells with high energetic demand, leading to onset of apoptosis. Our data has also shown that GPX1, an antioxidant enzyme regulating mitochondrial redox state, protects cells overexpressing MYC from apoptosis triggered by glutamine withdrawal. Thus a GPX1 inhibitor could be used for combination therapy with a glutaminase inhibitor.

Membrane potential

Even though it is widely accepted that energy crisis leads to apoptosis, the mechanism remains unclear. Decrease in mitochondrial membrane potential (MMP) has been observed during apoptosis triggered by different stimuli (Scarlett et al., 2000; Zamzami et al., 1995; Gottlieb et al., 2000). BCL-xL prevents the initial decrease in MMP during tumour necrosis factor alpha (TNF-α)-induced apoptosis (Gottlieb et al., 2000). Work from the same group has shown that decrease in MMP leads to mitochondrial structural changes, known as matrix condensation and cristae unraveling. These structural changes result in the redistribution of cytochrome c from the cristae to the intermembrane space, making it more susceptible to release from the mitochondria, thereby enhancing apoptosis (Gottlieb et al., 2003). These studies suggest that MMP could be the key factor that regulates apoptosis. There are multiple ways to decrease MMP, including lack of oxidisable substrates for mitochondria, inhibition of mitochondrial respiration (and therefore the electron transport chain), or uncoupling of the inner membrane. Exercising muscle cells are particularly susceptible to loss of MMP because of their high demand for energy. Under conditions in which electron transport chain activity is insufficient to maintain the MMP, muscle mitochondria can run the ATP synthase in reverse, consuming ATP and producing ADP. Reversal of the ATP synthase causes it to pump protons in reverse (i.e. out of the matrix) to maintain MMP. One possibility is that MYC-induced apoptosis, which we have shown is due to energy shortage, could occur through

failure to maintain the MMP by ATP synthase reversal because of mitochondrial ATP shortage. In this scenario, glutamine withdrawal would lead to MMP reduction due to lack of TCA cycle intermediates to drive electron transport chain. Under such conditions of MMP decrease, ATP hydrolysis by the ATP synthase can be used to maintain the MMP. This requires ATP availability in the mitochondrion and this ATP must be imported from the cytosol. However, in cells with activated MYC, the energy balance in the cytosol is low due to excessive transcription, restricting availability of ATP for mitochondrial transfer. Eventually, a failure to support the MMP leads to cytochrome c release and apoptosis. Research exploring this hypothesis is currently under way. Future work includes, measuring MMP during glutamine withdrawal and MYC-induced apoptosis to see if there is decrease in MMP, and inhibiting ATP synthase for ATP hydrolysis by inhibitors or genetic tools to look at their effect on apoptosis and MMP. These works can help us build the link between energy imbalance, MMP and apoptosis.

Model

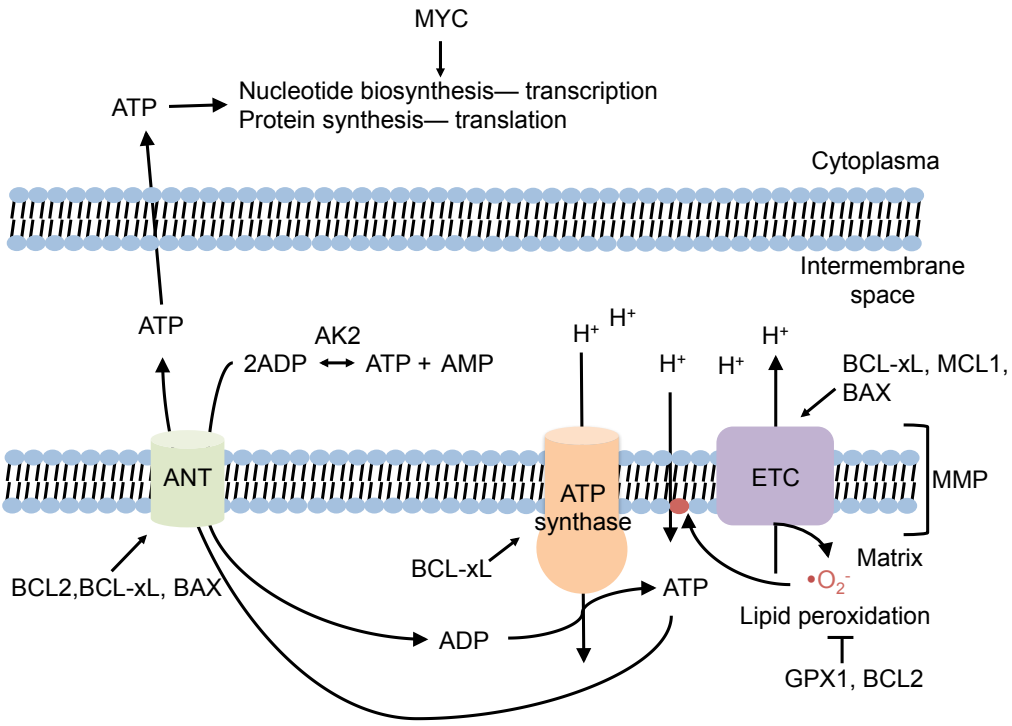


Figure 6.1. Model figure of the metabolic basis of MYC-induced apoptosis.

MYC drives global transcription and translation therefore creates high energetic demand. Insufficient energy supply for MYC leads to energy crisis and apoptosis. During this process, based on literature and our data, BCL2 family involves in MYC-induced apoptosis by regulating ANT for ATP/ADP exchange, regulating ATP synthase activity and the efficiency of ETC for ATP production. AK2 converts ATP, AMP to two ADP for ATP production therefore protects MYC-induced apoptosis by supporting energy supply. When the TCA cycle is compromised, ROS generated from the ETC leads to lipid peroxidation and this can be blocked by GPX1 and BCL2. GPX1 protects MYC-induced apoptosis suggesting that lipid peroxidation plays an important role in this process. Both energy crisis and lipid peroxidation may lead to decrease in MMP that can initiate apoptosis. These lead to our future work in studying the link of energy imbalance and MMP during MYC-induced apoptosis.

Chapter 7 - Bibliography

1. Hanahan, D. and R.A. Weinberg, *The hallmarks of cancer.* Cell, 2000. **100**(1): p. 57-70.
2. Hanahan, D. and R.A. Weinberg, *Hallmarks of cancer: the next generation.* Cell, 2011. **144**(5): p. 646-74.
3. Fernald, K. and M. Kurokawa, *Evading apoptosis in cancer.* Trends Cell Biol, 2013. **23**(12): p. 620-33.
4. Adams, J.M. and S. Cory, *The Bcl-2 apoptotic switch in cancer development and therapy.* Oncogene, 2007. **26**(9): p. 1324-37.
5. Lowe, S.W., E. Cepero, and G. Evan, *Intrinsic tumour suppression.* Nature, 2004. **432**(7015): p. 307-15.
6. Evan, G. and T. Littlewood, *A matter of life and cell death.* Science, 1998. **281**(5381): p. 1317-22.
7. Fukuhara, S. and J.D. Rowley, *Chromosome 14 translocations in non-Burkitt lymphomas.* Int J Cancer, 1978. **22**(1): p. 14-21.
8. Vaux, D.L., S. Cory, and J.M. Adams, *Bcl-2 gene promotes haemopoietic cell survival and cooperates with c-myc to immortalize pre-B cells.* Nature, 1988. **335**(6189): p. 440-2.
9. Delbridge, A.R., et al., *Thirty years of BCL-2: translating cell death discoveries into novel cancer therapies.* Nat Rev Cancer, 2016. **16**(2): p. 99-109.
10. Tsujimoto, Y., N. Ikegaki, and C.M. Croce, *Characterization of the protein product of bcl-2, the gene involved in human follicular lymphoma.* Oncogene, 1987. **2**(1): p. 3-7.
11. Chen-Levy, Z. and M.L. Cleary, *Membrane topology of the Bcl-2 proto-oncogenic protein demonstrated in vitro.* J Biol Chem, 1990. **265**(9): p. 4929-33.
12. Krajewski, S., et al., *Investigation of the subcellular distribution of the bcl-2 oncoprotein: residence in the nuclear envelope, endoplasmic reticulum, and outer mitochondrial membranes.* Cancer Res, 1993. **53**(19): p. 4701-14.
13. Weston, C.R., et al., *Activation of ERK1/2 by deltaRaf-1:ER* represses Bim expression independently of the JNK or PI3K pathways.* Oncogene, 2003. **22**(9): p. 1281-93.
14. Li, H., et al., *Cleavage of BID by caspase 8 mediates the mitochondrial damage in the Fas pathway of apoptosis.* Cell, 1998. **94**(4): p. 491-501.
15. Nakano, K. and K.H. Vousden, *PUMA, a novel proapoptotic gene, is induced by p53.* Mol Cell, 2001. **7**(3): p. 683-94.
16. Oda, E., et al., *Noxa, a BH3-only member of the Bcl-2 family and candidate mediator of p53-induced apoptosis.* Science, 2000. **288**(5468): p. 1053-8.

17. Andersen, J.L. and S. Kornbluth, *The tangled circuitry of metabolism and apoptosis.* Mol Cell, 2013. **49**(3): p. 399-410.
18. Green, D.R., L. Galluzzi, and G. Kroemer, *Cell biology. Metabolic control of cell death.* Science, 2014. **345**(6203): p. 1250256.
19. Brenner, C., et al., *Bcl-2 and Bax regulate the channel activity of the mitochondrial adenine nucleotide translocator.* Oncogene, 2000. **19**(3): p. 329-36.
20. Marzo, I., et al., *Bax and adenine nucleotide translocator cooperate in the mitochondrial control of apoptosis.* Science, 1998. **281**(5385): p. 2027-31.
21. Vander Heiden, M.G., et al., *Bcl-xL prevents cell death following growth factor withdrawal by facilitating mitochondrial ATP/ADP exchange.* Mol Cell, 1999. **3**(2): p. 159-67.
22. Alavian, K.N., et al., *Bcl-xL regulates metabolic efficiency of neurons through interaction with the mitochondrial F1FO ATP synthase.* Nat Cell Biol, 2011. **13**(10): p. 1224-33.
23. Chen, Z.X. and S. Pervaiz, *Bcl-2 induces pro-oxidant state by engaging mitochondrial respiration in tumor cells.* Cell Death Differ, 2007. **14**(9): p. 1617-27.
24. Meredith, M.J., et al., *Expression of Bcl-2 increases intracellular glutathione by inhibiting methionine-dependent GSH efflux.* Biochem Biophys Res Commun, 1998. **248**(3): p. 458-63.
25. Voehringer, D.W., et al., *Bcl-2 expression causes redistribution of glutathione to the nucleus.* Proc Natl Acad Sci U S A, 1998. **95**(6): p. 2956-60.
26. Hockenbery, D.M., et al., *Bcl-2 functions in an antioxidant pathway to prevent apoptosis.* Cell, 1993. **75**(2): p. 241-51.
27. Naderi, J., et al., *Water-soluble formulation of Coenzyme Q10 inhibits Bax-induced destabilization of mitochondria in mammalian cells.* Apoptosis, 2006. **11**(8): p. 1359-69.
28. Ahmad, K.A., et al., *Hydrogen peroxide-mediated cytosolic acidification is a signal for mitochondrial translocation of Bax during drug-induced apoptosis of tumor cells.* Cancer Res, 2004. **64**(21): p. 7867-78.
29. Vaughn, A.E. and M. Deshmukh, *Glucose metabolism inhibits apoptosis in neurons and cancer cells by redox inactivation of cytochrome c.* Nat Cell Biol, 2008. **10**(12): p. 1477-83.
30. Lowman, X.H., et al., *The proapoptotic function of Noxa in human leukemia cells is regulated by the kinase Cdk5 and by glucose.* Mol Cell, 2010. **40**(5): p. 823-33.
31. Reddy, E.P., et al., *Nucleotide sequence analysis of the proviral genome of avian myelocytomatosis virus (MC29).* Proc Natl Acad Sci U S A, 1983. **80**(9): p. 2500-4.

32. Taub, R., et al., *Translocation of the c-myc gene into the immunoglobulin heavy chain locus in human Burkitt lymphoma and murine plasmacytoma cells.* Proc Natl Acad Sci U S A, 1982. **79**(24): p. 7837-41.
33. Nesbit, C.E., J.M. Tersak, and E.V. Prochownik, *MYC oncogenes and human neoplastic disease.* Oncogene, 1999. **18**(19): p. 3004-16.
34. Blackwood, E.M. and R.N. Eisenman, *Max: a helix-loop-helix zipper protein that forms a sequence-specific DNA-binding complex with Myc.* Science, 1991. **251**(4998): p. 1211-7.
35. Peukert, K., et al., *An alternative pathway for gene regulation by Myc.* EMBO J, 1997. **16**(18): p. 5672-86.
36. Meyer, N. and L.Z. Penn, *Reflecting on 25 years with MYC.* Nat Rev Cancer, 2008. **8**(12): p. 976-90.
37. Sears, R., et al., *Ras enhances Myc protein stability.* Mol Cell, 1999. **3**(2): p. 169-79.
38. Magudia, K., A. Lahoz, and A. Hall, *K-Ras and B-Raf oncogenes inhibit colon epithelial polarity establishment through up-regulation of c-myc.* J Cell Biol, 2012. **198**(2): p. 185-94.
39. Palomero, T., et al., *Activating mutations in NOTCH1 in acute myeloid leukemia and lineage switch leukemias.* Leukemia, 2006. **20**(11): p. 1963-6.
40. Weng, A.P., et al., *c-Myc is an important direct target of Notch1 in T-cell acute lymphoblastic leukemia/lymphoma.* Genes Dev, 2006. **20**(15): p. 2096-109.
41. He, T.C., et al., *Identification of c-MYC as a target of the APC pathway.* Science, 1998. **281**(5382): p. 1509-12.
42. Evan, G.I., et al., *Induction of apoptosis in fibroblasts by c-myc protein.* Cell, 1992. **69**(1): p. 119-28.
43. Gibson, A.W., T. Cheng, and R.N. Johnston, *Apoptosis induced by c-myc overexpression is dependent on growth conditions.* Exp Cell Res, 1995. **218**(1): p. 351-8.
44. Felsher, D.W. and J.M. Bishop, *Transient excess of MYC activity can elicit genomic instability and tumorigenesis.* Proc Natl Acad Sci U S A, 1999. **96**(7): p. 3940-4.
45. Grandori, C., et al., *Werner syndrome protein limits MYC-induced cellular senescence.* Genes Dev, 2003. **17**(13): p. 1569-74.
46. Nilsson, J.A. and J.L. Cleveland, *Myc pathways provoking cell suicide and cancer.* Oncogene, 2003. **22**(56): p. 9007-21.
47. Hoffman, B. and D.A. Liebermann, *Apoptotic signaling by c-MYC.* Oncogene, 2008. **27**(50): p. 6462-72.
48. Green, D.R., *A Myc-induced apoptosis pathway surfaces.* Science, 1997. **278**(5341): p. 1246-7.

49. Zindy, F., et al., *Myc signaling via the ARF tumor suppressor regulates p53-dependent apoptosis and immortalization.* Genes Dev, 1998. **12**(15): p. 2424-33.
50. Jacobs, J.J., et al., *Bmi-1 collaborates with c-Myc in tumorigenesis by inhibiting c-Myc-induced apoptosis via INK4a/ARF.* Genes Dev, 1999. **13**(20): p. 2678-90.
51. Schmitt, C.A. and S.W. Lowe, *Bcl-2 mediates chemoresistance in matched pairs of primary E(mu)-myc lymphomas in vivo.* Blood Cells Mol Dis, 2001. **27**(1): p. 206-16.
52. Finch, A., et al., *Bcl-xL gain of function and p19 ARF loss of function cooperate oncogenically with Myc in vivo by distinct mechanisms.* Cancer Cell, 2006. **10**(2): p. 113-20.
53. Jain, M., et al., *Sustained loss of a neoplastic phenotype by brief inactivation of MYC.* Science, 2002. **297**(5578): p. 102-4.
54. Soucek, L., et al., *Modelling Myc inhibition as a cancer therapy.* Nature, 2008. **455**(7213): p. 679-83.
55. Verdine, G.L. and L.D. Walensky, *The challenge of drugging undruggable targets in cancer: lessons learned from targeting BCL-2 family members.* Clin Cancer Res, 2007. **13**(24): p. 7264-70.
56. Filippakopoulos, P., et al., *Selective inhibition of BET bromodomains.* Nature, 2010. **468**(7327): p. 1067-73.
57. Delmore, J.E., et al., *BET bromodomain inhibition as a therapeutic strategy to target c-Myc.* Cell, 2011. **146**(6): p. 904-17.
58. Yan, C. and P.J. Higgins, *Drugging the undruggable: transcription therapy for cancer.* Biochim Biophys Acta, 2013. **1835**(1): p. 76-85.
59. Whitfield, J.R., M.E. Beaulieu, and L. Soucek, *Strategies to Inhibit Myc and Their Clinical Applicability.* Front Cell Dev Biol, 2017. **5**: p. 10.
60. McCormick, F., *KRAS as a Therapeutic Target.* Clin Cancer Res, 2015. **21**(8): p. 1797-801.
61. Delbridge, A.R. and A. Strasser, *The BCL-2 protein family, BH3-mimetics and cancer therapy.* Cell Death Differ, 2015. **22**(7): p. 1071-80.
62. Otto, T., et al., *Stabilization of N-Myc is a critical function of Aurora A in human neuroblastoma.* Cancer Cell, 2009. **15**(1): p. 67-78.
63. Gustafson, W.C., et al., *Drugging MYCN through an allosteric transition in Aurora kinase A.* Cancer Cell, 2014. **26**(3): p. 414-427.
64. Hsieh, A.L. and C.V. Dang, *MYC, Metabolic Synthetic Lethality, and Cancer.* Recent Results Cancer Res, 2016. **207**: p. 73-91.
65. Dang, C.V., et al., *The c-Myc target gene network.* Semin Cancer Biol, 2006. **16**(4): p. 253-64.
66. Patel, J.H., et al., *Analysis of genomic targets reveals complex functions of MYC.* Nat Rev Cancer, 2004. **4**(7): p. 562-8.

67. Eilers, M. and R.N. Eisenman, *Myc's broad reach.* Genes Dev, 2008. **22**(20): p. 2755-66.
68. Kress, T.R., A. Sabo, and B. Amati, *MYC: connecting selective transcriptional control to global RNA production.* Nat Rev Cancer, 2015. **15**(10): p. 593-607.
69. Dang, C.V., *MYC, metabolism, cell growth, and tumorigenesis.* Cold Spring Harb Perspect Med, 2013. **3**(8).
70. Dansen, T.B., et al., *Specific requirement for Bax, not Bak, in Myc-induced apoptosis and tumor suppression in vivo.* J Biol Chem, 2006. **281**(16): p. 10890-5.
71. Juin, P., et al., *c-Myc functionally cooperates with Bax to induce apoptosis.* Mol Cell Biol, 2002. **22**(17): p. 6158-69.
72. Juin, P., et al., *c-Myc-induced sensitization to apoptosis is mediated through cytochrome c release.* Genes Dev, 1999. **13**(11): p. 1367-81.
73. Hotti, A., et al., *Caspases and mitochondria in c-Myc-induced apoptosis: identification of ATM as a new target of caspases.* Oncogene, 2000. **19**(19): p. 2354-62.
74. Bissonnette, R.P., et al., *Apoptotic cell death induced by c-myc is inhibited by bcl-2.* Nature, 1992. **359**(6395): p. 552-4.
75. Fanidi, A., E.A. Harrington, and G.I. Evan, *Cooperative interaction between c-myc and bcl-2 proto-oncogenes.* Nature, 1992. **359**(6395): p. 554-6.
76. Pelengaris, S., M. Khan, and G.I. Evan, *Suppression of Myc-induced apoptosis in beta cells exposes multiple oncogenic properties of Myc and triggers carcinogenic progression.* Cell, 2002. **109**(3): p. 321-34.
77. Soucie, E.L., et al., *Myc potentiates apoptosis by stimulating Bax activity at the mitochondria.* Mol Cell Biol, 2001. **21**(14): p. 4725-36.
78. Eischen, C.M., et al., *Bcl-2 is an apoptotic target suppressed by both c-Myc and E2F-1.* Oncogene, 2001. **20**(48): p. 6983-93.
79. Maclean, K.H., et al., *c-Myc augments gamma irradiation-induced apoptosis by suppressing Bcl-XL.* Mol Cell Biol, 2003. **23**(20): p. 7256-70.
80. de Alboran, I.M., E. Baena, and A.C. Martinez, *c-Myc-deficient B lymphocytes are resistant to spontaneous and induced cell death.* Cell Death Differ, 2004. **11**(1): p. 61-8.
81. Kamijo, T., et al., *Functional and physical interactions of the ARF tumor suppressor with p53 and Mdm2.* Proc Natl Acad Sci U S A, 1998. **95**(14): p. 8292-7.
82. Stott, F.J., et al., *The alternative product from the human CDKN2A locus, p14(ARF), participates in a regulatory feedback loop with p53 and MDM2.* EMBO J, 1998. **17**(17): p. 5001-14.
83. Eischen, C.M., et al., *Disruption of the ARF-Mdm2-p53 tumor suppressor pathway in Myc-induced lymphomagenesis.* Genes Dev, 1999. **13**(20): p. 2658-69.

84. Schmitt, C.A., et al., *INK4a/ARF mutations accelerate lymphomagenesis and promote chemoresistance by disabling p53.* Genes Dev, 1999. **13**(20): p. 2670-7.
85. Villunger, A., et al., *p53- and drug-induced apoptotic responses mediated by BH3-only proteins puma and noxa.* Science, 2003. **302**(5647): p. 1036-8.
86. Hsu, B., et al., *Evidence that c-myc mediated apoptosis does not require wild-type p53 during lymphomagenesis.* Oncogene, 1995. **11**(1): p. 175-9.
87. Blyth, K., et al., *Sensitivity to myc-induced apoptosis is retained in spontaneous and transplanted lymphomas of CD2-mycER mice.* Oncogene, 2000. **19**(6): p. 773-82.
88. Eischen, C.M., et al., *Bax loss impairs Myc-induced apoptosis and circumvents the selection of p53 mutations during Myc-mediated lymphomagenesis.* Mol Cell Biol, 2001. **21**(22): p. 7653-62.
89. Campone, M., et al., *c-Myc dependent expression of pro-apoptotic Bim renders HER2-overexpressing breast cancer cells dependent on anti-apoptotic Mcl-1.* Mol Cancer, 2011. **10**: p. 110.
90. Lee, Y.Y., et al., *CREB-binding protein (CBP) regulates beta-adrenoceptor (beta-AR)-mediated apoptosis.* Cell Death Differ, 2013. **20**(7): p. 941-52.
91. Hemann, M.T., et al., *Evasion of the p53 tumour surveillance network by tumour-derived MYC mutants.* Nature, 2005. **436**(7052): p. 807-11.
92. Muthalagu, N., et al., *BIM is the primary mediator of MYC-induced apoptosis in multiple solid tissues.* Cell Rep, 2014. **8**(5): p. 1347-53.
93. Harris, A.W., et al., *The E mu-myc transgenic mouse. A model for high-incidence spontaneous lymphoma and leukemia of early B cells.* J Exp Med, 1988. **167**(2): p. 353-71.
94. Strasser, A., et al., *Novel primitive lymphoid tumours induced in transgenic mice by cooperation between myc and bcl-2.* Nature, 1990. **348**(6299): p. 331-3.
95. McDonnell, T.J. and S.J. Korsmeyer, *Progression from lymphoid hyperplasia to high-grade malignant lymphoma in mice transgenic for the t(14; 18).* Nature, 1991. **349**(6306): p. 254-6.
96. Hueber, A.O., et al., *Requirement for the CD95 receptor-ligand pathway in c-Myc-induced apoptosis.* Science, 1997. **278**(5341): p. 1305-9.
97. Stine, Z.E., et al., *MYC, Metabolism, and Cancer.* Cancer Discov, 2015. **5**(10): p. 1024-39.
98. Vander Heiden, M.G., *Targeting cancer metabolism: a therapeutic window opens.* Nat Rev Drug Discov, 2011. **10**(9): p. 671-84.
99. Cantor, J.R. and D.M. Sabatini, *Cancer cell metabolism: one hallmark, many faces.* Cancer Discov, 2012. **2**(10): p. 881-98.
100. Dang, C.V., *Links between metabolism and cancer.* Genes Dev, 2012. **26**(9): p. 877-90.

101. Warburg, O., *On the origin of cancer cells.* Science, 1956. **123**(3191): p. 309-14.
102. Le, A., et al., *Inhibition of lactate dehydrogenase A induces oxidative stress and inhibits tumor progression.* Proc Natl Acad Sci U S A, 2010. **107**(5): p. 2037-42.
103. Kim, J.W., et al., *HIF-1-mediated expression of pyruvate dehydrogenase kinase: a metabolic switch required for cellular adaptation to hypoxia.* Cell Metab, 2006. **3**(3): p. 177-85.
104. Papandreou, I., et al., *HIF-1 mediates adaptation to hypoxia by actively downregulating mitochondrial oxygen consumption.* Cell Metab, 2006. **3**(3): p. 187-97.
105. Osthus, R.C., et al., *Deregulation of glucose transporter 1 and glycolytic gene expression by c-Myc.* J Biol Chem, 2000. **275**(29): p. 21797-800.
106. Shim, H., et al., *c-Myc transactivation of LDH-A: implications for tumor metabolism and growth.* Proc Natl Acad Sci U S A, 1997. **94**(13): p. 6658-63.
107. Doherty, J.R., et al., *Blocking lactate export by inhibiting the Myc target MCT1 Disables glycolysis and glutathione synthesis.* Cancer Res, 2014. **74**(3): p. 908-20.
108. Brahimi-Horn, M.C., G. Bellot, and J. Pouyssegur, *Hypoxia and energetic tumour metabolism.* Curr Opin Genet Dev, 2011. **21**(1): p. 67-72.
109. Kim, J.W., et al., *Hypoxia-inducible factor 1 and dysregulated c-Myc cooperatively induce vascular endothelial growth factor and metabolic switches hexokinase 2 and pyruvate dehydrogenase kinase 1.* Mol Cell Biol, 2007. **27**(21): p. 7381-93.
110. David, C.J., et al., *HnRNP proteins controlled by c-Myc deregulate pyruvate kinase mRNA splicing in cancer.* Nature, 2010. **463**(7279): p. 364-8.
111. Chaneton, B. and E. Gottlieb, *Rocking cell metabolism: revised functions of the key glycolytic regulator PKM2 in cancer.* Trends Biochem Sci, 2012. **37**(8): p. 309-16.
112. Wang, R., et al., *The transcription factor Myc controls metabolic reprogramming upon T lymphocyte activation.* Immunity, 2011. **35**(6): p. 871-82.
113. Morrish, F., et al., *c-Myc activates multiple metabolic networks to generate substrates for cell-cycle entry.* Oncogene, 2009. **28**(27): p. 2485-91.
114. Vazquez, A., E.K. Markert, and Z.N. Oltvai, *Serine biosynthesis with one carbon catabolism and the glycine cleavage system represents a novel pathway for ATP generation.* PLoS One, 2011. **6**(11): p. e25881.
115. Nikiforov, M.A., et al., *A functional screen for Myc-responsive genes reveals serine hydroxymethyltransferase, a major source of the one-carbon unit for cell metabolism.* Mol Cell Biol, 2002. **22**(16): p. 5793-800.

116. Wise, D.R., et al., *Myc regulates a transcriptional program that stimulates mitochondrial glutaminolysis and leads to glutamine addiction.* Proc Natl Acad Sci U S A, 2008. **105**(48): p. 18782-7.
117. Chang, T.C., et al., *Widespread microRNA repression by Myc contributes to tumorigenesis.* Nat Genet, 2008. **40**(1): p. 43-50.
118. Gao, P., et al., *c-Myc suppression of miR-23a/b enhances mitochondrial glutaminase expression and glutamine metabolism.* Nature, 2009. **458**(7239): p. 762-5.
119. DeBerardinis, R.J. and T. Cheng, *Q's next: the diverse functions of glutamine in metabolism, cell biology and cancer.* Oncogene, 2010. **29**(3): p. 313-24.
120. Le, A., et al., *Glucose-independent glutamine metabolism via TCA cycling for proliferation and survival in B cells.* Cell Metab, 2012. **15**(1): p. 110-21.
121. Murphy, T.A., C.V. Dang, and J.D. Young, *Isotopically nonstationary 13C flux analysis of Myc-induced metabolic reprogramming in B-cells.* Metab Eng, 2013. **15**: p. 206-17.
122. Yuneva, M., et al., *Deficiency in glutamine but not glucose induces MYC-dependent apoptosis in human cells.* J Cell Biol, 2007. **178**(1): p. 93-105.
123. Miltenberger, R.J., K.A. Sukow, and P.J. Farnham, *An E-box-mediated increase in cad transcription at the G1/S-phase boundary is suppressed by inhibitory c-Myc mutants.* Mol Cell Biol, 1995. **15**(5): p. 2527-35.
124. Liu, Y.C., et al., *Global regulation of nucleotide biosynthetic genes by c-Myc.* PLoS One, 2008. **3**(7): p. e2722.
125. Zhang, J., et al., *Asparagine plays a critical role in regulating cellular adaptation to glutamine depletion.* Mol Cell, 2014. **56**(2): p. 205-18.
126. Sullivan, L.B., et al., *Supporting Aspartate Biosynthesis Is an Essential Function of Respiration in Proliferating Cells.* Cell, 2015. **162**(3): p. 552-63.
127. Morrish, F., et al., *The oncogene c-Myc coordinates regulation of metabolic networks to enable rapid cell cycle entry.* Cell Cycle, 2008. **7**(8): p. 1054-66.
128. Zeller, K.I., et al., *An integrated database of genes responsive to the Myc oncogenic transcription factor: identification of direct genomic targets.* Genome Biol, 2003. **4**(10): p. R69.
129. Loven, J., et al., *Revisiting global gene expression analysis.* Cell, 2012. **151**(3): p. 476-82.
130. van Riggelen, J., A. Yetil, and D.W. Felsher, *MYC as a regulator of ribosome biogenesis and protein synthesis.* Nat Rev Cancer, 2010. **10**(4): p. 301-9.
131. Grandori, C., et al., *c-Myc binds to human ribosomal DNA and stimulates transcription of rRNA genes by RNA polymerase I.* Nat Cell Biol, 2005. **7**(3): p. 311-8.
132. Arabi, A., et al., *c-Myc associates with ribosomal DNA and activates RNA polymerase I transcription.* Nat Cell Biol, 2005. **7**(3): p. 303-10.
133. Gomez-Roman, N., et al., *Direct activation of RNA polymerase III transcription by c-Myc.* Nature, 2003. **421**(6920): p. 290-4.

134. Schlosser, I., et al., *A role for c-Myc in the regulation of ribosomal RNA processing.* Nucleic Acids Res, 2003. **31**(21): p. 6148-56.
135. Watson, J.D., et al., *Identifying genes regulated in a Myc-dependent manner.* J Biol Chem, 2002. **277**(40): p. 36921-30.
136. Schmidt, E.V., *The role of c-myc in regulation of translation initiation.* Oncogene, 2004. **23**(18): p. 3217-21.
137. Hofmann, J.W., et al., *Reduced expression of MYC increases longevity and enhances healthspan.* Cell, 2015. **160**(3): p. 477-88.
138. Barna, M., et al., *Suppression of Myc oncogenic activity by ribosomal protein haploinsufficiency.* Nature, 2008. **456**(7224): p. 971-5.
139. Morrish, F., C. Giedt, and D. Hockenbery, *c-MYC apoptotic function is mediated by NRF-1 target genes.* Genes Dev, 2003. **17**(2): p. 240-55.
140. Li, F., et al., *Myc stimulates nuclearly encoded mitochondrial genes and mitochondrial biogenesis.* Mol Cell Biol, 2005. **25**(14): p. 6225-34.
141. Zhang, H., et al., *HIF-1 inhibits mitochondrial biogenesis and cellular respiration in VHL-deficient renal cell carcinoma by repression of C-MYC activity.* Cancer Cell, 2007. **11**(5): p. 407-20.
142. Kim, J., J.H. Lee, and V.R. Iyer, *Global identification of Myc target genes reveals its direct role in mitochondrial biogenesis and its E-box usage in vivo.* PLoS One, 2008. **3**(3): p. e1798.
143. Graves, J.A., et al., *Mitochondrial structure, function and dynamics are temporally controlled by c-Myc.* PLoS One, 2012. **7**(5): p. e37699.
144. O'Donnell, K.A., et al., *Activation of transferrin receptor 1 by c-Myc enhances cellular proliferation and tumorigenesis.* Mol Cell Biol, 2006. **26**(6): p. 2373-86.
145. Fogal, V., et al., *Mitochondrial p32 protein is a critical regulator of tumor metabolism via maintenance of oxidative phosphorylation.* Mol Cell Biol, 2010. **30**(6): p. 1303-18.
146. Altman, B.J., Z.E. Stine, and C.V. Dang, *From Krebs to clinic: glutamine metabolism to cancer therapy.* Nat Rev Cancer, 2016. **16**(11): p. 749.
147. Lane, A.N. and T.W. Fan, *Regulation of mammalian nucleotide metabolism and biosynthesis.* Nucleic Acids Res, 2015. **43**(4): p. 2466-85.
148. Bhutia, Y.D., et al., *Amino Acid transporters in cancer and their relevance to "glutamine addiction": novel targets for the design of a new class of anticancer drugs.* Cancer Res, 2015. **75**(9): p. 1782-8.
149. Curthoys, N.P. and M. Watford, *Regulation of glutaminase activity and glutamine metabolism.* Annu Rev Nutr, 1995. **15**: p. 133-59.
150. Moreadith, R.W. and A.L. Lehninger, *The pathways of glutamate and glutamine oxidation by tumor cell mitochondria. Role of mitochondrial NAD(P)+-dependent malic enzyme.* J Biol Chem, 1984. **259**(10): p. 6215-21.
151. Metallo, C.M., et al., *Reductive glutamine metabolism by IDH1 mediates lipogenesis under hypoxia.* Nature, 2011. **481**(7381): p. 380-4.

152. Welbourne, T.C., *Ammonia production and glutamine incorporation into glutathione in the functioning rat kidney.* Can J Biochem, 1979. **57**(3): p. 233-7.
153. Ishimoto, T., et al., *CD44 variant regulates redox status in cancer cells by stabilizing the xCT subunit of system xc(-) and thereby promotes tumor growth.* Cancer Cell, 2011. **19**(3): p. 387-400.
154. Timmerman, L.A., et al., *Glutamine sensitivity analysis identifies the xCT antiporter as a common triple-negative breast tumor therapeutic target.* Cancer Cell, 2013. **24**(4): p. 450-65.
155. Hensley, C.T., A.T. Wasti, and R.J. DeBerardinis, *Glutamine and cancer: cell biology, physiology, and clinical opportunities.* J Clin Invest, 2013. **123**(9): p. 3678-84.
156. Ploessl, K., et al., *Comparative evaluation of 18F-labeled glutamic acid and glutamine as tumor metabolic imaging agents.* J Nucl Med, 2012. **53**(10): p. 1616-24.
157. Lieberman, B.P., et al., *PET imaging of glutaminolysis in tumors by 18F-(2S,4R)4-fluoroglutamine.* J Nucl Med, 2011. **52**(12): p. 1947-55.
158. Venneti, S., et al., *Glutamine-based PET imaging facilitates enhanced metabolic evaluation of gliomas in vivo.* Sci Transl Med, 2015. **7**(274): p. 274ra17.
159. Rajagopalan, K.N. and R.J. DeBerardinis, *Role of glutamine in cancer: therapeutic and imaging implications.* J Nucl Med, 2011. **52**(7): p. 1005-8.
160. Jacque, N., et al., *Targeting glutaminolysis has antileukemic activity in acute myeloid leukemia and synergizes with BCL-2 inhibition.* Blood, 2015. **126**(11): p. 1346-56.
161. Gross, M.I., et al., *Antitumor activity of the glutaminase inhibitor CB-839 in triple-negative breast cancer.* Mol Cancer Ther, 2014. **13**(4): p. 890-901.
162. Qing, G., et al., *ATF4 regulates MYC-mediated neuroblastoma cell death upon glutamine deprivation.* Cancer Cell, 2012. **22**(5): p. 631-44.
163. Griffin, J.L. and J.P. Shockcor, *Metabolic profiles of cancer cells.* Nat Rev Cancer, 2004. **4**(7): p. 551-61.
164. Untergasser, A., et al., *Primer3--new capabilities and interfaces.* Nucleic Acids Res, 2012. **40**(15): p. e115.
165. Koressaar, T. and M. Remm, *Enhancements and modifications of primer design program Primer3.* Bioinformatics, 2007. **23**(10): p. 1289-91.
166. Smith, C.A., et al., *XCMS: processing mass spectrometry data for metabolite profiling using nonlinear peak alignment, matching, and identification.* Anal Chem, 2006. **78**(3): p. 779-87.
167. Sumner, L.W., et al., *Proposed minimum reporting standards for chemical analysis Chemical Analysis Working Group (CAWG) Metabolomics Standards Initiative (MSI).* Metabolomics, 2007. **3**(3): p. 211-221.

168. Klefstrom, J., et al., *c-Myc induces cellular susceptibility to the cytotoxic action of TNF-alpha.* EMBO J, 1994. **13**(22): p. 5442-50.
169. Lutz, W., et al., *MycN and IFNgamma cooperate in apoptosis of human neuroblastoma cells.* Oncogene, 1998. **17**(3): p. 339-46.
170. Smith, C.A., et al., *METLIN: a metabolite mass spectral database.* Ther Drug Monit, 2005. **27**(6): p. 747-51.
171. Tullson, P.C. and R.L. Terjung, *Adenine nucleotide synthesis in exercising and endurance-trained skeletal muscle.* Am J Physiol, 1991. **261**(2 Pt 1): p. C342-7.
172. Jennings, R.B. and C. Steenbergen, Jr., *Nucleotide metabolism and cellular damage in myocardial ischemia.* Annu Rev Physiol, 1985. **47**: p. 727-49.
173. Chouchani, E.T., et al., *Ischaemic accumulation of succinate controls reperfusion injury through mitochondrial ROS.* Nature, 2014. **515**(7527): p. 431-435.
174. Dzeja, P. and A. Terzic, *Adenylate kinase and AMP signaling networks: metabolic monitoring, signal communication and body energy sensing.* Int J Mol Sci, 2009. **10**(4): p. 1729-72.
175. Drew, R. and J.O. Miners, *The effects of buthionine sulphoximine (BSO) on glutathione depletion and xenobiotic biotransformation.* Biochem Pharmacol, 1984. **33**(19): p. 2989-94.
176. Lubos, E., J. Loscalzo, and D.E. Handy, *Glutathione peroxidase-1 in health and disease: from molecular mechanisms to therapeutic opportunities.* Antioxid Redox Signal, 2011. **15**(7): p. 1957-97.
177. Esworthy, R.S., Y.S. Ho, and F.F. Chu, *The Gpx1 gene encodes mitochondrial glutathione peroxidase in the mouse liver.* Arch Biochem Biophys, 1997. **340**(1): p. 59-63.
178. Chaudiere, J. and A.L. Tappel, *Interaction of gold(I) with the active site of selenium-glutathione peroxidase.* J Inorg Biochem, 1984. **20**(4): p. 313-25.
179. Jastroch, M., et al., *Mitochondrial proton and electron leaks.* Essays Biochem, 2010. **47**: p. 53-67.
180. Willis, S.N., et al., *Apoptosis initiated when BH3 ligands engage multiple Bcl-2 homologs, not Bax or Bak.* Science, 2007. **315**(5813): p. 856-9.
181. Matsuyama, S., et al., *The Mitochondrial F0F1-ATPase proton pump is required for function of the proapoptotic protein Bax in yeast and mammalian cells.* Mol Cell, 1998. **1**(3): p. 327-36.
182. Gottlieb, E., M.G. Vander Heiden, and C.B. Thompson, *Bcl-x(L) prevents the initial decrease in mitochondrial membrane potential and subsequent reactive oxygen species production during tumor necrosis factor alpha-induced apoptosis.* Mol Cell Biol, 2000. **20**(15): p. 5680-9.
183. Narita, M., et al., *Bax interacts with the permeability transition pore to induce permeability transition and cytochrome c release in isolated mitochondria.* Proc Natl Acad Sci U S A, 1998. **95**(25): p. 14681-6.

184. Jiang, X., et al., *A Small Molecule That Protects the Integrity of the Electron Transfer Chain Blocks the Mitochondrial Apoptotic Pathway.* Mol Cell, 2016. **63**(2): p. 229-239.
185. Sabo, A., et al., *Selective transcriptional regulation by Myc in cellular growth control and lymphomagenesis.* Nature, 2014. **511**(7510): p. 488-492.
186. Weinberg, S.E. and N.S. Chandel, *Targeting mitochondria metabolism for cancer therapy.* Nat Chem Biol, 2015. **11**(1): p. 9-15.
187. Lee, K.M., et al., *MYC and MCL1 Cooperatively Promote Chemotherapy-Resistant Breast Cancer Stem Cells via Regulation of Mitochondrial Oxidative Phosphorylation.* Cell Metab, 2017. **26**(4): p. 633-647 e7.
188. Ye, J., et al., *Serine catabolism regulates mitochondrial redox control during hypoxia.* Cancer Discov, 2014. **4**(12): p. 1406-17.
189. Mullen, A.R., et al., *Reductive carboxylation supports growth in tumour cells with defective mitochondria.* Nature, 2011. **481**(7381): p. 385-8.
190. Scarlett, J.L., et al., *Changes in mitochondrial membrane potential during staurosporine-induced apoptosis in Jurkat cells.* FEBS Lett, 2000. **475**(3): p. 267-72.
191. Zamzami, N., et al., *Sequential reduction of mitochondrial transmembrane potential and generation of reactive oxygen species in early programmed cell death.* J Exp Med, 1995. **182**(2): p. 367-77.
192. Gottlieb, E., et al., *Mitochondrial membrane potential regulates matrix configuration and cytochrome c release during apoptosis.* Cell Death Differ, 2003. **10**(6): p. 709-17.